8-2016

REGULATION OF BREAST CANCER INITIATION AND PROGRESSION BY 14-3-3ZETA

Chia-Chi Chang

REGULATION OF BREAST CANCER INITIATION

AND PROGRESSION BY 14-3-3ζ

by

Chia-Chi Chang, M.S.

APPROVED:

_____
Dihua Yu, M.D., Ph.D.
Supervisory Professor

_____
Heinrich Taegtmeyer, M.D., D.Phil

_____
Richard Behringer, Ph.D.

_____
Peng Huang, M.D., Ph.D.

_____
Shao-Cong Sun, Ph.D.

APPROVED:

_____
Dean, Graduate School of Biomedical Sciences

The University of Texas Health Science Center at Houston

REGULATION OF BREAST CANCER INITIATION
AND PROGRESSION BY 14-3-3ζ

A

DISSERTATION

Presented to the Faculty of

The University of Texas

Health Science Center at Houston

and

The University of Texas

MD Anderson Cancer Center

Graduate School of Biomedical Sciences

In Partial Fulfillment

of the Requirements

for the Degree of

DOCTOR OF PHILOSOPHY

By

Chia-Chi Chang, M.S.

Houston, Texas

August, 2016

Copyright ©

2016 Chia-Chi Chang, M.S. All rights reserved.

Dedication

To my loving parents, who would never let go of a good idea. This work started primarily

to fulfill the curiosity to science and was done with family's love and support.

Acknowledgements

Foremost, I would like to express my gratitude to my supervisor, Dr. Dihua Yu, with her guidance throughout my graduate studies. I thank her for putting me as a primary person on the PO1 team when I was the second-year graduate student and for giving me many training opportunities. I am equipped and have seen my own growth to become an independent researcher. I thank her for the mentorship, support, and inspiration. Dr. Yu has a mindset for encouragement, drive, and innovation that has inspired me to pursue my research interests over the past 6 years. Importantly, Dr. Dihua Yu is an incredible role model of a woman scientist for me and her wisdom helps me to avoid mistakes and be a main part of my graduate school journey.

To my committee members, Dr. Heinrich Taegtmeyer, Dr. Peng Huang, Dr. Richard Behringer, Dr. Shao-Cong Sun, and Dr. Hui-Kuan Lin, who have always given me constructive comments and advice over the years, I am truly grateful. I especially appreciate Dr. Heinrich Taegtmeyer, who is always willing to spend time and share with me his wisdom and guidance. Dr. Taegtmeyer is a gracious person who has been a major part of my dissertation work and I learned a great deal from his deep insight. He encouraged me and also giving me an unflagging support throughout years. I thank Dr. Peng Huang for always having met me and having given precious advice and encouragements. I appreciate Dr. Richard Behringer for unconditionally sharing his knowledge and giving advice when I was new in working with animal models and developing my first transgenic mouse model for my dissertation work. I also want to express my gratitude to Dr. Shao-Cong Sun and Dr. Hui-Kuan Lin for their expertise in

REGULATION OF BREAST CANCER INITIATION
AND PROGRESSION BY 14-3-3ζ

Chia-Chi Chang, M.S.

Supervisor Professor: Dihua Yu, M.D., Ph.D.

14-3-3ζ is a ubiquitously expressed family member of proteins that have been implicated to have oncogenic potential through its interactions and involvement in cancer initiation and progression. 14-3-3ζ belongs to the highly conserved 14-3-3ζ protein family and modulates numerous pathways in cancer. Overexpression of 14-3-3ζ is an early event, occurs in more than 40% of human breast cancer cases, and is associated with disease recurrence and poor prognosis.

Metabolic reprogramming is a hallmark of cancer. Cancer cells elevate aerobic glycolysis to produce metabolic intermediates and reducing equivalents, thereby facilitating cellular adaptation to the adverse environment and sustaining fast proliferation. Interestingly, new evidence has emerged that metabolic alteration may arise at early stages of breast cancer. However, little is known about what triggers metabolic reprogramming and how it mechanistically contributes to breast cancer initiation and progression. In this dissertation, I have characterized the functional role of 14-3-3ζ in metabolic alteration, cancer initiation and progression. The bioinformatic analyses of gene expression profiling from early-stages breast premalignant lesions showed that the expression of 14-3-3ζ is strongly correlated with the expressions of glycolytic genes, especially lactate dehydrogenase A (LDHA). Interestingly, this positive correlation was

also preserved in the advanced stage of breast cancer. Experimentally, my work demonstrated that increasing 14-3-3ζ expression in human non-transformed mammary epithelial cells (hMECs), MCF10A and MCF12A, transcriptionally up-regulated LDHA expression and increased glycolytic activity, which increased colony formation and promoted early transformation of hMECs. Conversely, knockdown of LDHA in these 14-3-3ζ-overexpressing hMECs significantly decreased glycolytic activity and inhibited early transformation. Mechanistically, up-regulation of LDHA in 14-3-3ζ-overexpressing hMECs was directly mediated by the cAMP-response element-binding (CREB) transcription factor through 14-3-3ζ-mediated activation of the MEK-ERK signaling axis. Blocking MEK-ERK pathway in 14-3-3ζ-high expressing hMEC-derived MCF10DCIS.COM tumor lesions, significantly decreasing LDHA expression, reducing tumor cell proliferation, and effectively inhibiting tumor growth. Taken together, my studies demonstrate that 14-3-3ζ has pleiotropic functions on cancer metabolism dysregulation and tumorigenesis. While 14-3-3ζ has been identified as critical mediator in breast cancer initiation and early metabolic transformation, another key finding of this dissertation is that discovery of tumor cells selectively preserve high 14-3-3ζ expression during tumor progression process. 14-3-3ζ may involve in cell fitness mechanism that benefits cell survival and proliferation during cancer progression.

Cancer is a sequential process of cell clone selection and competition. During cell competition; a "fit" clone population with better growth advantages outcompetes other subclones and eliminates "unfit" subclones. I found that 14-3-3ζ-low cells are eradicated by 14-3-3ζ-high cells when they grow together (HET tumors); however, 14-3-3ζ-low cells can still survive only when surrounded by cells with similar expression levels of 14-3-3ζ.

Mechanistically, 14-3-3ζ-low tumor cells produce a high level of cytokine macrophage inhibitory factor (MIF). Juxtacrine signaling involving MIF, its receptor CXCR2 and downstream production of interleukin-8 (IL-8), augmented cell proliferation and reduced cell apoptosis in 14-3-3ζ-high cells. Disruption of IL-8 or its upstream signaling, MIF or CXCR2, led to diminish cell fitness in 14-3-3ζ-high tumor cells and reduced tumor growth. Moreover, unlike conventional cell fitness, this study has revealed that 14-3-3ζ-high cells out-compete to sequester MIF, thereby causing cell death of 14-3-3ζ-low cells. I show that cancer cells may utilize part of immunity to trigger winner-loser cell interaction that determines the cell fate in solid tumors. Targeting the MIF-CXCR2-IL-8 axis could be an effective strategy to intervene in breast cancer progression.

In summary, my work demonstrates that 14-3-3ζ has two distinct roles involving in cancer metabolism and cell competition, which may be developed into novel therapeutic strategies to target human breast cancer.

Table of Contents

CHAPTER 1. Introduction

CHAPTER 3. MIF-CXCR2-IL-8 pathway is required for 14-3-3ζ high tumor cells to induce cell competition

ABBREVIATIONS

5'-UTR	5'-untranslated region
ADH	Atypical ductal hyperplasia
AMPK	AMP-activated protein kinase
ATCC	American type cell collection
BM	Basement membrane
bp	Base pairs
BrdU	5-Bromo-2-deoxyuridine
CBA	Cytometric Bead Array
CRE	*c-AMP* response element
CREB	*c-AMP* response element binding
DCIS	Ductal carcinoma *in situ*
DH	Ductal hyperplasia
EGFR	Epidermal growth factor receptor
EMT	Epithelial-mesenchymal transition
ER	Estrogen receptor
FGF	Fibroblast growth factor
FH	Fumarate hydratase
FVB	Friend virus b-type mice
GADPH	Glyceraldehyde-3-phosphate dehydrogenase
GFP	Green fluorescent protein
GLUTs	Glucose transporter proteins
HA	Hemagglutinin
HAT	Histone acetyltransferase
HER2	Human epidermal growth factor receptor 2
HGF	Hepatocyte growth factor
HIF	Hypoxia-inducible factor 1
HMECs	Human mammary epithelial cells
IF	Immunofluorescence
IHC	Immunohistochemistry

MMPs	Extracellular matrix metalloproteases
PBS	Phosphate buffered saline
PFK-2	6-phosphofructo-2-kinase
PI	Propidium iodide
IP	Immunoprecipitation
IL-1β	Interleukin-1β
IL-8	Interleukin-8
IDC	Invasive ductal carcinoma
IBC	Invasive breast cancer
IDH	Isocitrate dehydrogenase
LDHA	Lactate dehydrogenase A
LKB1	Liver kinase B1
MIF	Macrophage inhibitory factor
MFPs	Mammary fat pads
MCM2	Minichromosome maintenance 2
MtDMA	Mitochondrial DNA
NGS	Next generation sequencing analyses
NLS	Nuclear localization sequence
NOX	NADPH oxidase
OXPHOS	Oxidative phosphorylation
PCD	Programmed cell death
PK	Pyruvate kinase
PKM2	Pyruvate kinase 2
PPP	Pentose phosphate pathway
PR	Progesterone receptor
PTM	Posttranslational modification
QUICK	Quantitative immunoprecipitation combined with knockdown method
ROS	Reactive oxygen species
ErbB2	Receptor tyrosine-protein kinase 2
tdRed	tdTomato red fluorescent protein

SDH	Succinate dehydrogenase
RTTA	Tetracycline-controlled transcriptional activation protein
TCGA	The Cancer Genome Atlas
TMA	Tissue microarray
T-ALL	T-lineage acute lymphoblastic leukemia
TESS	Transcription Element Search System
TAM	Tumor-associated macrophage formation
TILs	Tumor-infiltrating lymphocytes
GlcNAc	Acetylglucosamine
VEGF	Vascular endothelial growth factor
VEGF-A	Vascular endothelial growth factor-A
YWHAZ	Tyrosine 3-monooxygenase/tryptophan 5-monooxygenase activation protein Zeta

LIST OF TABLES

LIST OF FIGURES

Chapter 1. Introduction

CHAPTER 2. 14-3-3ζ-mediated LDHA upregulation facilitates breast cancer initiation and progression

CHAPTER 3. MIF-CXCR2-IL-8 pathway is required for 14-3-3ζ high tumor cells to induce cell competition

CHAPTER 4. Concluding remarks, future directions, and perspectives

Chapter 1
INTRODUCTION

1.1 Overview of Cancer

1.1.1 Cancer Epidemiology and Statistics

Cancer is the second leading cause of death in the United States, exceeded only by heart disease. In 2016, there is an overall estimation of about 1.68 million new cancer diagnoses, and it is estimated that about 595,000 of cancer deaths will occur in the U.S. (Figure 1) (1). The lifetime probability of developing an invasive cancer is about 42% in men and 38% in women. Interestingly, the cancer risk is higher for young women less than 50 years old (5.4%) than for young men (3.4%), due to relatively high incidences of breast, thyroid and genital cancer (1, 2). In 2016, the number of cancer survivors is the highest in American history with more than 15 million; in 2026, it is estimated that the number of cancer survivors will exceed 20 million in U.S. (Figure 2). The most prevalent cancers among males and females are prostate cancer and breast cancer, respectively (Figure 3) (2).

Despite the continuously increasing cancer survival over the past two decades, cancer death rates are still high and continue to rise in the two most fatal cancers, pancreatic cancer and hepatic cancer. To overcome this trend requires collaboration in both laboratory and clinical efforts towards the better therapeutic strategy, control, and prevention of cancer (3, 4). Currently, based on the increasingly growing population in U.S., the annual direct medical costs for cancer, which was estimated at $124 billion in 2011 (5), is expected to reach over $158 billion in 2020 (6). Recognition and advanced understanding of tumor biology will facilitate drug development for cancer treatment, improving clinical outcomes and ultimately leading to a significant increase of cancer survival rate.

Estimated New Cases

Males | Females

Site	Number	%		Site	Number	%
Prostate	180,890	21%		Breast	246,660	29%
Lung & bronchus	117,920	14%		Lung & bronchus	106,470	13%
Colon & rectum	70,820	8%		Colon & rectum	63,670	8%
Urinary bladder	58,950	7%		Uterine corpus	60,050	7%
Melanoma of the skin	46,870	6%		Thyroid	49,350	6%
Non-Hodgkin lymphoma	40,170	5%		Non-Hodgkin lymphoma	32,410	4%
Kidney & renal pelvis	39,650	5%		Melanoma of the skin	29,510	3%
Oral cavity & pharynx	34,780	4%		Leukemia	26,050	3%
Leukemia	34,090	4%		Pancreas	25,400	3%
Liver & intrahepatic bile duct	28,410	3%		Kidney & renal pelvis	23,050	3%
All Sites	**841,390**	**100%**		**All Sites**	**843,820**	**100%**

Estimated Deaths

Males | Females

Site	Number	%		Site	Number	%
Lung & bronchus	85,920	27%		Lung & bronchus	72,160	26%
Prostate	26,120	8%		Breast	40,450	14%
Colon & rectum	26,020	8%		Colon & rectum	23,170	8%
Pancreas	21,450	7%		Pancreas	20,330	7%
Liver & intrahepatic bile duct	18,280	6%		Ovary	14,240	5%
Leukemia	14,130	4%		Uterine corpus	10,470	4%
Esophagus	12,720	4%		Leukemia	10,270	4%
Urinary bladder	11,820	4%		Liver & intrahepatic bile duct	8,890	3%
Non-Hodgkin lymphoma	11,520	4%		Non-Hodgkin lymphoma	8,630	3%
Brain & other nervous system	9,440	3%		Brain & other nervous system	6,610	2%
All Sites	**314,290**	**100%**		**All Sites**	**281,400**	**100%**

Figure 1. Expected number of new cancer cases and deaths in United States in 2016. In 2016, an estimated 841,390 new cases of cancer in males and 843,820 new cases in females will occur in United States. *Reprinted with permission from Siegel RL, Miller KD, Jemal A. Cancer statistics, 2016. CA: A Cancer Journal for Clinicians 2016; 66:7-30.*

As of January 1, 2016

Male	Female
Prostate 3,306,760	Breast 3,560,570
Colon & rectum 724,690	Uterine corpus 757,190
Melanoma 614,460	Colon & rectum 727,350
Urinary bladder 574,250	Thyroid 630,660
Non-Hodgkin lymphoma 361,480	Melanoma 612,790
Kidney & renal pelvis 305,340	Non-Hodgkin lymphoma 324,890
Testis 266,550	Lung & bronchus 288,210
Lung & bronchus 238,300	Uterine cervix 282,780
Leukemia 230,920	Ovary 235,200
Oral cavity & pharynx 229,880	Kidney & renal pelvis 204,040
Total survivors 7,377,100	**Total survivors 8,156,120**

As of January 1, 2026

Male	Female
Prostate 4,521,910	Breast 4,571,210
Colon & rectum 910,190	Uterine corpus 942,670
Melanoma 848,020	Colon & rectum 885,940
Urinary bladder 754,280	Thyroid 885,590
Non-Hodgkin lymphoma 488,780	Melanoma 811,490
Kidney 429,010	Non-Hodgkin lymphoma 436,370
Testis 335,790	Lung & bronchus 369,990
Leukemia 318,430	Uterine cervix 286,300
Lung & bronchus 303,380	Kidney & renal pelvis 284,380
Oral cavity & pharynx 293,290	Ovary 280,940
Total survivors 9,983,900	**Total survivors 10,305,870**

Figure 2. Expected number of cancer survivors in United States by 2016 and 2026.

There is a fast growing number of cancer survivors. It is expected that there will be nearly 21 million of cancer survivors in United States by 2026. *Miller KD, Siegel RL, Lin CC; Mariotto AB, Kramer JL, Rowland JH, Stein KD, Alteri R; Ahmedin Jemal A. Cancer treatment and survivorship statistics, 2016 CA: A Cancer Journal for Clinicians 2016.*
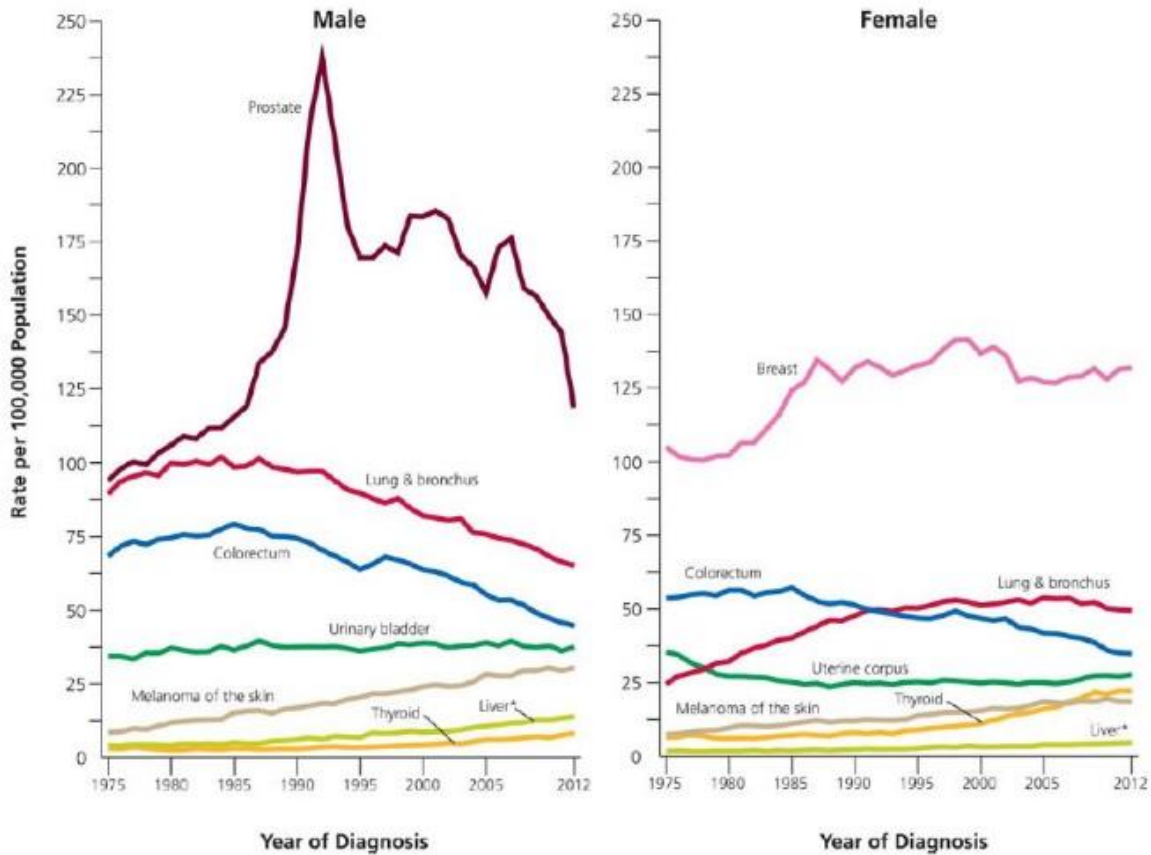
Figure 3. Trends in cancer incidence by sex in United States from 1975 to 2012.

Prostate cancer and lung and bronchus caner are the most prevalent cancer in men; breast cancer and lung and bronchus caner are the most prevalent cancer in women. *Reprinted with permission from Siegel RL, Miller KD, Jemal A. Cancer statistics, 2016. CA: A Cancer Journal for Clinicians 2016; 66:7-30.*

1.1.2 Cancer Hallmarks

Cancer is a term originally described by Greek physician, Hippocrates, who used it to illustrate the structure of veins on the external outside invasive surface of solid tumors . In the past century, researchers have been intensively investigating at the cancer genetic, molecular, cellular, and physiological levels, which has led us to a better understanding and categorization of the causes of cancer. Each tumor is a complex tissue containing diverse cell types that support each other and secure enough oxygen and nutrients to sustain tumor growth. Many lines of study discovered that tumorigenesis is caused by multiple steps such as DNA mutation and epigenetic alteration, which allow tumor cells to grow, survive and disseminate.

A well-known review on the common features of cancer was put forth by Dr. Douglas Hanahan and Dr. Robert Weinberg, who enumerated the complexities of tumor biology and emerging knowledge of distinct cancer-associated mechanisms. Tumors are not only comprised of proliferating cells, instead involving diverse cell types able to interact with each other and even recruit cells from other organs to support their need for growth. Ten emerging cancer hallmarks describe eight acquired functional features and two empowering characteristics during carcinogenesis (Figure 4) (7, 8). These capabilities allow cancer cells to grow, proliferate, and disseminate to distant organs to form metastasis. Additionally, the acquired hallmarks are common features shared by almost all types of cancers, and those are: 1) sustaining proliferative signaling, 2) resisting apoptosis, 3) evading growth suppressors, 4) inducing angiogenesis, 5) enabling replicative immortality, 6) activating invasion and metastasis, 7) avoiding immune destruction, 8) dysregulating cellular energetic. Previous studies showed that acquisition

of cancer hallmarks requires two enabling characteristics, genome instability and tumor-promoting inflammation, to increase genetic alteration in tumor cells, thereby fostering the development of incipient neoplasms into bulk tumor masses. In the following text, I will discuss several acquired capabilities of cancer hallmarks that are commonly shared by cancers. In-depth knowledge of tumor-promoting mechanisms will allow us to understand the biology of cancer in a comprehensive manners.
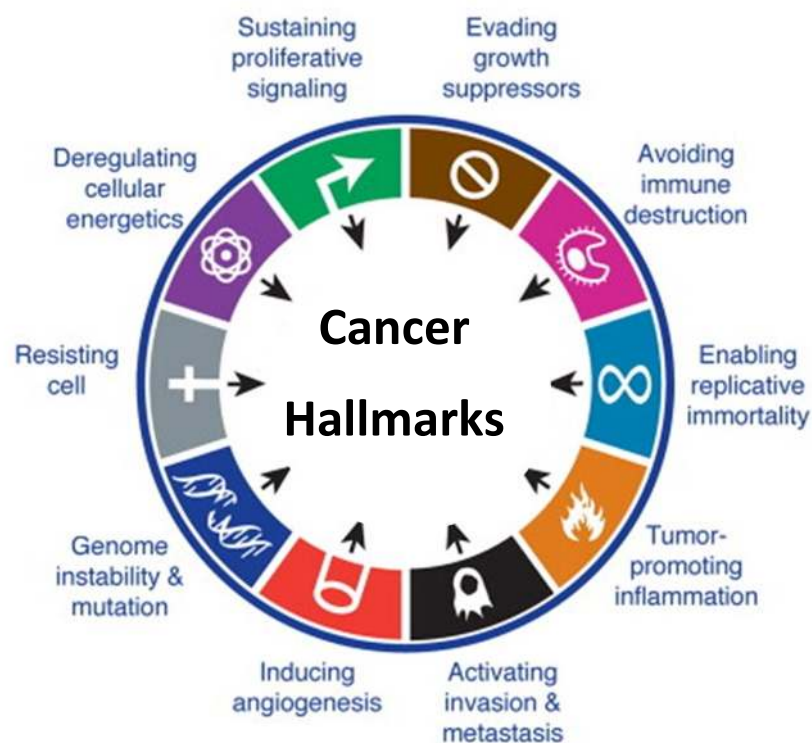
Figure 4. Ten emerging cancer hallmarks. There are ten characteristics and features that tightly link to cancer development. These capabilities allow cancer cells grow, survive, and disseminate to distant organs to form metastasis. *Reprinted with permission from Hanahan D, Weinberg RA. Hallmarks of cancer: the next generation. Cell 2011; 144:646-674.*

1.1.2.1 Sustaining proliferative signaling

Normal cells require growth factor signals to control cell growth and proliferation. Growth signaling is transmitted in a spatially regulated fashion from a cell to its neighboring cells, thereby controlling total cell numbers and maintaining architecture of the tissues. It is still unclear how normal cells control the release of mitogenic signals; however, multiple studies have emerged showing how cancer cells are involving in mitogenic signaling and using it to gain advantage in tumor growth. Interestingly, unlike normal cells, cancer cells can provide growth factor ligands themselves, and use them to promote growth by receiving the signal through binding to cell-surface receptors that usually contain tyrosine kinase domain. This activates a signal cascade, and can result in unstoppable proliferation (9, 10). Monoclonal antibody inhibitors and small molecular inhibitors have been designed to block epidermal growth factor receptor (EGFR), a receptor tyrosine kinase, through distinct mechanisms that target either the extracellular ligand binding domain or cytoplasmic side of receptor, respectively. Cetuximab and panitumumab are examples of monoclonal antibody inhibitors; Gefitinib and Erlotinib represent small molecular inhibitors. Both classes of drugs are wildly used in the clinic.

1.1.2.2 Resisting apoptosis

Programmed cell death (PCD), plays a key role in tissue development and homeostasis (11), but can also occur when cells experience irreparable DNA damage or receive certain extracellular factors from the innate immune response to viral infection (12). Apoptosis is a type of PCD that is attenuated in tumors, commonly driven by a loss of TP53 tumor suppressor function. Alternatively, cancer cells can avoid apoptosis by upregulating protein expression of anti-apoptotic regulators such as Bcl-2, or reducing

expression levels of pro-apoptotic factors such as Bax, Bim, and Puma. Potential strategies to target cells that evade the apoptosis machinery are to use BH3 mimetic and other small molecules (13-16). The BH3 is a conserved domain shared by pro-apoptotic proteins such as Bim. The putative BH-3 mimetic, a small peptide inhibitor that mimics the BH3 domain, can bind to Bcl-2 pro-survival family members and initiate apoptosis (13, 17). Studies of BH-3 mimetic, in particular ABT-737, showed a good clinical outcome through targeting Bcl-2, and thus inducing cell resensitization to apoptosis (16). However, optimization of therapy of BH3 treatment needs further study in the mechanism of BH3-mediated apoptosis (18).

1.1.2.3 Inducing angiogenesis

Nutrients and oxygen are crucial to maintain tissue homeostasis and cell functions. Like all cells, tumor cells rely on blood vessels to obtain sufficient amounts of nutrients and oxygen while eliminating waste products to meet the demands for energy and proliferation. In 1971, Dr. Judah Folkman proposed that solid tumors are dependent on de novo angiogenesis to increase the supply of blood and nutrients (19). Following his hypothesis, he, together with Dr. Bert Vallee, soon identified fibroblast growth factor (FGF) as the first angiogenic factor, and began to deliver drugs attempting to target angiogenesis (20-22). Later in the 1980s, two other well-known angiogenic factors, vascular endothelial growth factor (VEGF) and angiogenin, were identified by other teams that had been inspired by Folkman's work (23-25).

During tumor development, angiogenesis may be stimulated by hypoxia or activated by vascular endothelial growth factor-A (VEGF-A) that is produced by tumor cells. Interestingly, VEGF can be further induced by low oxygen levels. Therefore, VEGF

signaling can be regulated at different levels, depending on its end purposes. VEGF can also be induced by proangiogenic signals such as fibroblast growth factor (FGF) to increase new vessel formation. Surprisingly, many studies reported that angiogenesis can occur in early neoplasms or non-invasive lesions, confirming that adequate nutrients and oxygen are critical factors for incipient neoplasms growth and survival. The development of anti-angiogenesis therapy showed promising results in inhibiting growth by reducing capillary buds to outgrow and spread into tumor masses. Bevacizumab, a first-line drug to inhibit growth of blood vessels, has shown promising results to prolong overall survival and reduce disease progression in many cancers and metastatic diseases (26-28).

1.1.2.4 Enabling replicative immortality

Telomerase, a terminal transferase that adds telomere repeat sequence the ends of 3' telometric DNA, is expressed at a significant amount in immortalized cells such as cancer cells. Previous studies have shown that telomerases can protect the end of chromosomes, resulting in unlimited replicative potential and ultimately development into full-grown tumor (29). Telomerase functions to cause resistance to the induction of apoptosis and cellular senescence. In addition to cell senescence, some current studies show that telomerase is also involved in the regulation of cellular proliferation independent of its canonical function. This indicates that regulation of telomere maintenance and proliferation by telomerase are key requirement to fitness in terms of sustaining unlimited replicative potential and enabling replicative immortality. There are multiple inhibitors currently be developed for tackling telomerase, but they need further investigation in the field in order to translate into improved cancer prognoses (30).

1.1.2.5 Activating invasion and metastasis

Metastasis is the leading cause of cancer death, and it affects millions of cancer patients (31, 32). Major neoplastic diseases such as breast cancer, colon cancer and melanoma have high incidences of metastasis (33, 34). Metastasis is extremely complex and dynamic, and generally presents as the advanced stage of cancer. Despite the continuous advances of modern medicine in better controlling disease, the circumstance of metastases steadily increases (35). Successful establishment and initiation of metastases requires a sequential process: cell invasion, migration, intravasation, transportation through blood vessels, extravasation, and colonization at secondary organ site (36). Epithelial-mesenchymal transition (EMT) plays an important role in promoting metastatic dissemination, and regulating cell invasiveness and migration in epithelium-derived carcinoma (37, 38). Studies have shown that neoplastic cells that obtain invasive capability are able to transform cells into malignant cells. Pre-malignant cells that become invasive that are able to degrade the surrounding basement membrane (BM) through activating matrix degrading enzymes, extracellular matrix metalloproteases (MMPs), which reduce the barriers to migration, and dissemination and can ultimately result in a successful colonization (39).

Unfortunately, there is no standard approach for targeting metastatic cancer. When patients are diagnosed with symptomatic metastases, the disease is likely too advanced to be controlled by any current treatments. Clearly, earlier detection/diagnosis combined with more effective treatments could provide better clinical management of metastasis to enhance the quality of life and prolong survival of patients (40). c-Met receptor tyrosine kinase/Hepatocyte growth factor (HGF) pathway has been shown to be involved in cell

migration and growth control in cancer development (41, 42). Additionally, c-Met is upregulated in many types of cancers and regulates cellular motility, migration and metastasis (43, 44). In preclinical models, knockdown of MET expression resulted in a decrease in cell invasion and migration, as well as impairing tumor growth and metastases *in vivo*. In addition to genetic approaches, crizotinib, a small molecule inhibitor that was developed to inhibit c-Met receptor phosphorylation, has been shown to successfully inhibit invasion and metastasis (40, 45, 46). Therefore, c-Met may be a potential drug target for treating metastasis (43, 47, 48).

1.1.3 Overview of Cancer Metabolism

Altered metabolism is one of the hallmarks of cancer (7, 49). Cancer cells are dependent on reprogramming multiple metabolic pathways, including carbohydrate metabolism, lipid metabolism, amino acid metabolism, to provide both energy and chemical building blocks for growth and proliferation (49-52).

1.1.3.1 Warburg Effect and Glucose Metabolism

The concept of metabolic dysregulation in cancer cells was first brought to light approximately ninety years ago by a physician scientist, Dr. Otto Warburg (53, 54). In the 1920s, Dr. Otto Warburg found that tumor tissues have heavily increased glucose uptake and fermentation of glucose into lactic acid production, at the rate 10 times higher than normal tissues and even in the presence of oxygen; this observation is known as the Warburg effect (Figure 5) (55). In the 1950s, Warburg hypothesized that cancer cells have

an impaired capability for mitochondrial respiration, which results in unstoppable lactate production in the presence of oxygen (56). However, in fact, it was later reported that some cancer cells still maintain certain levels of oxidative phosphorylation (OXPHOS) and have a fully functioning mitochondria, even while displaying Warburg effect (57-61). Due to the phenomenon of an increase in glycolysis and lactate production while in the presence of oxygen, the Warburg effect is also named "aerobic glycolysis".

Why do cancer cells perform to aerobic glycolysis? Even today, the exact function of aerobic glycolysis is still controversial. Hypothetical explanations abound with one possible explanation being that cancer cells obtain a growth advantage through the Warburg effect (62, 63). They are six main functions of how the Warburg effect supports cell proliferation: 1) increases access to ATP by rapid ATP synthesis, 2) promotes flux into biosynthetic pathway, 3) enhances disruption of tissue architecture and tumor microenvironment, 4) allows for more reactive oxygen species (ROS) production, 5) modify chromatin structure, 6) alters immune function (Figure 6) (64).
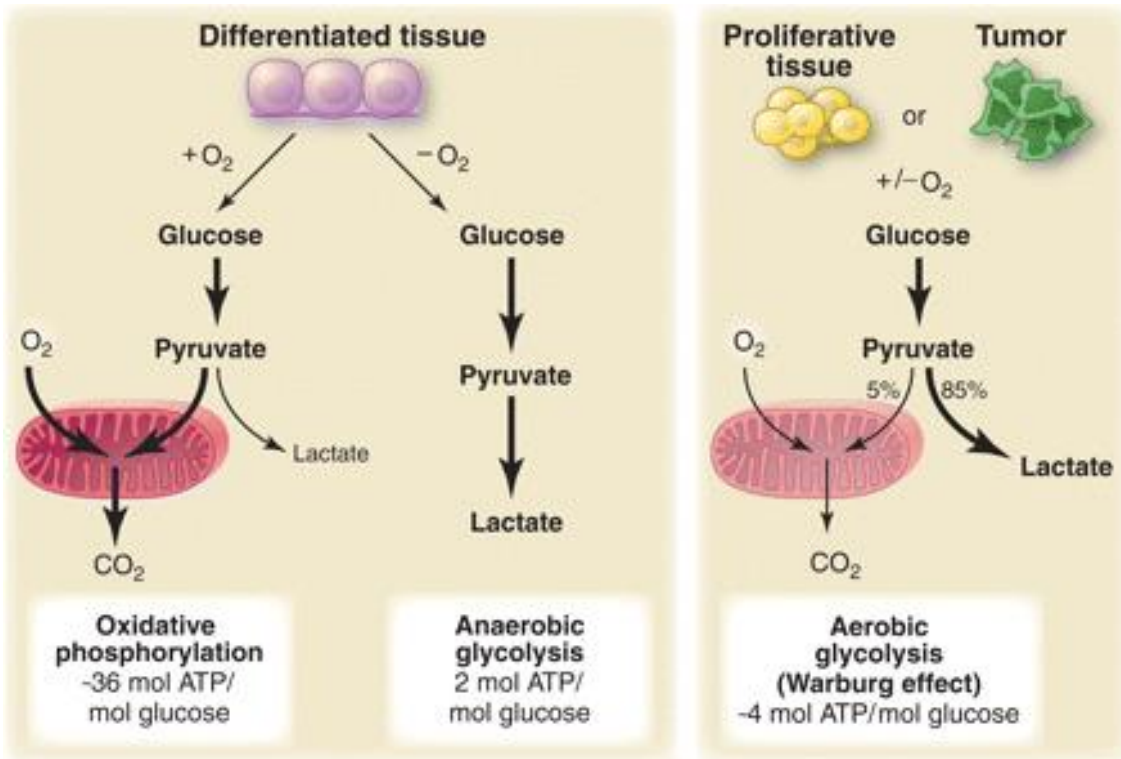
Figure 5. Comparison between aerobic glycolysis (Warburg effect), oxidative phosphorylation (OXPHOS), and anaerobic glycolysis. Schematic representation of the difference in ATP production and biological flux under OXPHOS, fermentation, and aerobic glycolysis**.** *Reprinted with permission from Vander Heiden MG, Cantley LC, Thompson CB. Understanding the Warburg effect: the metabolic requirements of cell proliferation. Science 2009; 324:1029-1033.*
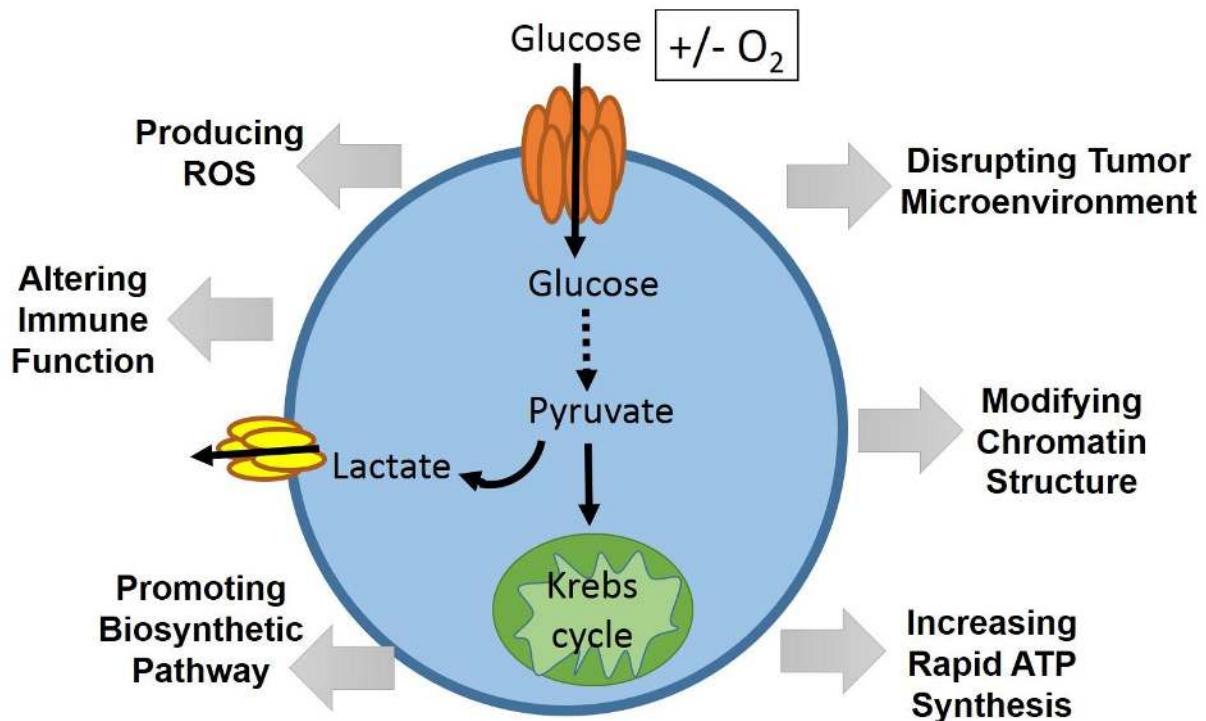
Figure 6. Six proposed functions of Warburg effect. Cancer cells increase glucose uptake and lactate production to support rapid glycolysis. There are six proposed purposes of Warburg effect that have been wildly reported. ROS, reactive oxygen species. *Modified and reprinted with permission from Liberti MV, Locasale JW. The Warburg Effect: How Does it Benefit Cancer Cells? Trends Biochem Sci 2016; 41:211-218.*

Interestingly, the process of aerobic glycolysis only produces two ATPs at a time, which means that it does not efficiently utilize glucose to maximize ATP production (62). Instead, it generates biosynthetic building blocks to support rapid proliferation (64, 66). Although the Warburg effect in cancer cells is a relatively an inefficient way to generate ATP compared to the amount that is generated through OXPHOS in normal cells, it has been reported that in cancer cells 1) the glucose metabolism rate is 10-100 times that of normal cells, and 2) the total amount of ATP production is higher in cancer cells in a given time period. Therefore, the phenomenon of Warburg effect in cancer cells may due to competition for limited glucose and other nutrient resources to support high-energy demand for ATP synthesis in tumor microenvironment (67, 68). Notably, in addition to higher ATP production rate, the Warburg effect has been proposed to utilize glucose as a carbon source for anabolic process such as generation of lipids, proteins, ketone bodies, steroids, and nucleotides to maintain the high flux supply and keep the *de novo* biosynthesis pathway active. For instance, glycolysis can feed into the serine biosynthesis pathway that mediates production of nucleotides for cell division (69, 70).

Interestingly, glucose metabolism also plays an important role to support T cell function and immune system. T cell activation requires a flux shift from OXPHOS into glycolysis via the regulation of mTOR pathway (71). Therefore, availability of glucose in tumor microenvironment may affect activity of tumor-infiltrating lymphocytes (TILs). Indeed, cancer cells can compete for the limited glucose with TILs in order to suppress the immune function in a living organism (72, 73). Rapid glycolysis in cancer cells could serve as a cell fitness mechanism to suppress T lymphocyte function and promote tumor growth. Moreover, lactate production allows cells to regenerate reducing equivalents of

NAD+, which recycles back into glycolysis and sustains active glycolysis (62, 65). Elevated aerobic glycolysis may result in a lower pH tumor microenvironment that affect tumor cells' capabilities and change the immune system. For example, a decrease in pH in tumors by higher lactate triggers local cancer cell invasion (74). In addition, recent studies showed that tumor-derived lactic acid may contribute to M2 tumor-associated macrophage formation (TAM) (75).

The Warburg effect may also cause an increase in generating reactive oxygen species (ROS) (76). Elevated glycolysis in cancer cells increases pentose phosphate pathway (PPP), leading to ROS production through NADPH oxidase (NOX). NOX is a critical enzyme to convert NADPH to ROS, which keeps active glycolysis by providing unlimited NADP+ (77). Maintaining the homoeostasis of superoxide is essential to keep mitochondria functions (78). Changes in redox potential contribute to oxidative stress that ultimately leads to damage in mitochondria and induces mutation of mitochondrial DNA (79-81). Multiple lines of studies have showed the link between mitochondrial dysfunction and cancer formation, implying that mutations in mitochondrial DNA (mtDNA) may result in mitochondrial dysfunction, thereby causing cancer initiation and progression (82). Taken together, these findings demonstrated the interplay between Warburg effect, ROS, and mitochondrial function in cancer. Both aerobic glycolysis and mitochondrial metabolism are essential for cell proliferation (64).

In addition to the Warburg effect, several studies have addressed the link between glucose metabolism and histone acetylation (83). Histone acetylation, a critical element of gene regulation, is usually catalyzed by histone acetyltransferase (HAT). The amount of acetyl-coA in cells determines the level of histone acetylation through HAT, which may

impact tumor growth (84). The enzyme ATP-citrate lyase is primarily responsible for determining the synthesis of acetyl-coA, which is a precursor of thousands of metabolites that connects multiple cell signaling pathways (85, 86). Furthermore, knockdown of ATP-citrate lyase decreased histone acetylation and changed global chromatin structure, thereby resulting in a reduction of expression of glucose-related enzymes (87). Additionally, acetyl-coA can serve as a substrate for protein lysine acetylation, which is a critical post-translational modification that affects enzymatic activity. Remarkably, almost every metabolic enzyme that catalyzes metabolic pathway can be acetylated (88). This implies that glucose metabolism has many effects on global epigenetic regulation, which in turn feeds back to regulate metabolism.

Metabolic rewiring in cancer cells can be tightly linked to alteration of tumor-associated genes. Tumor suppressor genes such as *p53* and oncogenes like *c-myc* and *HIF-1α* were found to directly cause cancer, as well as being involved in reprogramming cancer metabolism (89-95). Recently, many lines of evidence showed that mutations in metabolic enzymes such as isocitrate dehydrogenase (IDH), succinate dehydrogenase (SDH), pyruvate kinase 2 (PKM2), and fumarate hydratase (FH) are sufficient to induce cancer initiation and progression (52). Importantly, mutations are also found in enzymes that have direct functions in mitochondrial metabolism (57), which implies that not only tumor-associated genes, but also mitochondrial-related genes can have pleiotropic functions on cancer metabolism dysregulation and tumorigenesis.

One of the most famous metabolic genes that mediates carcinogenesis is embryonic isoform 2 of pyruvate kinase (PKM2). Cancer cells have been shown to express PKM2 to promote tumor growth by switching from mitochondrial oxidative

phosphorylation to glucose metabolism in order to generate ATP (96, 97). PKM2 expression is necessary to drive aerobic glycolysis and confer advantages on tumor growth. The regulation of PKM2 activity is tightly controlled by metabolic master regulators such as hypoxia-inducible factor 1 (HIF-1). PKM2 can both be activated by, and activate HIF. Under hypoxia, knockdown of PKM2 reduces transcription of HIF1-dependent target genes (96) and decreases glucose metabolism by inhibiting glycolytic gene expression in HeLa cells (98). However, PKM2 function in cells is controversial (85, 99), as some studies have shown that inhibition of PKM2 may support tumor growth (100, 101). These effects appear to be context-dependent and merit need further investigation. Interestingly, a PKM2 signature is also preserved in the failing human heart where decreases with mechanical unloading (102).

1.1.3.2 Building Cells with Glucose and Glutamine

It still remains elusive which comes first, alteration of cancer-associated genes or metabolism? In other words: are the oncometabolites always the cause or the consequence of increased cell proliferation? Due to the unique architecture of each tumor, it is always a "chicken and egg" situation. No matter which is the consequence or which is the cause, there is no doubt that cancer cells have common features of markedly utilizing glucose and glutamine as fuels to fulfill their demands for cell proliferation and survival. The catabolism of glucose and glutamine can generate pools of various carbon metabolites to use as building blocks to form thousands of macromolecules and maintain a complex metabolic network. In addition to the functions of glucose metabolism, glutamine uniquely provides nitrogen-containing intermediates for *de novo* nucleotide synthesis of purine and pyrimidine in cells (103-106). The increased glutamine uptake in

tumors was described by Dr. Harry Eagle, who found that HeLa cells consumed 10 times more glutamine than any other amino acid (107). Therefore, both glucose and glutamine are essential carbon sources for cancer cells (108). Furthermore, Craig Thompson and colleagues found that cancer cells can also use the hexosamine pathway to stimulate cell growth and rescue cells from cell death under glucose deprivation (109). The hexosamine biosynthesis leads to UDP-N-acetyl glucosamine (UDP-N-GlcNAc) synthesis and has been associated with posttranslational modification (PTM) via glycosylation. Under glucose deprivation, cells maintain hexosamine pathway which serves as a fuel signal to modulate growth factor receptor activity in a manner dependent on N-linked glycosylation. The activated hexosamine pathway sustains growth factor signaling, supports cell growth, and ultimately leads to stimulating glutamine uptake for cell growth and survival (109).

A major question is: under nutrient-limiting conditions, how do tumor cells differentiate between available nutrients and selectively uptake one over others? Many studies have shown that influx of nutrients into tumor cells is not only stimulated to supply bioenergetics needs, but also by extracellular growth factors. Sustaining proliferative signaling is a hallmark of cancer (7). Therefore, when tumor cells are in a nutrient-deprived situation, or the absence of growth factors, a compensatory signal can stimulate glucose transporter proteins (GLUTs) to traffic to the plasma membrane and activate glucose uptake (110-112). It is notable that hypoxic conditions can increase the rate of glucose uptake through activation of hypoxia-inducible factor 1 (HIF-1) (93, 113). Despite intensive studies to understand the mechanisms underlying specific metabolic alterations, it is now generally accepted that combinational therapy will be needed to tackle multiple targets of cancer metabolism due to the metabolic heterogeneity within tumors (114, 115).

1.1.4 Clonal Evolution and Tumor Heterogeneity

Cancer is also considered an evolutionary process of cell clone selection and expansion (116, 117); over time, a clone population arises with comprehensive advantages that out-compete other tumor subclones for the limited space and resources within tumors (118). This clonal evolution theory was originated proposed by Dr. Peter Nowell, who hypothesized that cancer evolve from a single cell, and tumor progression acquired a sequential selection of competitive subpopulations that contains various genetic mutations, resulting in tumor growth (Figure 7) (116). Somatic mutations, epigenetic dysregulation, cellular context and microenvironmental stress all contribute to different levels of positive selection of clones for fitness, which results in intratumor heterogeneity and interpatient heterogeneity (118, 119). Advances in genome-scale approaches, such as next-generation sequencing analyses (NGS), enable the timely monitoring of clonal dynamics and assess regional heterogeneity directly in tumors (120, 121). Recently, intratumor heterogeneity gained more attention because a patient can greatly benefit from genomic biomarker-guided therapy (122). Tumor heterogeneity explains the cellular complexity and dynamics that post challenges for current therapeutic strategies (123, 124). A full understanding of clonal evolution and dynamics of cell fitness may improve targeted therapy efficacy and may ultimately benefit personalized treatment medicine.
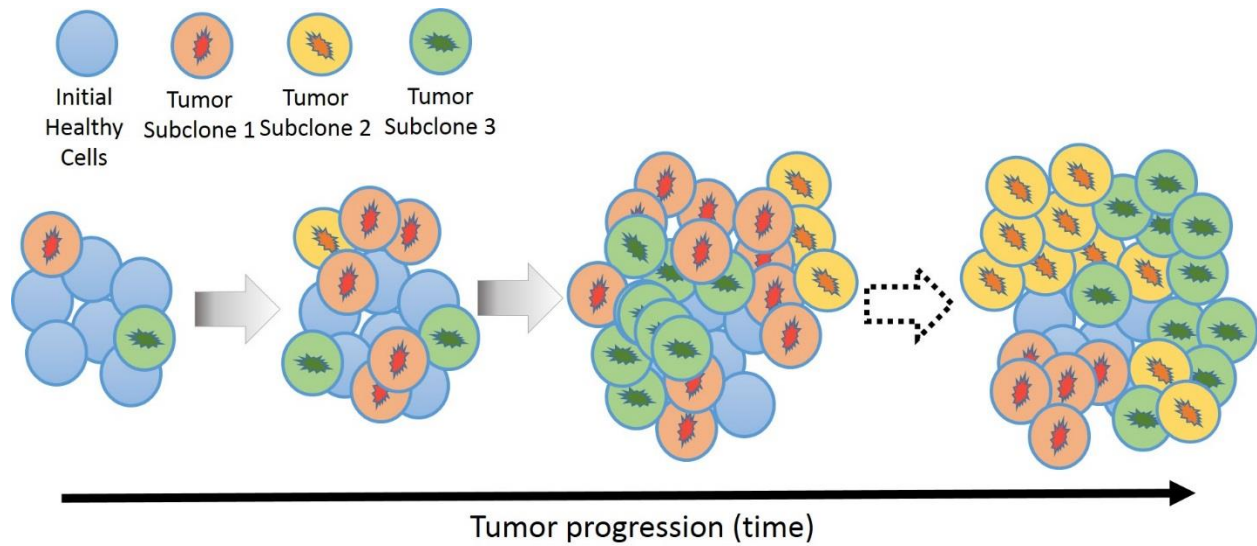
Figure 7. Schematic representation of tumor evolution. Cancer is a series processes of cell clone selection and expansion. As the tumor progresses, a sequential selection of competitive subpopulations with appearance of various morphological features. Somatic mutation is one of the proposed mechanism that contributes to intratumor phenotypic heterogeneity. *Modified and reprinted with permission from http://www.cs.carleton.edu/faculty/loesper/research.html.*

1.2 Breast cancer

1.2.1 Breast Cancer Facts and Statistics

After lung cancer, breast cancer is the most common cancer in women. According to the American Cancer Society, about 1 in 8 (12%) women in the United States will develop invasive breast cancer (IBC), and the chance that a woman will die from breast cancer is about 3% (1, 125-127). Moreover, breast cancer is also among the most common in female cancer survivors. In the United States, the annual estimation of newly diagnosed cases is about 236,660 for IBC cases; and 61,000 for ductal carcinoma *in situ* (DCIS) cases (128). Interestingly, 19% of breast cancer is diagnosed in women aged 30-49 years, meaning that it develops earlier than other cancers such as lung and colorectal cancer. Although the death rate from breast cancer has significantly declined since 1989, the 5-year overall survival rate of breast cancer patients rapidly decreases from 100% for stage I disease to 22% for stage IV disease. Thus, there are unmet needs for prevention and early intervention (Table 1).

1.2.2 Breast Cancer Initiation and Evolution

Breast cancer is a genetically heterogeneous disease that contains multiple distinct cells, which contributes to diverse histological characteristics and different clinical outcomes (129, 130). In a simplified scenario, many breast cancers develop through multiple linear steps from normal epithelium, to ductal hyperplasia (DH), to atypical ductal hyperplasia (ADH or atypia), to ductal carcinoma *in situ* (DCIS), to invasive (infiltrating) ductal carcinoma (IDC), and finally, to metastatic breast cancer (Figure 8) (131-134). During disease progression, cells accumulate both genetic and non-genetic alterations

(135). However, it has been reported that metastatic cells may not necessarily go through a general mechanism of tumor development, but instead disseminate at the early stages of primary tumor development and grow in parallel with primary tumors (136, 137). The parallel metastasis theory implies that certain high fitness tumor clones with specific capabilities can disseminate into distant organs to form metastasis independent from the primary tumor.
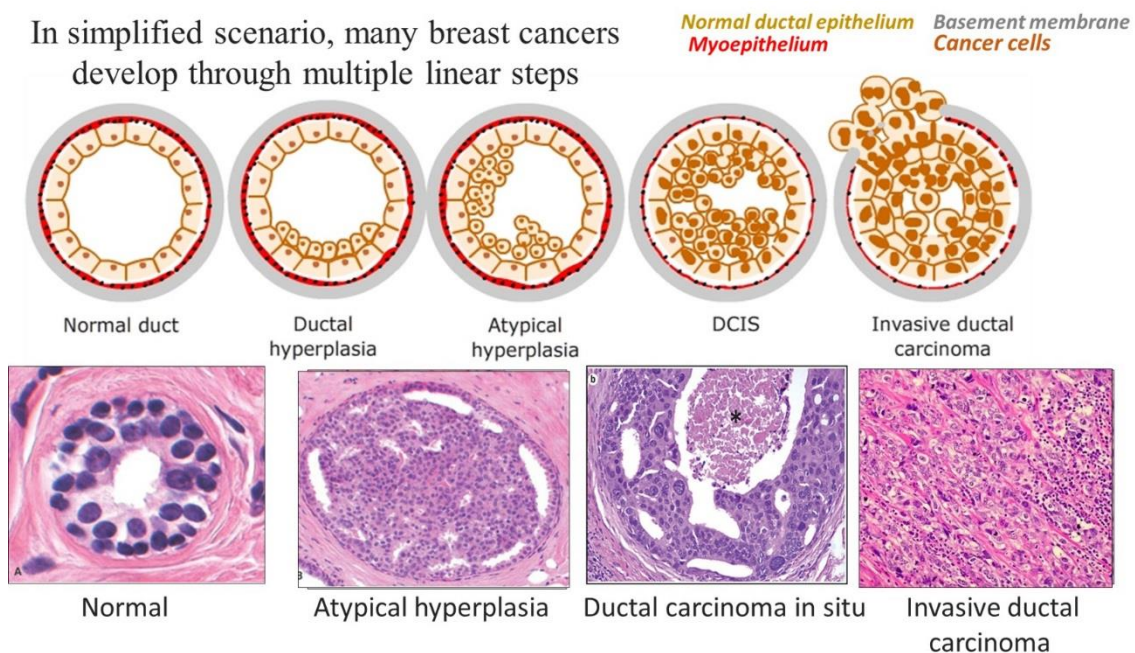
Figure 8. A linear progression model of ductal breast cancer development. In a simplified scenario, many breast cancers develop from normal epithelium, to pre-malignant cells (ductal hyperplasia, atypical ductal hyperplasia and ductal carcinoma *in situ*), and to invasive ductal carcinoma. The bottom panel of IHC revealed the morphological structure of each stage of breast cancer. *Modified and reprinted with permission from Moulis S, Sgroi DC. Re-evaluating early breast neoplasia. Breast Cancer Res 2008, 10: 302. And http://www.rnceus.com/dcis/sub.html.*

Stage	5-year survival rate	Symptom
0	100%	Stage 0 includes ductal hyperplasia (DH), atypical ductal hyperplasia (ADH or atypia), and ductal carcinoma *in situ* (DCIS). In DCIS, cancer cells are still within a duct and have not invaded deeper into the surrounding fatty breast tissue In all cases in stage 0, the cancer has not spread to lymph nodes or distant sites.
I	100%	The tumor is 2 cm or less across and has not no distant sites. The cancer hasn't spread to distant sites.
II	93%	The tumor is larger than 2 cm but less than 5 cm across. The cancer hasn't spread to distant sites.
III	72%	The tumor is any size and may or may not spread to lymph nodes. The cancer hasn't spread to distant sites.
IV	22%	The cancer can be any and may or may not have spread to nearby lymph nodes. It has spread to distant organs or to lymph nodes far from the breast. The most common sites of spread are the bones, liver, brain, or lungs.

Table 1. Staging of breast cancer and 5-year survival rate. Breast cancer is staged base on pathologic features *Table was modified and reprinted with permission from American cancer society. http://www.cancer.org/cancer/breastcancer/detailedguide/breast-cancer-staging.*

Despite different routes of evolution and progression that breast cancer cells may take, there are stringent histopathological features that define the neoplastic stages and invasive stages of breast cancer (Figure 8). A normal breast duct contains a basement membrane and a bilayer of epithelial cells, in which luminal epithelial cells are surrounded by myoepithelial cells (130). In the DH and ADH pre-malignant breast diseases, the lumen is filled with non-invasive cells, which are considered as the precursor stage of DCIS. In DCIS lesions, proliferating cells are still confined within the basement membrane, showing no invasion into neighboring stroma cells and heterogeneously expressing basal cytokeratin markers (138). IDC may arise from DCIS (139), and the transition from DCIS to IDC is a critical trait of breast cancer progression. Loss of myoepithelial cells and basement membrane are characterized as the features of invasive breast cancer, in which cancer cells invade into the surrounding tissues and ultimately circulate to distant organs and forms metastases.

1.2.3 Risk, Early Detection and Intervention

Breast cancers initiate and develop through a series of stages of genetic and non-genetic alteration. To reduce breast cancer death, it is critical to develop early prevention and detection approaches to interfere with breast cancer development at early stages. This requires better understanding mechanism of the critical mediators, driving early lesions (atypia) to progress to cancer and developing new interventions based on the understanding.

Based upon (1) molecular characteristics, (2) histological/clinical features of hormone receptor status of the human epidermal growth factor receptor 2 (HER2), estrogen receptor (ER), and progesterone receptor (PR), breast cancer can be grouped into different subtypes (Figure 9) (140-143). Current clinical treatment for breast cancer patients is dependent upon hormone receptor status. The basal-like/triple-negative (ER-, PR-, HER2-) BRAC1 mutation group has the worst prognosis and poor clinical outcome (144).
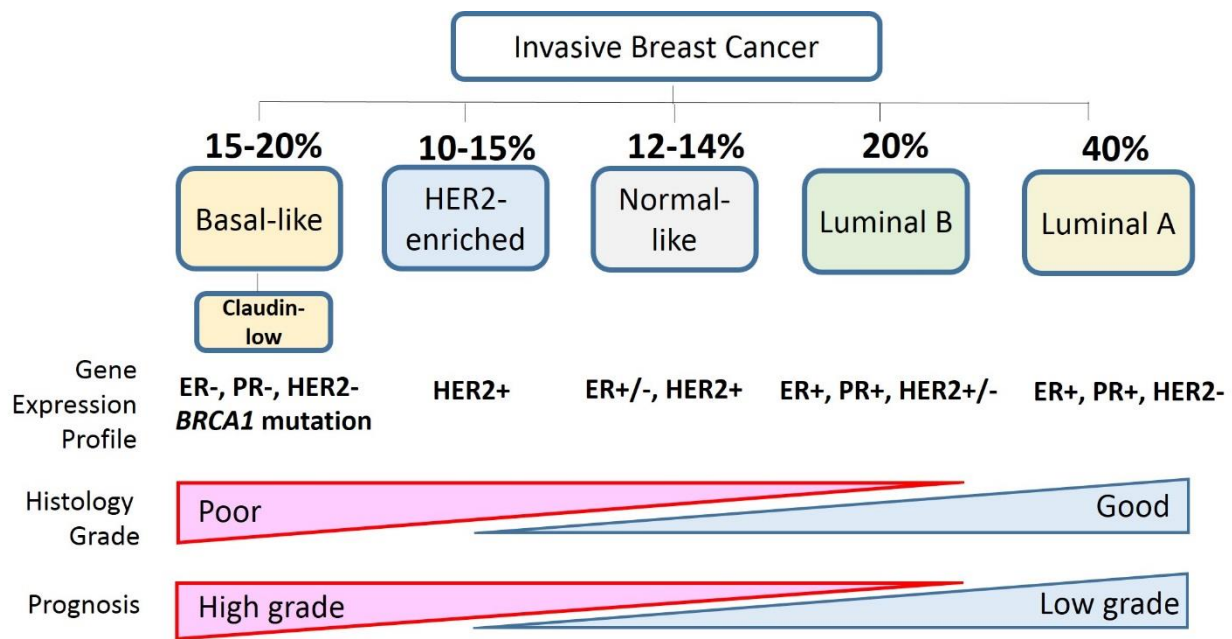
Figure 9. Breast cancer subtypes. Based on gene expression profiles and clinical features, invasive breast cancer can be categorized into different subtypes include basal-like, Her-2 enriched, luminal A, luminal B and normal-like breast cancer (140-143). *Modified and reprinted with permission from McMaster Pathophysiology Review.*

Because of the improvement in early detection and treatment, the overall 5-year relative cancer survival rate has greatly improved in breast cancer patients. Early detection has been aided by such advances such as mammography; the early interventions such as hormone therapy, chemotherapy, and targeted therapy have shown high efficacy in reducing breast cancer risk and continuously increasing the numbers of cancer survivors (2). Ultimately, the most effective way to reduce breast cancer mortality is prevention of early disease; however, progress in breast cancer prevention has been extremely limited with no true prevention options available at this time. Thus, there is an urgent need to identify the molecular alterations driving the initiation of breast cancer in order to rapidly test and develop targeted prevention strategies. Historically, progress has been limited by the inability to serially sample mammary cells from women who have pre-malignant breast disease and prospectively test for predictors of cancer initiation and progression. Currently, there is a lack of biomarkers which would facilitate an early diagnosis. Therefore, it is important to find out the mechanism of cancer initiation and develop effective prevention strategies to win the battle with cancer.

1.3 14-3-3 Proteins

1.3.1 Overview of 14-3-3 proteins, structure, and functions

The 14-3-3 proteins are a family of evolutionarily conserved molecules that are encoded by separate genes and expressed across all kinds of eukaryotic cells (145).The 14-3-3 proteins are abundant in brain and neurons, and were originally described back in 1967 by Dr. Moore and Dr. Perez (146). There are seven 14-3-3 isoforms in mammals:

β, γ, η, ζ, ε, σ, τ, and θ, which typically form homo and hetero-dimers with other isoforms to influence numerous signaling transduction events including the regulation of cell cycle, transcription, ion channels, intracellular trafficking, cytoskeleton rearrangement and apoptosis in cells (147-149).

Through peptide library analyses, it was shown that proteins containing the consensus motifs, RSXpSXP or RXXXpSXP can be recognized by and directly interact with 14-3-3 proteins (150-152). Although 14-3-3 primarily binds to ligands with a phosphorylated motif, several experts have shown that there are some interactions between 14-3-3 and non-phosphorylated ligands as well (146, 152); these interactions can even show high affinity similar to those with phosphorylated proteins. However, most of the interactions between 14-3-3 and non-phosphorylated ligands can be out-competed and inhibited by phosphorylated ligands, leading to the notion 14-3-3 responds efficiently to signal transduction via heightened binding affinity to phosphorylated ligands. Besides targeting phosphorylated protein motifs, 14-3-3 proteins can be phosphorylated by kinases, which affect their ability to bind to target partners. Thus, many 14-3-3 cellular signaling cascades are tightly regulated by protein phosphorylation.

Dimerized 14-3-3 is the predominant form to orchestrate signal transduction and cellular processes in cells (151). Crystal structures of 14-3-3 dimer have revealed that the 14-3-3 protein can interact with two ligands concurrently with one ligand serving as a gatekeeper (Figure 10). Once the gatekeeper site is phosphorylated and binds to one of the monomers of the 14-3-3 dimer, it accelerates the secondary interaction between

another ligand and the second monomer (146, 147), thereby modulating protein function and subcellular localization. For example, Raf-1 has multiple 14-3-3 recognition motifs, and 14-3-3 dimer may bind to both affinity sites and induce a structural changes of Raf-1, thereby regulating its activity. The binding of 14-3-3 dimer may also change the subcellular localization of a target protein by interfering with the nuclear localization sequence (NLS) on the target protein (153). The major proportion of 14-3-3 proteins are located in the cytoplasm; thus they might serve as cytoplasmic anchors that inhibit 14-3-3 binding proteins from being translocated into the nucleus or promote the 14-3-3-bound complex exporting from the nucleus into the cytoplasm. The impact of 14-3-3-mediated subcellular localization of binding proteins could enormous to cellular functions and signal transduction cascades. For example, in neoplastic cells, 14-3-3 promotes YAP-1 cytoplasmic localization via binding and retaining YAP-1 in the cytoplasm, thereby inhibiting YAP-1-mediated gene expression. (154).
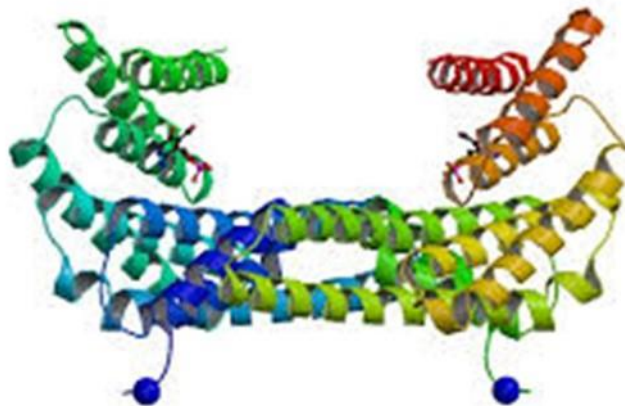
Figure 10. Crystal structure of dimerized 14-3-3 protein. Dimerized of 14-3-3 is critical for 14-3-3 function and activation. Software Pymol is used to make figure. PDB: 4E2E.

1.3.2 Role of 14-3-3 proteins in Cancer

Dimerized 14-3-3 binds to many partners that drive diverse functions and control cell checkpoints. Accordingly, the biological functions of 14-3-3 are thought to highly be dependent on their binding proteins. In support of this notion, many studies have emerged in dissecting 14-3-3 binding partners (155, 156). Dr. Feng and colleagues showed by quantitative immunoprecipitation (IP) combined with a knockdown method (QUICK), more than 200 novel 14-3-3ζ binding substrates in multiple myeloma cells (155). Interestingly, this list included several metabolism-related pathways which had not been previously linked to 14-3-3 proteins. Their results strongly suggested that 14-3-3 participates in many of the networks in cell signaling pathways which may include cancer metabolism.

Over the past two decades, 14-3-3 has gained the attention from the field due to its position at the center of signaling transduction. 14-3-3 proteins have hundreds of binding partners, which are involved in cell cycle control, nucleic acid synthesis and processing, cellular organization, storage and transportation, energy and metabolism, cellular communication, and signal transduction. Each individual isoform has distinct functions in cancer. For example, 14-3-3σ serves as tumor a suppressor. In contrast to 14-3-3σ, 14-3-3ζ is a ubiquitously expressed family member that has been implicated to have oncogenic potential through its interactions and involvement in cancer initiation and progression. Through TCGA dataset (RNAseq) analyses, 14-3-3ζ (YWHAZ) overexpression has been observed across different cancer types (Figure 11). Interestingly, only a few mutations were found in 14-3-3ζ protein (Figure 11). However, 14-3-3ζ (YWHAZ) overexpression was observed in > 40% of breast cancer and neuroendocrine prostate cancer, and part of overexpression was contributed by gene

amplification (Figure 12). Additionally, 14-3-3ζ (YWHAZ) overexpression occurs in > 10% tumors in more than fifteen different cancers.
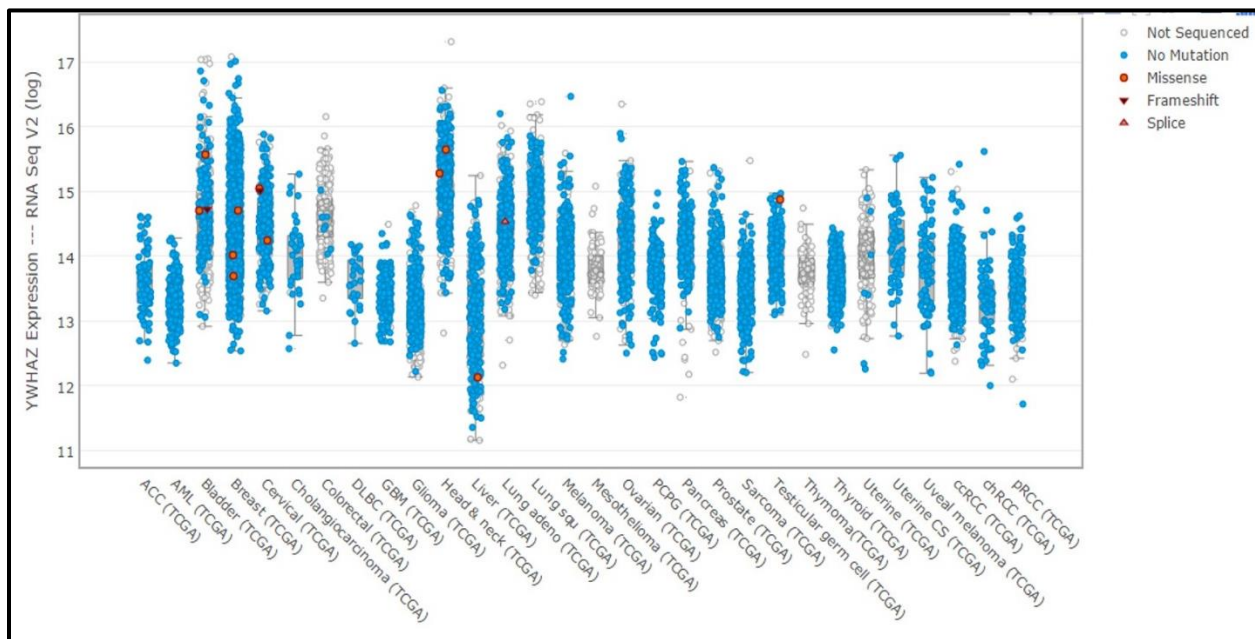
Figure 11. 14-3-3ζ (YWHAZ) overexpression across different cancer types. 14-3-3ζ overexpression has been observed across different cancer types. TCGA Data eBioPortal (http://www.cbioportal.org/) is the tool for data analysis. Each dot represents a patient sample. Blue dot: no mutation; red dot: missense: black triangle: frameshift; red triangle splicing; grey dot: not sequenced.
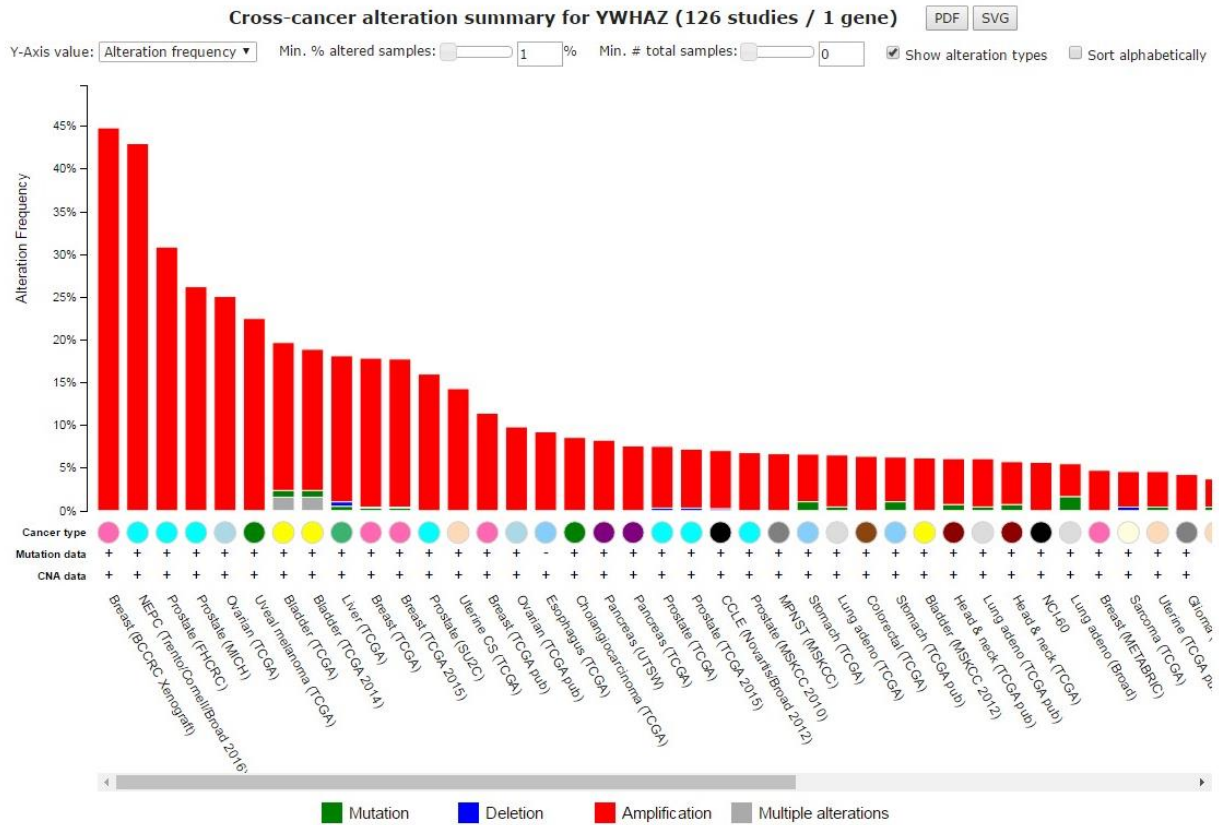
Figure 12. Alteration frequency of 14-3-3ζ (YWHAZ) across different cancer types.
The most frequent alteration for 14-3-3ζ overexpression is gene amplification which has been observed in 126 patients across different cancer types. Data analysis is using TCGA Data eBioPortal (http://www.cbioportal.org/). Red columns indicate gene amplification; green columns indicate gene mutation; blue columns indicate gene deletion; grey columns indicate multiple alterations.

1.3.2.1 14-3-3ζ and Cancer

14-3-3ζ belongs to the highly conserved 14-3-3 protein family and modulates numerous pathways in cancer (157). A heritable increase in 14-3-3ζ expression in cancer is associated with a poor prognosis and disease recurrence (158). As I discussed in the following chapters, in pre-malignant cells, 14-3-3ζ overexpression induces glycolysis through upregulation of LDHA (159), binds to metabolic proteins, which include fructose-2,6,-bisphosphate kinase promoting metabolic functions (160), leads to Akt phosphorylation by activation of the PI3K pathway (161), destabilizes the p53/Smads complex by binding to YAP-1 (154), and triggers epithelial-to-mesenchymal transition, which may increase the transition of ductal carcinoma in situ (DCIS) to invasive breast cancer (162). In cancers, 14-3-3ζ overexpression enhances MAPK/c-Jun signaling (163) and regulates tumor immune response by modulation of expression of multiple cytokines (164, 165). Interestingly, quite a number of 14-3-3ζ-mediated cellular networks appear reported to be involved in cancer metabolism and cell competition, such as the Hippo pathway, the JNK pathway and the PI3K-Akt pathway (166). Moreover, 14-3-3ζ has distinct functions in regulating treatment resistance. Knockdown of 14-3-3ζ sensitizes cells to UV-induced apoptosis, which is mediated by the JNK/p38 signaling (145). Taken together, cancer cells with high 14-3-3ζ expression tend to promote cancer initiation and progression.

1.4 Gap in Knowledge and Hypothesis

After cardiovascular diseases, cancer is the second leading cause of death in the United States (1). Growing tumor cells must find alternative metabolic mechanisms to

take advantage of the limited nutrient resources provided by the body. Metabolic dysregulation has been recognized as a distinct hallmark of tumorigenesis and cancer progression.

14-3-3ζ binds to and regulates phosphorylated proteins involved in numerous important cellular processes, including those essential for metabolic regulation, signaling transduction, and apoptosis. 14-3-3ζ overexpression is known to occur at the early neoplastic stage (ADH and DCIS) of breast disease and is found in >40% of invasive breast cancer patients. Remarkably, 14-3-3ζ overexpression persists throughout breast cancer progression (167).

Additionally, as many reports showed that metabolic alteration is an early event in pre-malignant cells, I hypothesized that 14-3-3ζ overexpression in neoplastic cells may rewire metabolism and induce cancer initiation. In this dissertation, I therefore sought to investigate the role of 14-3-3ζ in metabolic alterations that may impact breast cancer initiation and progression **(Chapter 2)**. Meanwhile, many lines of evidence exists reporting that cancer cells always grow in environments with limited nutrient resources and must compete fiercely to win the race of tumor formation and progression (116-118). Pathological gain of 14-3-3ζ function may confer advantages on cancer progressing in a heterogeneous tumor environment with individual cancer cells competing for limited resources. The level of 14-3-3ζ may determine the outcome of the competitive race for nutrients in primary tumor formation and progression. Therefore, I hypothesized that 14-3-3ζ is a critical molecular mediator to secure limited nutrient resources among heterogeneous tumor cell populations. Consequently, I investigated the pathological function of 14-3-3ζ in breast cancer progression *in vivo* in **Chapter 3**.

Effective breast cancer prevention cannot be accomplished without combining knowledge from multiple disciplines. Metabolic alteration and tumor heterogeneity are two distinct cancer hallmarks, and 14-3-3ζ seems to be a key regulator directly involved in these two hallmarks. By comprehensively examining the characteristics of 14-3-3ζ in both preclinical models and clinical human samples, the results I obtained will lead to the discovery of new and better biomarkers for prognostic values and will further guide us to develop a novel therapeutic strategy for breast cancer that overexpresses 14-3-3ζ.

Chapter 2

14-3-3ζ–MEDIATED LDHA UPREGULATION FACILIATES BREAST CANCER INITIATION AND PROGRESSION

Notes

- *This chapter is based upon "Chia-Chi Chang, Chenyu Zhang, Qingling Zhang, Ozgur Sahin, Hai Wang, Jia Xu, Yi Xiao, Jian Zhang, Sumaiyah K. Rehman, Ping Li, Mien-Chie Hung, Fariba Behbod, Dihua Yu, Upregulation of lactate dehydrogenase a by 14-3-3ζ leads to increased glycolysis critical for breast cancer initiation and progression. Oncotarget, 2016, Vol. 7, No. 23, 25370-25383".*

- *Permission of the copyright by publisher of Oncotarget: Oncotarget applies the Creative Commons Attribution License 3.0 (CCAL, https://creativecommons.org/licenses/by/3.0/) to all works we publish (read the human-readable summary or the full license legal code). Under the CCAL, authors retain ownership of the copyright for their article, but authors allow anyone to download, reuse, reprint, modify, distribute, and/or copy articles in Oncotarget journal, so long as the original authors and source are cited. <u>No permission is required from the authors or the publishers</u>. PII: 9136. In most cases, appropriate attribution can be provided by simply citing the original article. If the item you plan to reuse is not part of a published article (e.g., a featured issue image), then please indicate the originator of the work, and the volume, issue, and date of the journal in which the item appeared. For any reuse or redistribution of a work, you must also make clear the license terms under which the work was published. This broad license was developed to facilitate open access to, and free use of, original works of all types. Applying this standard license to your own work will ensure your right to make your work freely and openly available.*

2.1 Introduction

2.1.1 Metabolic dysregulation and cancer initiation

Breast cancers initiate and develop through a series of stages from normal cells to ductal hyperplasia (DH), to atypical ductal hyperplasia (ADH), to ductal carcinoma *in situ* (DCIS), to invasive (infiltrating) ductal carcinoma (IDC), and finally, to metastatic breast cancers (131). About 20% of the breast cancer patients present ADH and/or DCIS early-stage breast disease in the clinic (158). Although advances in targeted therapies have shown efficacy to increase breast cancer survival rates (168), a better understanding of mechanisms underlying cancer initiation will allow us to improve early detection and intervention, which may further lead to a reduction of mortality from breast cancer.

Breast cancer initiation and progression involve cascades of genetic and non-genetic alterations, including metabolic perturbation (51, 169, 170). Recently, multiple lines of evidence have reported that metabolic reprogramming may occur at an early stage of neoplasia and contribute to cancer initiation and malignant transformation (103, 171, 172). The Warburg effect is a phenomenon of an increase in glycolysis and lactate production while in the presence of oxygen, which promotes flux into the biosynthetic pathway to support cell proliferation (62). By examination of blood flow entering and leaving tumor lesions, Dr. Otto Warburg made the seminal discovery that cancer cells mainly exhibit a high rate of glycolysis. Major regulators of the Warburg effect include tumor suppressor genes, such as *p53* and oncogenes like *c-MYC* and *HIF-1α* (173), which were found to directly cause cancer, as well as being involved in rewiring cancer

metabolism. These genes are critical because they can have pleiotropic functions on cancer metabolism alteration and tumorigenesis. However, it still remains elusive what other mediators may involve in mediating aerobic glycolysis at the early-stage of breast cancer.

2.1.2 The role of LDHA in cancer metabolism

Lactate dehydrogenase A (LDHA) is a critical enzyme that metabolizes the final step of glycolysis to generate lactate and provide enough NAD+ to support rapid proliferation of cancer cells (174, 175). Interestingly, lactate can be further used as a fuel for mitochondria functions and biosynthesis pathway in cancer cells (176). Elevated levels of LDHA are a cancer hallmark that is tightly associated with poor prognosis and critically involved in the tumor progression (177-180). LDHA has been reported as a key enzyme for highly glycolytic phenotype in many types of cancer (174, 181) and has gradually been considered as a high-priority target for cancer drug therapy. Several LDHA inhibitors have been developed (181), and Gossypol (AT-101) is one of the noncompetitive inhibitors binding to the lactate dehydrogenase isoenzyme that is being tested in multiple clinical trials (181-183). Selective LDHA inhibitor FX-11 can suppress the enzymatic function *in vivo* that blocks the conversion of pyruvate to lactate (184) and inhibits tumor growth both *in vitro* and *in vivo* (175). These inhibitors are promising to target LDHA; a further mechanistic understanding of the interplay between glucose metabolism and tumorigenesis can lead to optimize the efficacy of these agents in cancer treatment.

2.1.3 14-3-3ζ and cancer metabolism

14-3-3ζ is a key protein that critically involves in numerous signal transduction and tumorigenesis (154, 185). In the past two decades, multiple high-throughput proteomic screenings have identified that 14-3-3ζ-targeted partners massively participate in various biological function, especially in the modulation of cellular metabolism (155, 186-190). These potential binding targets including enzymes that are in the center of glycolysis such as pyruvate kinase (PK), glyceraldehyde-3-phosphate dehydrogenase (GADPH) and 6-phosphofructo-2-kinase (PFK-2) (191). AMP-activated protein kinase (AMPK), a master sensor in metabolic checkpoint, responds to cellular energy stress and mediates homeostasis. In cancer cells, 14-3-3ζ physically interacts with phosphorylated liver kinase B1 (LKB1, or STK11) (192) and suppresses binding and activation of its substrate AMPK, suggesting that 14-3-3ζ could be an important mediator of cellular metabolism.

2.1.4 Hypothesis

14-3-3ζ overexpression is an early event in human breast cancer, taking place as early as during the atypical ductal hyperplasia (ADH) (158, 167). Recent evidence suggests that metabolic alternation may occur at an early stage of neoplasia and contribute to cancer metabolic transformation (103, 171). Given the known roles that 14-3-3ζ mediates numerous mechanisms in the early stage of breast epithelial cells and its probable involvement in metabolic alteration, I therefore **<u>hypothesized</u>** that pathological

14-3-3ζ overexpression in breast epithelial cells may trigger metabolism rewiring and contribute to the initiation of cancer.

Briefly, in **this chapter**, I examined gene expression profiling data on three datasets: 1) a microarray dataset (GSE16873) generated from histologically normal epithelia, 2) RNAseq-derived Cancer Genome Atlas (TCGA), and 3) the microarray-derived breast cancer dataset GSE2109 (193, 194). The bioinformatic analysis revealed that the expression of 14-3-3ζ is positively correlated with a number of genes in the glycolysis pathway, especially LDHA. Therefore, I sought to determine whether 14-3-3ζ modulates cellular glycolysis and metabolic flux in breast cancer. I identified a direct mechanistic link between 14-3-3ζ overexpression and LDHA upregulation, and showed that 14-3-3ζ-mediated LDHA upregulation is critical to early transformation of human mammary epithelial cells (hMECs). These data provide a direct evidence that 14-3-3ζ overexpression in early-stage breast cancer contributes to the metabolic dysregulation of breast epithelial cells. Importantly, I also demonstrate that targeting 14-3-3ζ could be an efficacious strategy for clinical intervention of early-stage breast cancer for the prevention of further disease progression.

2.2 Materials and Methods

2.2.1 Cell lines and cell culture

MCF10A and MCF12A cells were obtained from American type cell collection (ATCC) and were maintained in human mammary epithelial cells (hMECs) medium (154). MCF10DCIS.COM cells, provided by Dr. Fariba Behbod (195), were maintained in DMEM/F-12 media (#DFL13-500, Caisson,USA) supplemented with 5% horse serum (Gibco). All cell lines were authenticated and validated by MD Anderson Cancer Center's Characterized Cell Line Core.

2.2.2 Plasmids and shRNAs

MCF10A, MCF12A and MCF10DCIS.COM cell lines were transfected with pcDNA3-HA-14-3-3ζ or pcDNA3 empty vector (Thermo Fisher Scientific, USA), which were constructed by Lu et al. (162), and selected with neomycin for 14-3-3ζ-overexpressing sublines. 14-3-3ζ shRNA (clone, NM_003406.2-418s1c1) and LDHA shRNA (NM_005566) were used to make 14-3-3ζ and LDHA knockdown cell lines.

2.2.3. Bioinformatics

Glycolysis-related genes were extracted from the Gene Ontology database under the term "glycolytic process" (accession #GO: 0006096). The corresponding patient-derived gene expression values were retrieved from the Gene Expression Omnibus data

repository microarray datasets for early-stage breast neoplasia (GSE16873) and advanced breast cancers (GSE2109), as well as the The Cancer Genome Atlas (TCGA) breast cancer datasets (http://cancergenome.nih.gov/). The clustering analysis of gene expression and heatmap visualization of the correlation matrix were performed in the corrplot package (v0.73) on the statistical computation software R (v3.1.2, https://www.r-project.org/). Breast cancer patient-derived gene expression dataset GSE3494 had clinical follow-up information and was used to investigate the relationship between 14-3-3ζ and/or LDHA expression and patient prognosis. Patients were stratified as having either "low" or "high" expression of the gene by median expression values of 14-3-3ζ and LDHA in the data cohort, respectively. Patients with "low" or "high" expression of both 14-3-3ζ and LDHA genes were further extracted to investigate whether there is synergistic predictive effect to combine the two biomarkers together. The Kaplan-Meier plots and survival analysis of breast cancer patients (GSE3494) were performed using R package survival (v2.38).

2.2.4 Real-time PCR analyses

Total RNA was extracted with Trizol reagent (Thermo Fisher Scientific) following manufacturer's protocol. *LDHA, CREB, MYC* mRNA expression were determined by the qRT-PCR using TaqMan primers (Hs00855332_g1, Hs00231713_m1 and Hs00153408_m1) and normalized to 18S rRNA endogenous control (#4310893E).

2.2.5 Metabolic assays

For glucose uptake assays, cells ($2x10^5$) were plated in 6-well plate with DMEM /F12 media (#DFL13-500, Caisson,USA) supplemented 10% fetal bovine serum (Gibco) with for 24 hours before starting experiments. Then cells were replaced with DMEM/F-12 media for 3 hours in order to cause a starving condition before 2-deoxy-D-glucose-[1,2-^{3}H(N)] (Moravek Biochemicals) was added in. The stock of 2-deoxy-D-glucose-[1,2-^{3}H(N)] contains tritium with specific activity for 1 millicurie. 1µl 2-deoxy-D-glucose-[1,2-3H(N)] was added into 6-well plate for 1 hour. Therefore, each experiment contains 1 microcurie trillium signal. The cells were then trypsinized, and tritium signal was measured by liquid scintillation counting. For lactate production assay, cells were plated for 24 hours, followed by fresh-medium incubation for 1 hour. Lactate production was measured according to the manufacturer's instructions (BioVision Inc). For oxygen consumption assays, cells ($2x10^5$) were plated in a 96-well oxygen biosensor system (BD Biosciences) covered with mineral oil to prevent oxygen leakage. according to the manufacturer's instructions (196). The signals (Ex/Em: 485/630 nm) were read using a Synergy 2 microplate reader (BioTek, Winooski) immediately after cell plating (baseline) and 1 hour after plating. The oxygen consumption rate was calculated and normalized to baseline. The overall cellular glycolytic activity was evaluated as previously described by Xu et al. (197).

2.2.6 Soft agar colony formation assay

Colony formation assay was analyzed by plating 0.5% top agar (BD, New Jersey) that contained cells ($2x10^5$) with medium into 6-well plates coated with 1% agar. Cells

were maintained with the addition of fresh medium twice weekly. The average culture timing depends on the tumorigenicity of the cells which is typically three to five weeks. The cells were then stained with 0.005% crystal violet, and the cell colonies were counted manually. This assay was further adopted and analyzed by the methods previously described by Danes et al (167).

2.2.7 Luciferase reporter assay

The LDHA promoter fragments were amplified from a bacterial artificial chromosome (#RP11-107C21) and cloned into a pGL3-basic vector (Promega). The promoter constructs were co-transfected with a *Renilla* luciferase control reporter vector into cells using the Amaxa HMEC Nucleofector kit, program T-24 (Lonza). Bioluminescence activity was assessed by methods previously described (154). The primers for different fragments are listed as following.

Fragment	Forward primer sequence	Reverse primer sequence
-2000 to +272	5'GTTCTGCCTAAGAAGCCTG AAGCTGTG	5'GTCAGCATAGCTGTTCCACT TAA
-2000 to -1	5'GTTCTGCCTAAGAAGCCTG AAGCTGTG	5' TGCTCCACGTGCGCTGGG
-500 to -1	5'GCAGAATAAAATGTACATTT GAACTGAGTCACC	5' TGCTCCACGTGCGCTGGG

+1 to +272	5'AGCAGCGTCGAGTTTTGGA GGTCA	5'GTCAGCATAGCTGTTCCACT TAA
+1 to +85	5'AGCAGCGTCGAGTTTTGGA GGTCA	5'GTGGGTTCCCGCACGTCCG
+1 to +33	5'AGCAGCGTCGAGTTTTGGA GGTCA	5'CCCGGGCCTCTCCAGTGC
+85 to +150	5'TCACACGTGGGTTCCCGC	5' TTAAGTGGAACAGCTATG

2.2.8 Chromatin Immunoprecipitation (ChIP) Assay

ChIP assays were performed following previously described methods (198). Immunoprecipitation antibodies: phospho-CREB and IgG antibodies (#9198 and #2729, Cell Signaling). Primers for qPCR: Fwd 5'-TGGCTCGGCATCCAC-3' and Rev 5'-CTGCAGCACTCTGAGCTG-3'.

2.2.9 siRNAs and chemical inhibitors

siRNA negative control #1 and siRNAs were purchased from Sigma for CREB(SAS1-Hs01_00116985), MYC (SAS1-Hs01_00215897), ATF1 (SAS1-Hs02_00313621), USF1(SAS1-Hs01_00185068), and SP1 (SAS1-Hs01_00070994) knockdown *in vitro*. Cells were transfected with siRNAs using Pepmute siRNA Transfection Reagent (SignaGen Laboratories) according to manufacturer's protocol. The final siRNA concentration was 25nM for each transfection. AZD6244 (Selumetinib) was

obtained from Selleck Chemicals and AdooQ Bioscience (#A10257). AZD6244 (10µM) was used to treat cells *in vitro* for at least 5 hours prior to lysate collection from cell culture.

2.2.10 Three-dimensional (3D) culture and immunofluorescence staining

Human non-transformed mammary epithelial cells (hMECs), MCF10A and MCF12A, were cultured in 100% matrigel (BD Biosciences, USA) for 3D morphogenesis. The 3D culture of hMECs on a matrigel results in a polarized, acini-like spheroids that recapitulate ductal and glandular structure *in vivo*. Cells ($2x10^3$) were suspended in 2% Matrigel medium, placed in an 8-well chamber slide precoated with Matrigel (#356231, BD Biosciences, San Jose). The cells were then fixed with 4% paraformaldehyde and stained with mouse monoclonal anti–laminin V (Millipore, Bellerica), rabbit polyclonal anti-Ki67 (Cell Signaling Technology, Danvers), and rabbit polyclonal anti-cleaved caspase-3 (Cell Signaling Technology) antibodies using methods described previously described previously by Debnath et al. (199). Immunofluorescence staining was analyzed using a Zeiss 520 confocal microscope (Carl Zeiss AG, Germany).

2.2.11 Tumor xenograft studies

All the mouse experiments were carried out in accordance with protocols approved by MD Anderson's Institutional Animal Care Committee. We established breast cancer xenografts by injecting $5x10^5$ MCFDCIS.COM.Vec or MCFDCIS.COM.ζ cells orthotopically into the mammary fat pads of 6-week-old female SWISS[nu/nu] mice obtained

from MD Anderson's Department of Experimental Radiation Oncology. We then divided the mice randomly into two groups, AZD6244 treatment or vehicle control group. Each group contained 5 mice. AZD6244 was suspended in sterile HPMC solution and given to mice through oral gavage daily at a dose of 16 mg/kg body weight or with vehicle control. Tumor volume was calculated using the formula volume = length x $(\text{width})^2/2$ previously described by Tomayko and Reynolds (200). Mice were sacrificed 20 days after treatment started and tumors were collected and embedded in paraffin following a routine pathological procedure.

2.2.12 Immunohistochemistry (IHC) analyses and tissue microarray (TMA)

For general immunohistochemistry (IHC), mouse tumor tissues were embedded in paraffin and cut into slides. We used the following antibodies: anti-14-3-3ζ (clone C-19, Santa Cruz Biotechnology, Santa Cruz, CA); anti-β-actin (Sigma, Australia); anti-LDHA, anti-cAMP response element-binding protein (CREB), anti-phospho-CREB, anti-ERK, anti-phospho-ERK (catalog no. 3582, 9197, 9198, 4695, and 4370, respectively, Cell Signaling Technology); anti-Ki67 (catalog no. ab92353, AbCam, England); and anti–minichromosome maintenance 2 (MCM2) (clone EP40, Epitomics). We also used the In Situ Cell Death Detection Kit (Roche, Germany) to detect apoptosis in tissue sections. The IHC staining scores for 14-3-3ζ, p-CREB, CREB, p-ERK and ERK were defined as 0, 1+, 2+, or 3+. 3+ indicates higher expression; 1+ indicates lower expression. The staining scores for Ki67 defined as percentages. Antigen retrieval and IHC analyses were performed as described previously (162). For TMA, we used a 70-case, 208-core breast

cancer tissue microarray (catalog no. BR208, US Biomax Inc.). The antigen retrieval and staining process are adopted using general IHC protocol. The optimal antibody dilutions for IHC is 1:100 as working solution.

2.2.13 Statistical analyses

Between-group differences were assessed using the Student's t test or ANOVA. P values < 0.05 were considered statistically significant.

2.3 Results

2.3.1 14-3-3ζ overexpression increases glycolysis

Since metabolic dysregulations has recently been implicated to take place during the early-stage of neoplastic transformation (103, 171), and abnormal 14-3-3ζ overexpression was also observed in pre-cancerous breast lesions (167), I hypothesized that 14-3-3ζ overexpression contributes to metabolic dysregulations in early-stage breast cancer. To gain insights on this conjecture, I first examined the relationship between 14-3-3ζ expression and genes involved in metabolic functions, using a microarray dataset (GSE16873) generated from histologically normal epithelia, simple ductal hyperplasia (SDH), atypical ductal hyperplasia (ADH) and ductal carcinoma in situ (DCIS) (201). Remarkably, the 14-3-3ζ expression level was most strongly correlated with the expressions of genes involved in glycolysis (Gene Ontology, GO: 0006096) in these pre-cancerous and early-stage breast lesions (Figure 13). In addition, this strong correlation between 14-3-3ζ expression level and glycolytic genes persisted in breast cancer patients (GSE2109 and TCGA datasets) (Figure 14 and 15) (194).
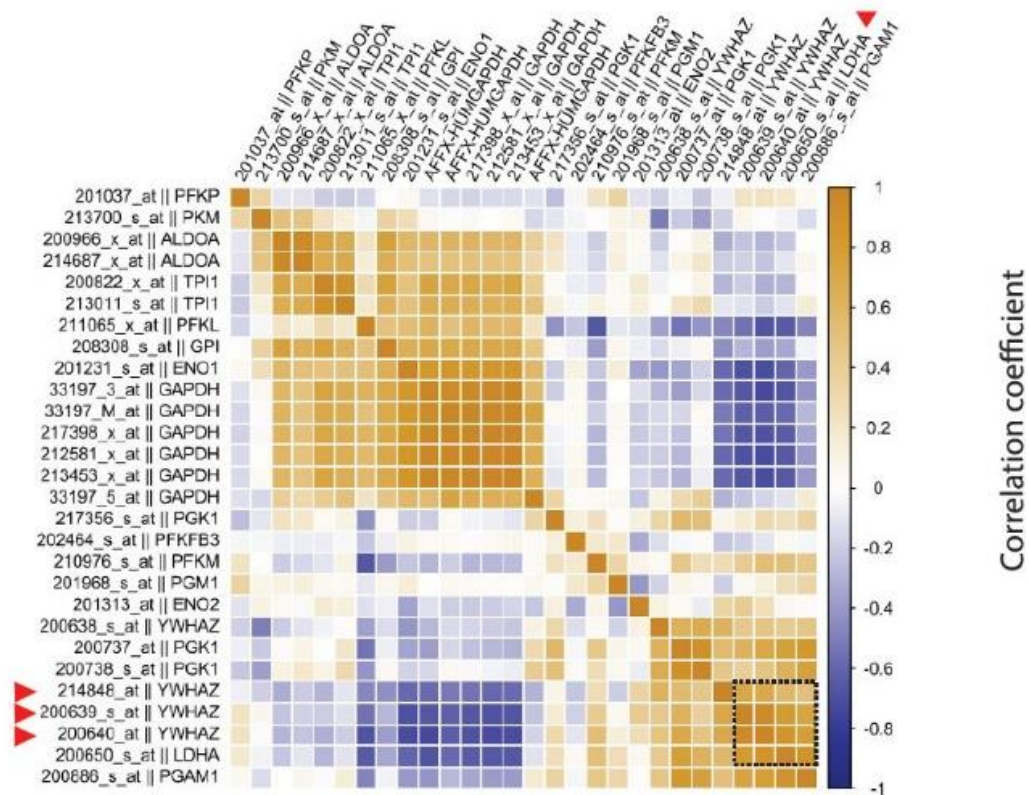
Figure 13. The correlation between 14-3-3ζ expression levels and glycolytic genes. Heat map of pairwise correlation on 14-3-3ζ (YWHAZ) and glycolytic gene (Gene Ontology, GO:0006096) expression levels in the early-stage breast lesions (GSE16873). Triangles indicate the high correlation between 14-3-3ζ and LDHA. The correlative relationship between the expression levels of 14-3-3ζ (YWHAZ) and LDHA reaches $R^2>0.8$. The data are in collaboration with Dr. Chenyu Zhang.
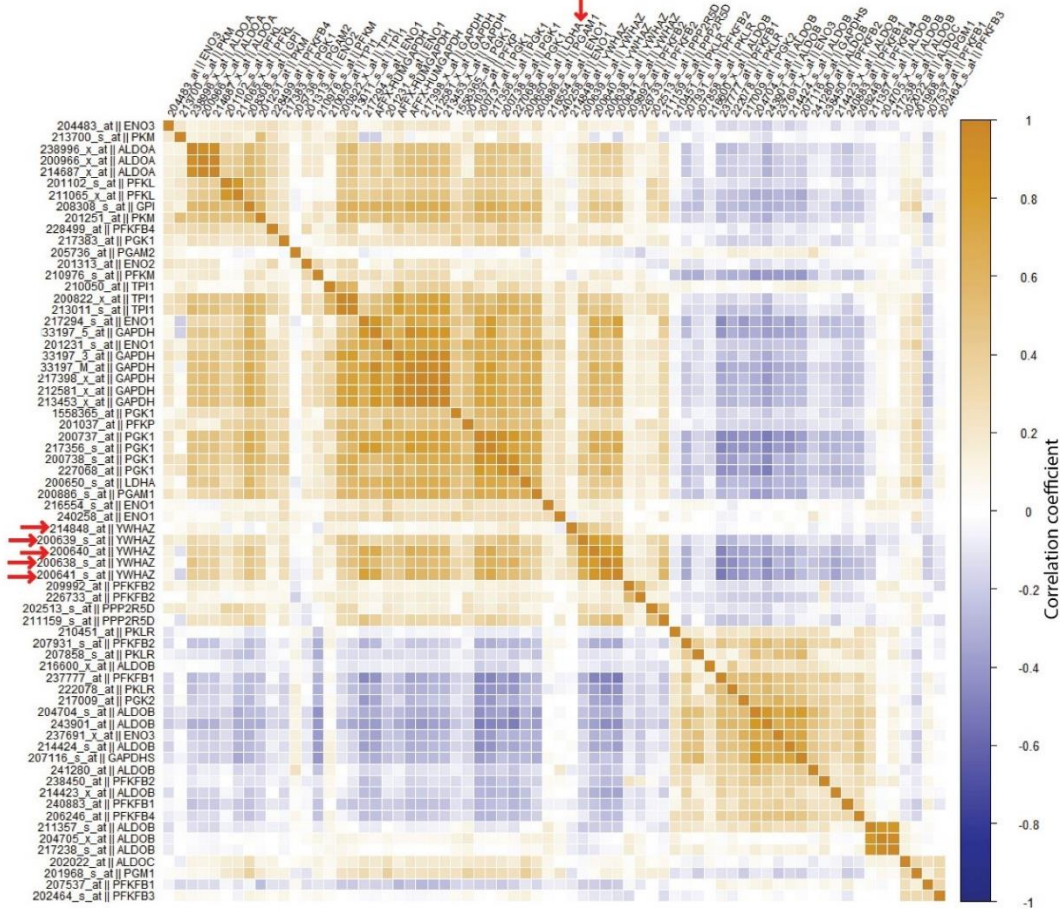
Figure 14. Heat map of pairwise correlation on 14-3-3ζ and glycolytic gene expression. Heat map of pairwise correlation in breast cancer patients profiled with cDNA microarray (expO, GSE2109). The datasets contain data from 353 breast cancer patients. Five 14-3-3ζ (YWHAZ) probe sets were analyzed together with glycolysis-related genes (GO: 0006096). Probe sets were ordered according to clustering analysis. Arrow indicates the strong correlation between 14-3-3ζ and LDHA. The correlative relationship between the expression levels of 14-3-3ζ (YWHAZ) and LDHA reaches R^2=0.31. The data are in collaboration with Dr. Chenyu Zhang.
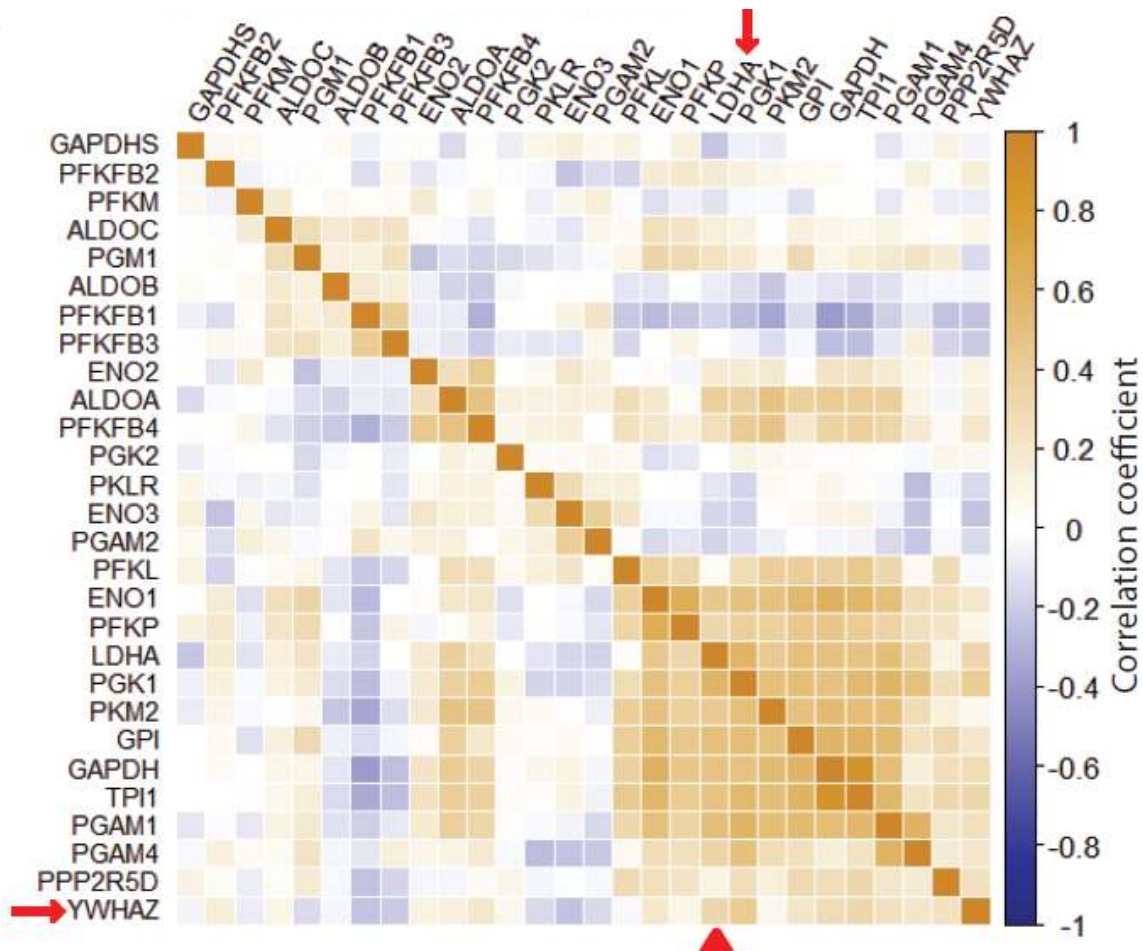
Figure 15. The correlation between 14-3-3ζ and glycolytic gene expression in TCGA.
Heat map of pairwise correlation on 14-3-3ζ (YWHAZ) and glycolytic gene expression levels in the TCGA breast cancer datasets. Arrow and indicates the high correlation between 14-3-3ζ and LDHA. The correlative relationship between the expression levels of 14-3-3ζ (YWHAZ) and LDHA reaches $R^2=0.32$. The data are in collaboration with Dr. Chenyu Zhang.

To test whether 14-3-3ζ functionally modulates cellular glycolytic activity in pre-cancerous mammary epithelial cells, I measured glycolytic activities in widely used and validated models of pre-cancerous mammary epithelial cells, i.e., MCF10A and MCF12A hMECs. I compared three glycolytic indices (i.e., glucose uptake, lactate production, and oxygen consumption) in MCF10A and MCF12A hMECs that had either exogenous 14-3-3ζ overexpression (10A.ζ and 12A.ζ cells) or endogenous 14-3-3ζ knockdown (10A.shζ, and 12A.shζ cells) (Fig. 16A) (154). Indeed, glucose uptake and lactate production significantly increased in both 10A.ζ and 12A.ζ cells compared to this control cells, but significantly reduced in both 10A.shζ, and 12A.shζ cells compared to their control cells (Figure 16B and 16C). Cells with higher glycolysis activity tend to reduce the rates of oxidative phosphorylation and oxygen consumption and shift the metabolic flux from the ATP-generating Krebs cycle to the biomass-producing glycolysis. Consistently, the oxygen consumption rates of the 14-3-3ζ-overexpressing 10A.ζ and 12A.ζ cells were significantly reduced than that of the control cells (Figure 16D). However, no significant difference in oxygen consumption was detected between the 10A.shζ and 12A.shζ cells and their control cells (Figure 16D), suggesting that 14-3-3ζ does not modulate basal oxygen consumption in the 14-3-3ζ low-expressing MCF10A and MCF12A cells. Next, I evaluated the overall impact of 14-3-3ζ on cellular glycolytic activity by calculating the glycolytic index, G x L / O, where G is for glucose uptake rate, L is for lactate generation production, and O is for oxygen consumption rate (197). 14-3-3ζ-overexpressing 10A.ζ and 12A.ζ cells had 4 to 5 fold increases, whereas 14-3-3ζ knockdown 10A.shζ and 12A.shζ cells had approximately 70% decreases, in their glycolytic index compared to their respective control cells (Table 2A and 1B). Collectively, these data demonstrate that

14-3-3ζ positively modulates glycolytic activity in nontransformed MCF10A and MCF12A cells.
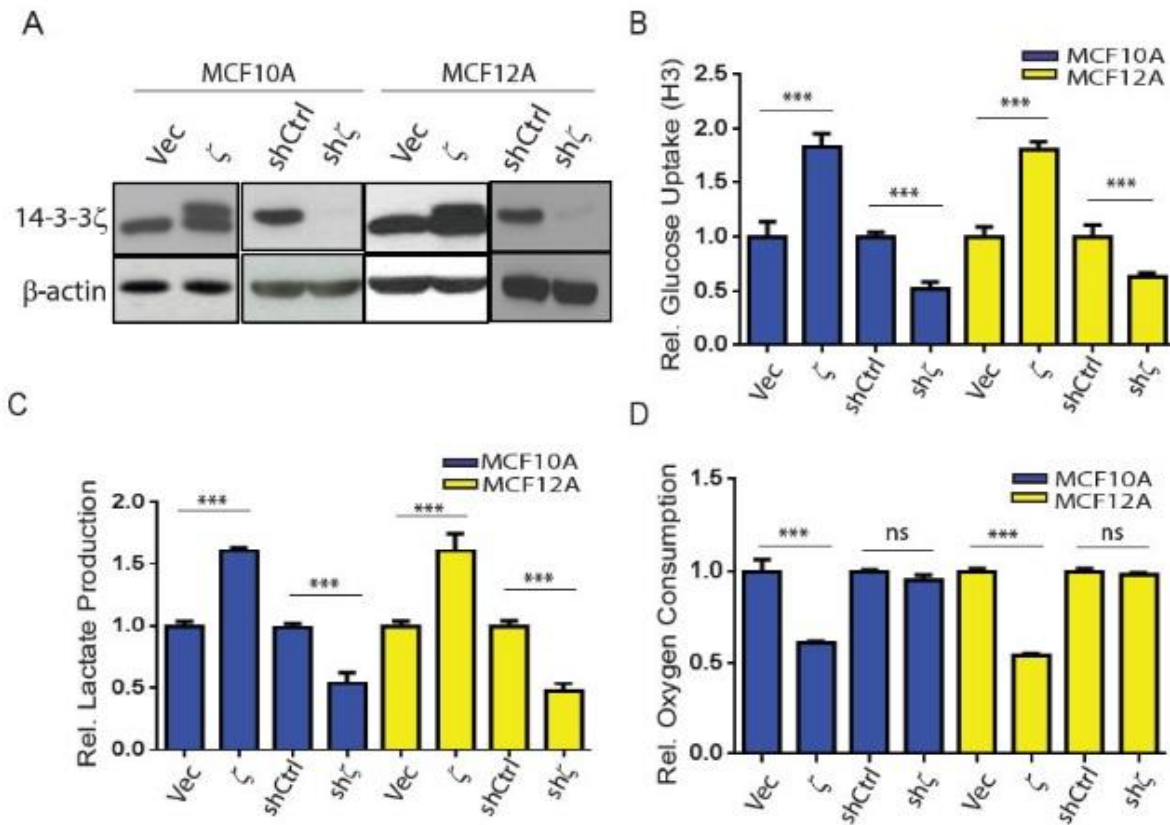
Figure 16. Overexpression of 14-3-3ζ increases glycolysis in hMECs. A, western blotting for 14-3-3ζ protein expression in hMEC sublines. B-D, MCF10A and MCF12A cells with 14-3-3ζ-overexpression (10A.ζ and 12A.ζ) and 14-3-3ζ-knockdown (10A.shζ and 12A.shζ) were assessed for glucose uptake (B), lactate production (C), and oxygen consumption (D). The relative levels of glucose uptake, lactate production, and oxygen consumption of the 10A.ζ cells and 12A.ζ cells were normalized to those of the control 10A.Vec and 12A.Vec cells, respectively; and the relative levels of glucose uptake, lactate production, and oxygen consumption of the 10A.shζ cells and 12A.shζ cells were normalized to those of the control 10A.shCtrl and 12A.shCtrl cells, respectively. Absolute

measurements were normalized to the corresponding controls. Bars indicate standard deviations. ***, $P<0.001$; n.s., not significant by the Student t-test.

A

hMEC lines / Glycolytic Indices	10A.Vec	10A.ζ	12A.Vec	12A.ζ
Glucose Uptake (G)	2.72	4.99	4.95	8.95
Lactate Production (L)	1.55	2.50	2.55	4.12
Oxygen Consumption (O)	2.97	1.80	2.44	1.32
Glycolytic Index (G x L / O)	1.42	6.93	5.17	27.93
Fold Change (Normalized by control)	1.00	4.88	1.00	5.40

B

hMEC lines / Glycolytic Indices	10A.shCtrl	10A.shζ	12A.shCtrl	12A.shζ
Glucose Uptake (G)	2.79	1.46	1.69	1.08
Lactate Production (L)	1.48	0.80	0.99	0.47
Oxygen Consumption (O)	2.57	2.20	2.53	2.32
Glycolytic Index (G x L / O)	1.61	0.53	0.66	0.22
Fold Change (Normalized by control)	1.00	0.32	1.00	0.33

Table 2. Cellular glycolytic index of 14-3-3ζ-overexpressing and 14-3-3ζ-knockdown hMECs. A. The glycolytic activity of 14-3-3ζ overexpressing 10A.ζ and 12A.ζ cells was significantly increased than that of control 10A.Vec and 12A.Vec cells. B. the glycolytic activity of 14-3-3ζ-knockdown 10A.shζ and 12A.shζ cells was significantly reduced than that of control shRNA-transfected 10A.shCtrl and 12A.shCtrl cells.

2.3.2 14-3-3ζ-mediate LDHA upregulation increases aerobic glycolysis

To investigate the molecular mechanisms of the 14-3-3ζ-mediated increase of glycolysis, we focused on LDHA because its expression, compared with that of other glycolytic genes in human pre-cancerous lesions, is more strongly associated with 14-3-3ζ expression level. Furthermore, 14-3-3ζ-overexpressing 10A.ζ and 12A.ζ cells had significantly increased levels of LDHA mRNA and protein expression compared to their vector control cells; whereas knockdown of 14-3-3ζ in 10A.shζ and 12A.shζ cells led to significantly decreased LDHA mRNA and protein levels compared to the control shCtrl cells (Figure 17A and 17B).

These findings led us to investigate whether 14-3-3ζ-mediated LDHA upregulation directly contributes to the increase of glycolytic activity. We knocked down the LDHA gene expression in the 14-3-3ζ overexpressing 10A.ζ and 12A.ζ cells by shRNA (10A.ζ.shLDHA and 12A.ζ.shLDHA cells) and measured the three glycolytic indices. The 10A.ζ.shLDHA and 12A.ζ.shLDHA cells had significantly less glucose uptake and lactate production than the control cells (Figure 17C and 17D); whereas oxygen consumption in 10A.ζ.shLDHA and 12A.ζ.shLDHA cells was not significantly different from that in the control cells (data not shown). Overall, the glycolytic indices were reduced with LDHA knockdown by approximately 70% (10A.ζ.shLDHA versus 10A.ζ.shCtrl cells) and 60% (12A.ζ.shLDHA versus 12A.ζ.shCtrl cells) (Table 3). Together, these data indicate that 14-3-3ζ-mediated LDHA upregulation is a key promoting factor of glycolysis in 14-3-3ζ overexpressing hMECs.
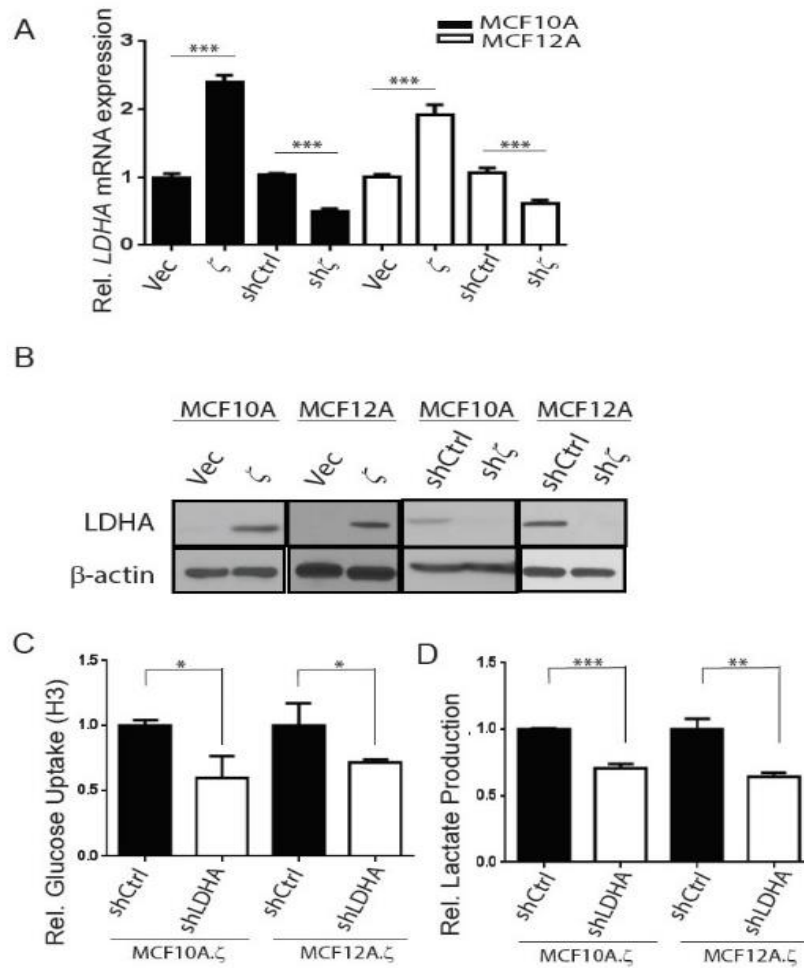
Figure 17. 14-3-3ζ overexpression increases glycolysis by upregulating LDHA in hMECs. A-B, qRT-PCR analysis of relative *LDHA* mRNA expression (A), western blotting for LDHA protein expression (B) in 14-3-3ζ overexpressing (10A.ζ and 12A.ζ) and 14-3-3ζ-knockdown (10A.shζ and 12A.shζ) MCF10A and MCF12A cells, compared to control cells. C-D, 14-3-3ζ overexpressing cell lines with LDHA knockdown (10A.ζ.shLDHA and 12A.ζ.shLDHA) were assessed for glucose uptake (C) and lactate production (D). The relative levels of glucose uptake and lactate production were normalized to those of the shCtrl cells, respectively. Bars indicate standard deviations. *, $P<0.05$; **, $P<0.01$; ***, $P<0.001$ using the Student t-test.

hMEC lines / Glycolytic Indices	10A.ζ.shCtrl	10A.ζ.shLDHA	12A.ζ.shCtrl	12A.ζ.shLDHA
Glucose Uptake (G)	1.84	1.10	2.05	1.47
Lactate Production (L)	7.86	5.56	6.75	4.35
Oxygen Consumption (O)	1.20	1.40	1.40	1.56
Glycolytic Index (G x L / O)	12.05	4.37	9.88	4.02
Fold Change (Normalized by control)	1.00	0.36	1.00	0.42

Table 3. Glycolytic activity of 14-3-3ζ-overexpressing hMECs with LDHA knockdown. 10A.ζ and 12A.ζ cells transfected with LDHA shRNA (10A.ζ.shLDHA and 12A.ζ.shLDHA); or with control shRNA (10A.ζ.shCtrl and 12A.ζ.shCtrl). The glycolytic activity of hMECs cells was calculated by glycolytic index.

2.3.3 14-3-3ζ-mediated LDHA upregulation contributes to early-stage transformation of hMECs

As increased glycolysis has been implicated in early-stage neoplastic transformation (62), we examined whether 14-3-3ζ-mediated LDHA upregulation is a critical determinant of hMEC transformation. We previously reported that 14-3-3ζ overexpression in MCF10A cells (10A.ζ) led to increased colony formation in soft agar and dysregulated acini (158, 167). The 3D culture of normal hMECs on a matrigel results in a polarized and acini-like spheroids that recapitulate normal ductal architecture *in vivo*. When oncogene induces cell transformation, which results in a dysregulated acini structure that mimics several aspects of early transformation of mammary gland *in vivo*. Consistent with our previous findings in MCF10A cells, the colony numbers of 14-3-3ζ-overexpressing MCF12A cells (12A.ζ) were also significantly increased compared to vector control (12A.Vec) cells (Figure 18A). Remarkably, LDHA knockdown in 14-3-3ζ-overexpressing MCF10A (10A.ζ.shLDHA) and MCF12A (12A.ζ.shLDHA) cells reversed the transforming effects of 14-3-3ζ overexpression, yielding significantly fewer colonies compared to their control cells (Figure 18A and Figure 19A).

Furthermore, in the 3D culture system, 14-3-3ζ-overexpressing 12A.ζ cells also developed dysregulated acini with filled lumen resulting from reduced apoptosis (Figure 18B) and increased proliferation (202) (Figure 18C) compared to control 12A.Vec cells. Notably, LDHA knockdown in 14-3-3ζ high expressing 10A.ζ and 12A.ζ (10A.ζ.shLDHA and 12A.ζ.shLDHA) partially reversed the dysregulated acini phenotype with increased cleaved-caspase 3 (Figure 18B, and Figure 19B), suggesting that LDHA has an anti-apoptosis effect in hMECs. In addition, 12A.ζ.shLDHA cells had reduced proliferation

(reduced both Ki67 and MCM2 levels) but 10A.ζ.shLDHA showed a mild reduction in proliferation (Figure 18C and Figure 19C). Further analysis revealed that the 10A.ζ.shLDHA and 12A.ζ.shLDHA cells had fewer disruptive acini structures and more rounding acini than their control cells (Figure 18D and Figure 19D), demonstrating a partial restoration of normal epithelial morphology. Collectively, these data demonstrate that 14-3-3ζ overexpression-mediated LDHA upregulation contributes, at least partially, to hMEC transformation and aberrant acinar formation through, increased glycolysis, increased proliferation, and decreased apoptosis that can be reversed by LDHA downregulation.
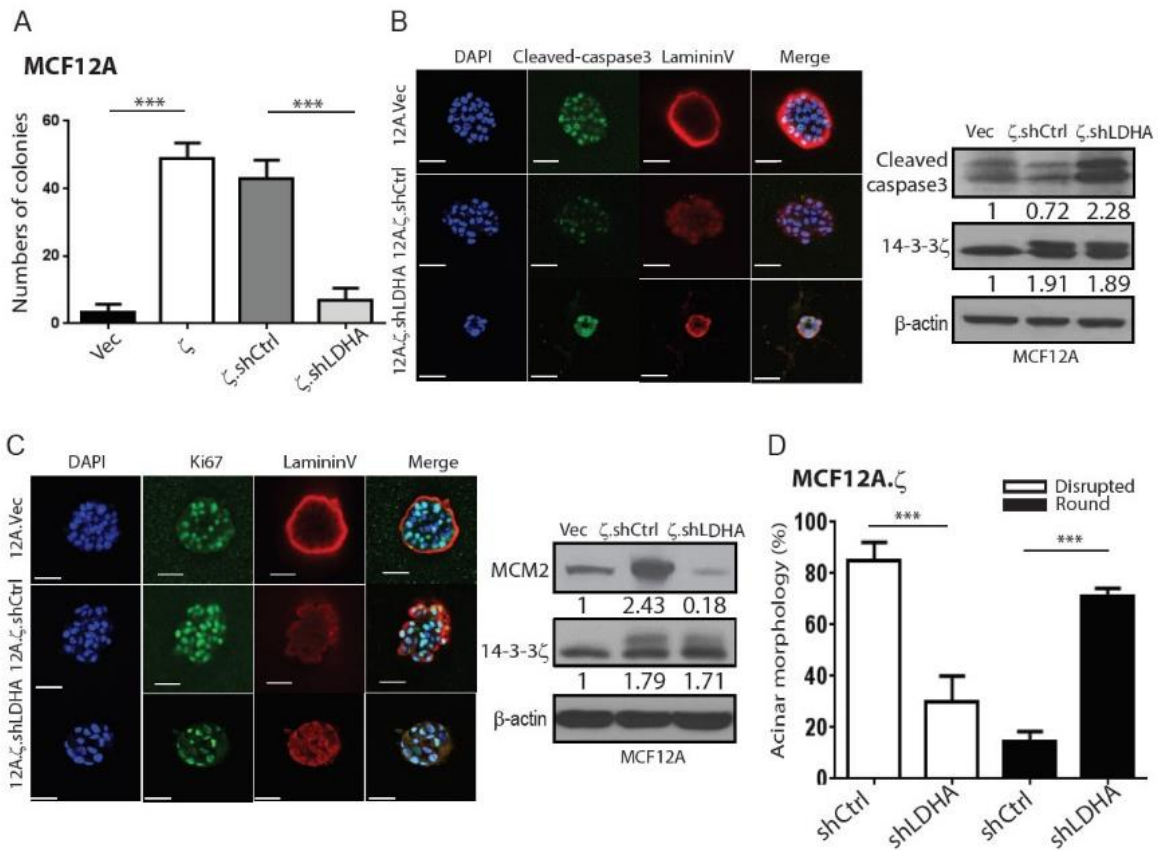
Figure 18. The contributions of 14-3-3ζ-mediated LDHA upregulation in hMECs. A, Quantified soft colony formation assay of the MCF12A sublines. Cells were cultured in 0.5% soft agar for 21 days. B, Detection of apoptosis (cleaved caspase 3, green), polarity markers (Laminin V, red) and DAPI (blue) in MCF12A sublines cultured in Matrigel for 8 days. Left: Right: Western blotting of cleaved caspase-3 and 14-3-3ζ in acini lysate collected from 3D culture. C, Detection of proliferation marker (Ki-67, green), polarity marker (Laminin V, red) and DAPI (blue) in MCF12A sublines cultured in 3D culture for 15 days. Scale bars, 50 μm. Right: Western blotting of MCM2, and 14-3-3ζ in acini lysate collected from 3D culture. D, MCF12A sublines in 3D culture for 20 days, rounded or disrupted acinar morphology were counted.
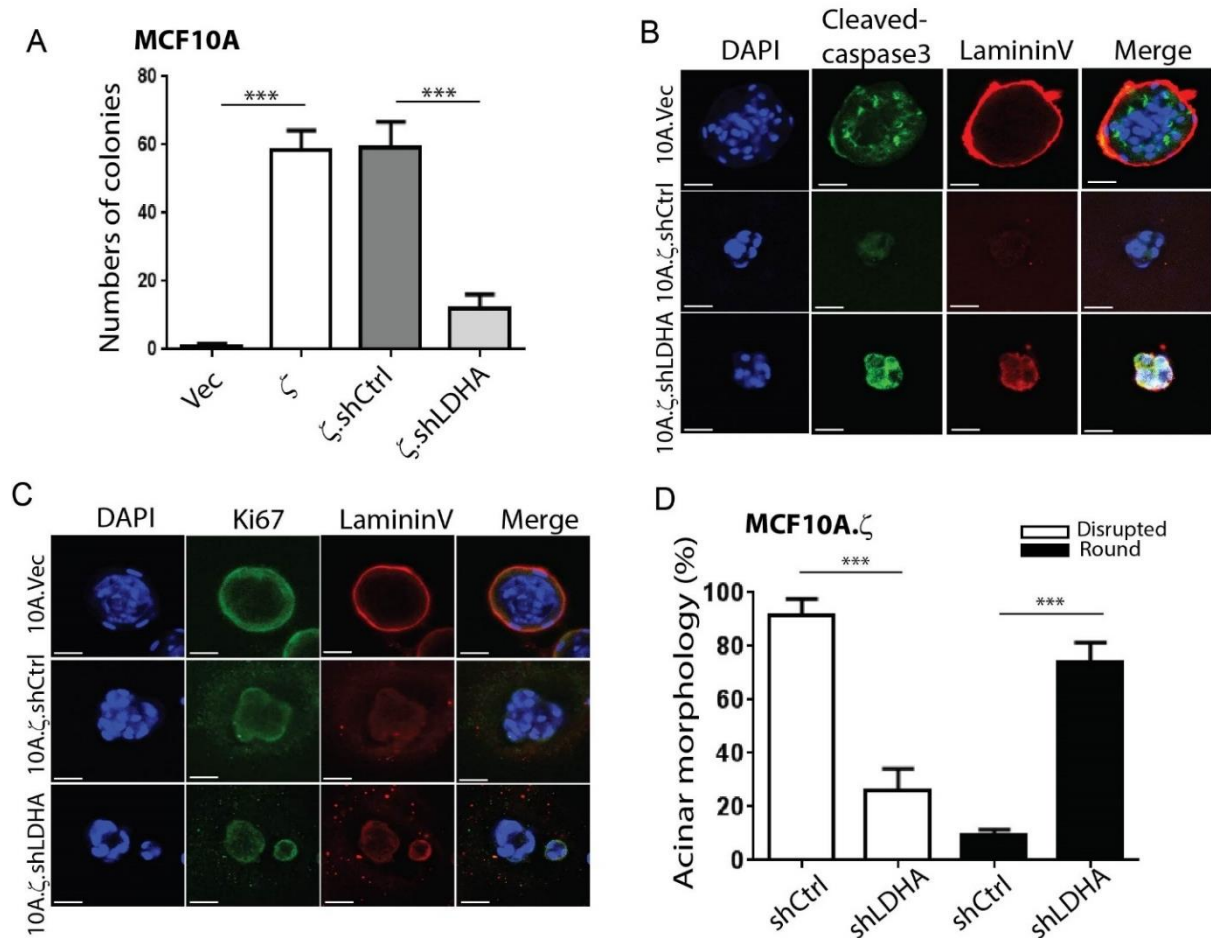
Figure 19. LDHA upregulation contributes to early-stage transformation of MCF10A cells. A, Quantified soft colony formation assay of the MCF10A sublines which were cultured in 0.5% soft agar for 45 days, and the cell colonies were counted. B, Detection of apoptosis (cleaved caspase-3, green) and polarity marker (laminin V, red) and DAPI (blue) in MCF10A sublines cultured in Matrigel. Representative images of immunofluorescence staining. Scale bars, 50 μm. C, Detection of proliferation markers (Ki-67, green), polarity marker (laminin V, red), and DAPI (blue) in MCF10A sublines cultured in Matrigel. Representative images of MCF10A sublines subjected to immunofluorescence staining. D, MCF10A sublines cultured for 30 days were assessed for rounded or disrupted acinar morphology.

2.3.4 14-3-3ζ overexpression leads to up-regulation of LDHA

Since LDHA upregulation contributes to 14-3-3ζ-mediated hMEC transformation, it is important to identify the underlying molecular mechanisms of 14-3-3ζ-induced LDHA upregulation. Because 14-3-3ζ overexpression increases LDHA expression at both mRNA and protein levels in hMECs (Figure 17A and 17B) and is known to regulate protein stability (157, 203), I initially compared the LDHA protein stability of the 10A.ζ cells with that of the control 10A.Vec cells, but found no significant difference between them (Figure 20A and 20B). This led us to focus on studying mechanisms of *LDHA* mRNA upregulation by 14-3-3ζ. I examined *LDHA* mRNA stability by treating 10A.ζ and 10A.Vec cells with actinomycin D, and measured *LDHA* mRNA degradation rate. No significant difference in *LDHA* mRNA stability was found between the 10A.ζ and 10A.Vec cells (Figure 20C), suggesting that 14-3-3ζ might modulate *LDHA* mRNA expression through transcriptional regulation.
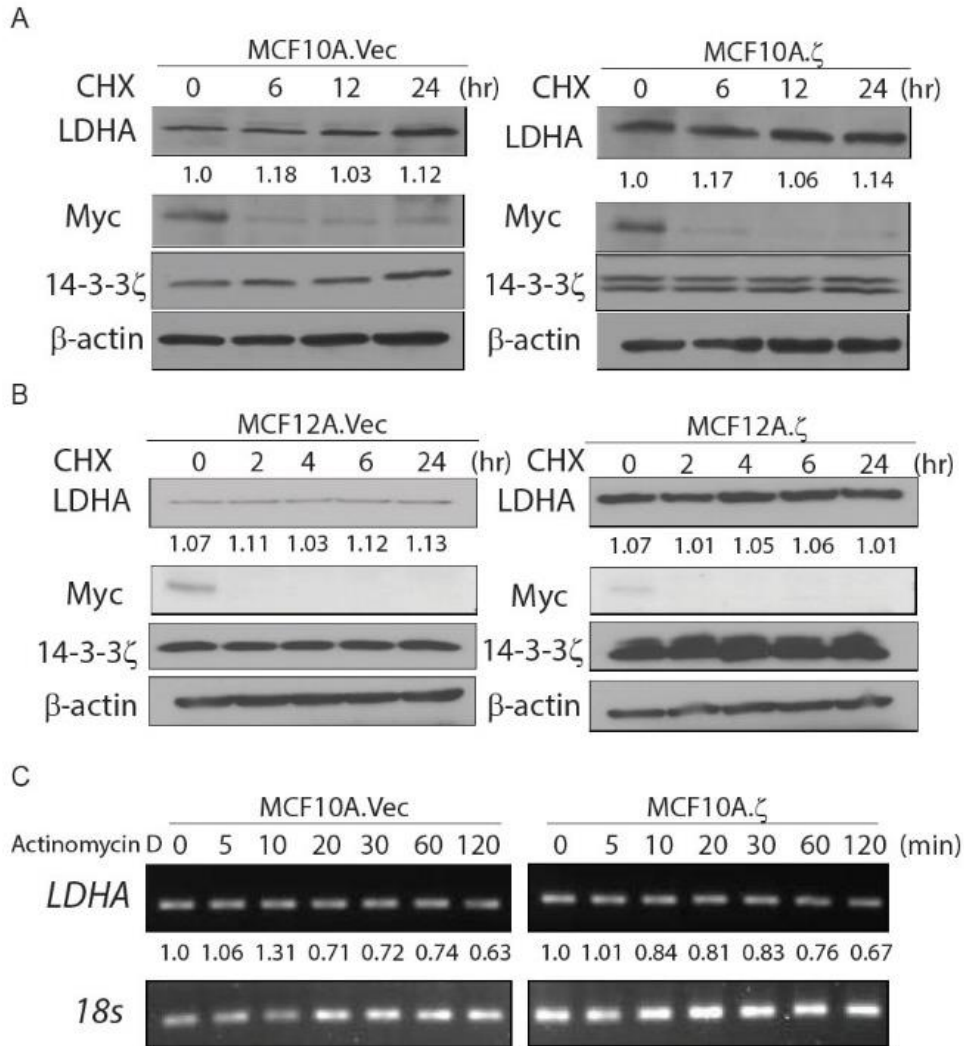
Figure 20. Comparison between protein and mRNA stability in hMECs. A-B, MCF10A and MCF12A sublines were treated with 100 µg/mL cycloheximide (CHX) from 0 to 24 hours and compared the LDHA degradation rate over the time. Myc served as a positive control to show that CHX worked effectively during treatment. The LDHA expression levels were normalized to β-actin and also to their time zero of treatment. C, MCF10A sublines were treated with actinomycin D from 0 to 2 hours and compared the mRNA level of *LDHA* over the time. The *LDHA* mRNA expression levels were normalized to *18s* and also to their time zero of treatment.

To determine whether 14-3-3ζ transcriptionally upregulates *LDHA*, I cloned the LDHA promoter from 2000 base pairs (bp) upstream of the transcription start site plus the entire 272bp 5'-untranslated region (5'-UTR) into the pGL3-Basic vector to drive luciferase reporter gene expression (-2000 to +272-Luc), and transfected this reporter vector into the 10A.ζ versus 10A.Vec cells and the 10A.shζ versus 10A.shCtrl cells (Fig. 4A). I detected an increase of luciferase activity in 10A.ζ compared to 10A.Vec cells, but a decreased luciferase activity in 10A.shζ compared to 10A.shCtrl cells, indicating that 14-3-3ζ transcriptionally upregulates *LDHA* mRNA expression (Figure 21A).

To identify the cis-regulatory element in the -2000bp LDHA promoter and 5'-UTR region that is responsible for 14-3-3ζ-induced transcriptional upregulation, I made a series of deletion constructs in the -2000 to +272 region, subcloned them into the pGL3-Basic vector, and transfected them into the 10A.ζ, 10A.Vec, 10A.shζ, and 10A.shCtrl cells (Fig. 21A, left). Remarkably, a specific 65bp region (+85 to +150) in the 5'-UTR of LDHA gene was necessary and sufficient to induce the luciferase gene expression (Figure 21A). Transfection of this 65bp 5'-UTR region resulted in higher luciferase activity in 10A.ζ than in vector control cells (Figure 21A, middle). In contrast, the luciferase activity driven by the 65bp 5'-UTR was lower in the 10A.shζ cells compared to the 10A.shCtrl cells (Figure 21A, right). Next, to identify the transcription factors that bind to the 65bp 5'-UTR region of LDHA and are responsible for transcriptional upregulation by 14-3-3ζ, I analyzed this DNA sequence for putative transcription factor binding sites using the Transcription Element Search System (TESS) and University of California-Santa Cruz (UCSC) genome browser online analysis tools (204, 205). I identified potential binding sites for five transcription factors USF1, CREB, MYC, SP1, and ATF-1 (Figure 21B), knocked them

down individually in the 10A.ζ cells and compared their luciferase activities. Knocking down each of the five genes reduced the LDHA 65bp 5'-UTR driven luciferase activity in 10A.ζ cells to various degrees, and knocking down CREB led to the most significant reduction (Figure. 21C).

Furthermore, I examined *LDHA* mRNA and protein levels in the 10A.Vec and 10A.ζ cells that had the five transcription factors knocked down individually. Among these five transcription factors, CREB and MYC knock down in the 10A.ζ cells (Figure 21D and 21E), significantly reduced *LDHA* protein and mRNA compared to shCtrl cells (Figure 21F and 21G). However, CREB knockdown had less effect on the LDHA protein level in the control 10A.Vec cells compared to MYC knockdown cells (Figure 21F), suggesting that CREB has a more specific role in regulating LDHA expression in 14-3-3ζ overexpressing cells. Therefore, I focused on the question how 14-3-3ζ overexpression leads to CREB transactivation of LDHA that contributes to early transformation in 14-3-3ζ overexpressing hMECs.

A

B

```
                    +1
                    |
+1 to +50   5'- GTCTGCCGGTCGGTTGTCTGGCTGCGCGCGCCACCCGGGCCTCTCCAGTG

                                                        +85
                                                        |
+51 to +100    CCCCGCCTGGCTCGGCATCCACCCCCAGCCCGACTCACACGTGGGTTCCC
                                                        ‾‾‾‾‾‾
                                                        Myc
                                                        USF1
                                                                    +150
                                                                    |
+101 to +150   GCACGTCCGCCGGCCCCCCCCCGCTGACGTCAGCATAGCTGTTCCACTTAA
                    ‾‾‾‾‾                ‾‾‾‾‾‾
                    SP1                  CREB
                                         ATF-1

+151 to +200   GGCCCCTCCCGCGCCCAGCTCAGAGTGCTGCAGCCGCTGCCGCCGATTCC

+201 to +250   GGATCTCATTGCCACGCGCCCCCGACGACCGCCCGACGTGCATTCCCGAT

+251 to +272   TCCTTTTGGTTCCAAGTCCAAT -3'
                                |
                              +272
```

C   D   E

(Legends of Figure 21 were listed in the next page)
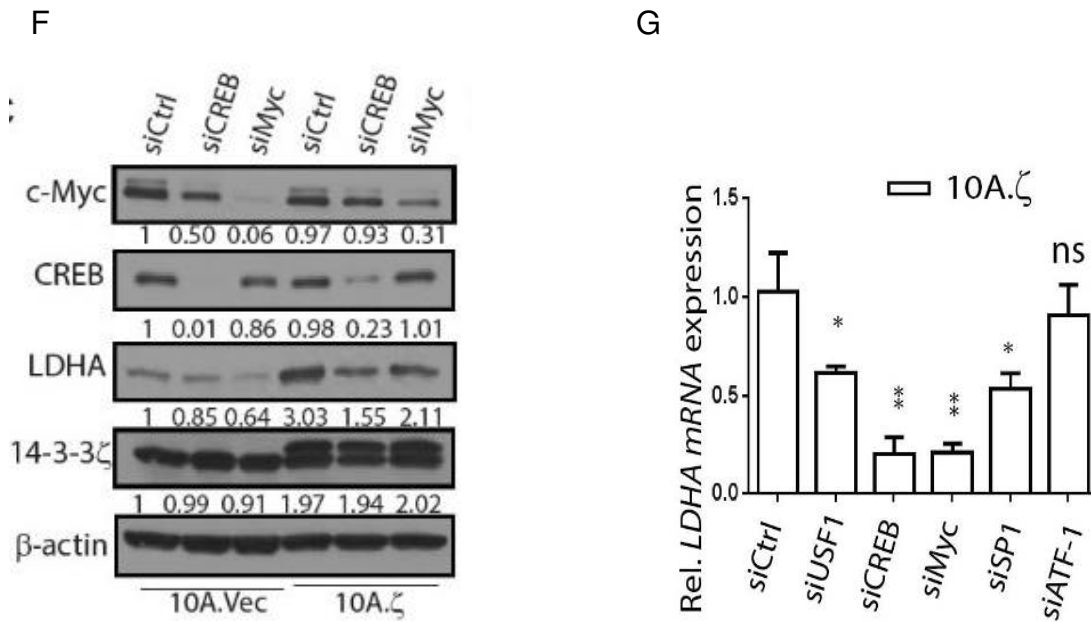
Figure 21. Identification of transcription factors involved in LDHA upregulation. A, Schematic design of the LDHA regulatory region deletion assay. Series of deletion constructs were transfected into 10A.ζ, 10A.Vec, 10A.shζ and 10A.shCtrl cells. B, Schematic overview of the transcription factor binding sites from +1 to +272 bp of LDHA's 5'-UTR annotated using the TESS. C, Cells with individual knockdown of five indicated transcription factors were subject to luciferase activity assays after transfection with the construct with the 65bp 5'UTR region driving the luciferase reporter gene. The relative luciferase activity of the cells was normalized to that of 10A.ζ cells with control siRNA. D, qRT-PCR analysis of relative *CREB* mRNA and E) *MYC* mRNA expression in the indicated cells was normalized by 18s mRNA expression. F, Western blotting of c-Myc, CREB, LDHA, and 14-3-3ζ in MCF10A sublines. G, qRT-PCR analysis of relative *LDHA* mRNA expression in cells with five transcription factors individually knocked down and control cells

14-3-3ζ has been shown to directly bind to Raf and activate MEK/ERK (206-208), which directly phosphorylate p90 ribosomal S6 kinase, that in turn activates and phosphorylates of CREB at Ser-133 (209, 210). Thus, I tested whether CREB-mediated transcriptional upregulation of LDHA could be modulated through the 14-3-3ζ-ERK-RSK signaling axis. Indeed, I detected a dramatically higher activation of the ERK pathway and increased phosphorylation of CREB at Ser-133 in both 10A.ζ and 12A.ζ cells compared to control 10A.Vec and 12A.Vec hMECs (Figure 22A). Furthermore, treating the 14-3-3ζ-overexpressing 10A.ζ and 12A.ζ cells with a potent MEK/ERK inhibitor, AZD6244, dramatically inhibited the ERK pathway, reduced CREB phosphorylation and decreased the LDHA mRNA and protein expressions to similar levels as in the 10A.Vec and 12A.Vec hMECs (Figure 22B and 22C), suggesting that LDHA upregulation in the 14-3-3ζ overexpressing 10A.ζ and 12A.ζ cells is primarily dependent on the ERK/CREB pathway. To determine whether the transcription factor CREB directly binds to the *LDHA* promoter, I performed chromatin immunoprecipitation assay using anti-p-Ser-133-CREB followed by LDHA promoter-specific PCR (ChIP-PCR). I found significantly more *LDHA* promoter-bound pCREB proteins (~1.8 to 2 fold) in the 14-3-3ζ-overexpressing 10A.ζ and 12A.ζ cells than in the control cells (Figure 22D). In contrast, knockdown of 14-3-3ζ in MCF10A hMECs significantly reduced pCREB protein binding to the LDHA promoter compared to the 10A.shCtrl cells (Figure 22D). Together, these data indicate that 14-3-3ζ overexpression activates the MEK/ERK pathway and consequently increases the binding of pCREB to the LDHA promoter, leading to LDHA transcriptional upregulation.
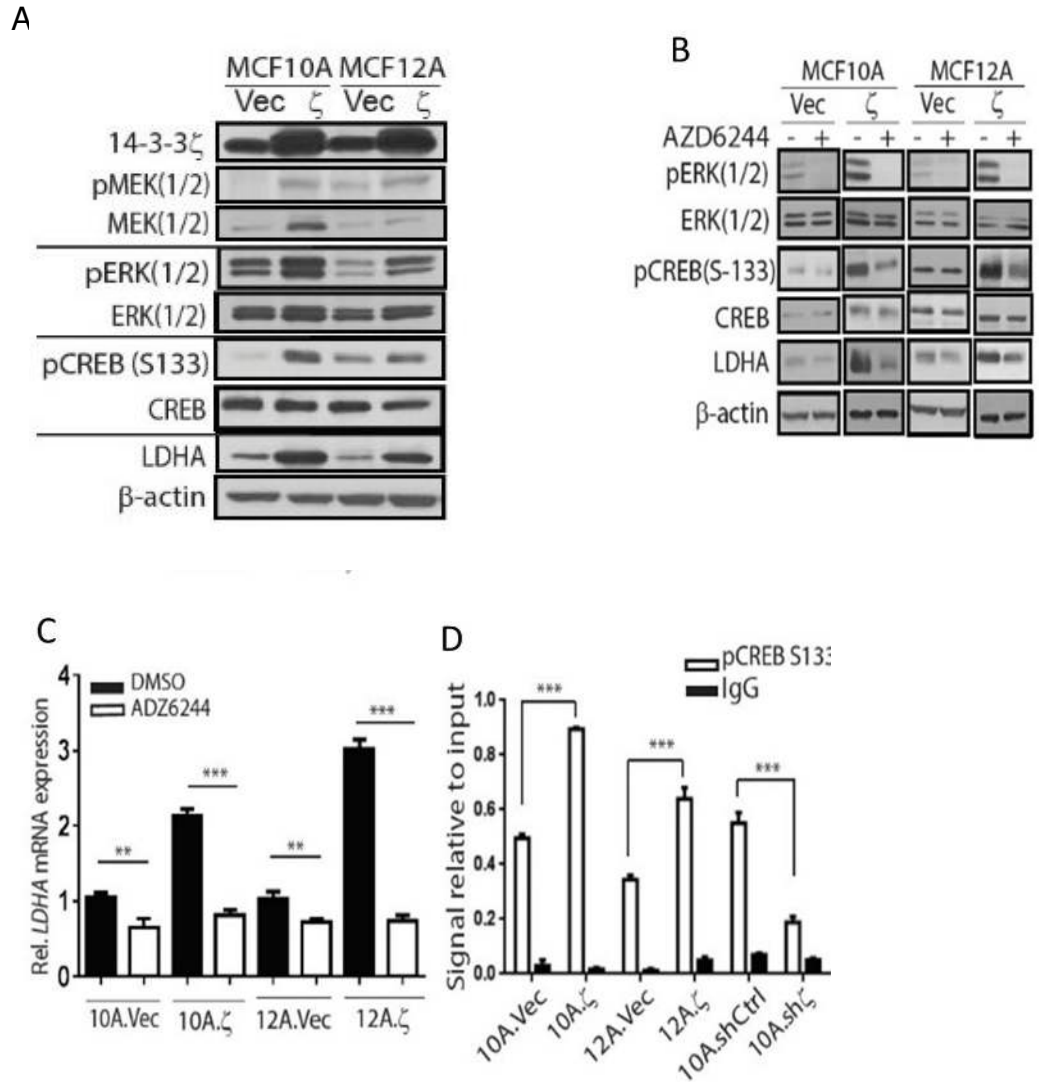
Figure 22. 14-3-3ζ overexpression transcriptionally upregulates LDHA. A, Western blotting of c-Myc, CREB, LDHA, and 14-3-3ζ in MCF10A sublines. B, Western blotting detecting the phospho-ERK, phospho-CREB, total ERK, CREB, LDHA, and 14-3-3ζ in10A.Vec, 10A.ζ, 12A.Vec and 12A.ζ cells treated with AZD6244 or DMSO. C, qRT-PCR analysis of *LDHA* mRNA expression in the hMEC sublines following by treatment with AZD6244 or DMSO. D, Chromatin immunoprecipitation assay using anti-phospho-CREB (Ser-133) followed by PCR (ChIP-PCR) of the LDHA promoter region.

2.3.5 Targeting the MEK/ERK/CREB pathway inhibits tumor outgrowth

Because the MEK/ERK/CREB pathway is critical for 14-3-3ζ-induced LDHA upregulation which contributes to hMEC early transformation. I proposed that targeting this pathway to inhibit metabolic adaptation of early-stage breast cancer cells towards glycolysis may be an effective strategy to intervene cancer progression. Therefore, I next investigated whether targeting the 14-3-3ζ downstream from the MEK/ERK pathway may effectively prevent or intervene the early-stage breast cancer further progression *in vivo.* To this end, I exogenously overexpressed 14-3-3ζ in early-stage DCIS model of MCF10DCIS.COM cells. The MCF10DCIS.COM line is a MCF10A cells-derived model that forms DCIS-like mammary lesions and ultimately progresses to invasive mammary tumors in nude mice (195). Recent studies revealed almost identical genomic profiles between the MCF10A and MCF10DCIS.COM cells, supporting our efforts to extend the above studies of MCF10A to in vivo investigations using the MCF10DCIS.COM line (211). Consistent with the MCF10A and MCF12A cells, exogenous overexpression of 14-3-3ζ in the MCF10DCIS.COM cells (DCIS.COM.ζ) led to activation of the ERK/CREB pathway and LDHA upregulation; whereas 14-3-3ζ knockdown in MCF10DCIS.COM led to decreased ERK/CREB activity and LDHA downregulation (Figure 23 and Figure 24).
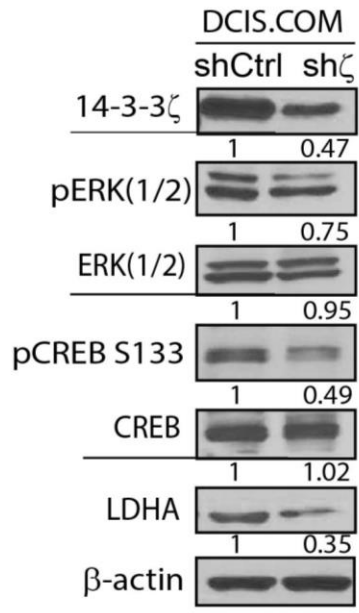
Figure 23. DCIS.COM breast cancer cells. Western blotting of proteins in DCIS.COM sublines.
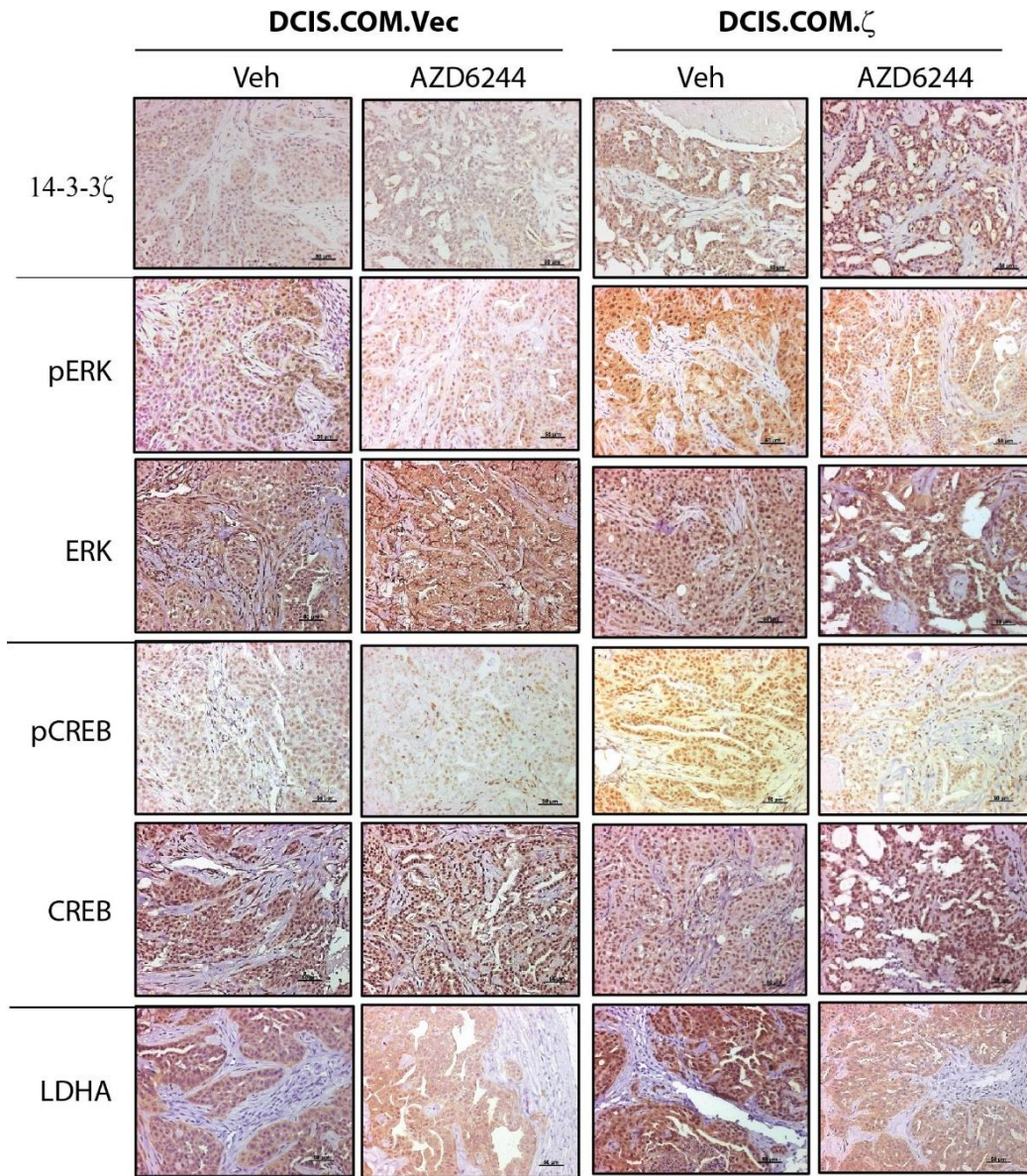
Figure 24. Figure 24. Representative IHC staining of DCIS.COM.Vec and DCIS.COM tumors. 14-3-3ζ, phospho-ERK, ERK, phospho-CREB, CREB, and LDHA in DCIS.COM.Vec and DCIS.COM.ζ tumors with indicated treatments. Scale bars, 50 µm. The data are in collaboration with Dr. Qingling Zhang.

Next, I implanted DCIS.COM.ζ and control DCIS.COM.Vec cells into the mammary fat pads (m.f.ps) of nude mice (day 0) to produce tumor xenografts and started treating these mice with vehicle or MEK/ERK inhibitor AZD6244 on day 10 (Figure 25A). Treatment continued until day 30, when the mice were sacrificed and their mammary tumors were collected. Vehicle-treated 14-3-3ζ overexpressing DCIS.COM.ζ (DCIS.COM.ζ.Vehicle) tumors had significantly higher tumor growth rate compared to vehicle-treated DCIS.COM.Vec (DCIS.COM.Vec.Vehicle) tumors (Figure 25B), suggesting that overexpression of 14-3-3ζ can promote tumor outgrowth. Interestingly, AZD6244 inhibited >75% DCIS.COM.ζ tumor growth but <50% DCIS.COM.Vec tumor growth, suggesting that the 14-3-3ζ overexpressing DCIS.COM.ζ tumors were more dependent on the MEK/ERK pathway and its downstream targets. These data indicate that 14-3-3ζ overexpression-mediated tumor progression in this DCIS model can be effectively targeted by MEK/ERK inhibitor.

To determine the impact of MEK/ERK inhibitor treatment on 14-3-3ζ/ERK/CREB/ LDHA, as well as on tumor cell proliferation and apoptosis, I collected tumors from control and treatment groups. IHC showed that 14-3-3ζ overexpressing DCIS.COM.ζ tumors had increased phospho-ERK and phospho-CREB levels that correlated with higher LDHA expression compared with DCIS.COM.Vec tumors (Figure 25C) but had no significant effect on total ERK, CREB or 14-3-3ζ expression levels (Figure 24). AZD6244 treatment significantly reduced phospho-ERK, phospho-CREB and LDHA levels in DCIS.COM.ζ and DCIS.COM.Vec tumors compared to vehicle treatment (Figure 25C and Table 4). Compared to the DCIS.COM.Vec.Vehicle tumors, the DCIS.COM.ζ.Vehicle tumors showed no significant difference in apoptosis, but a singnificantly increased Ki67 positive

proliferating cells (Figure 25C and 25D), which were inhibited by AZD6244 (Figure 25C and 25D). These data indicate that AZD6244 effectively inhibit the MEK/ERK/CREB/LDHA axis and proliferation of 14-3-3ζ overexpressiong tumor cells, thereby suppressing DCIS-like tumor outgrowth.
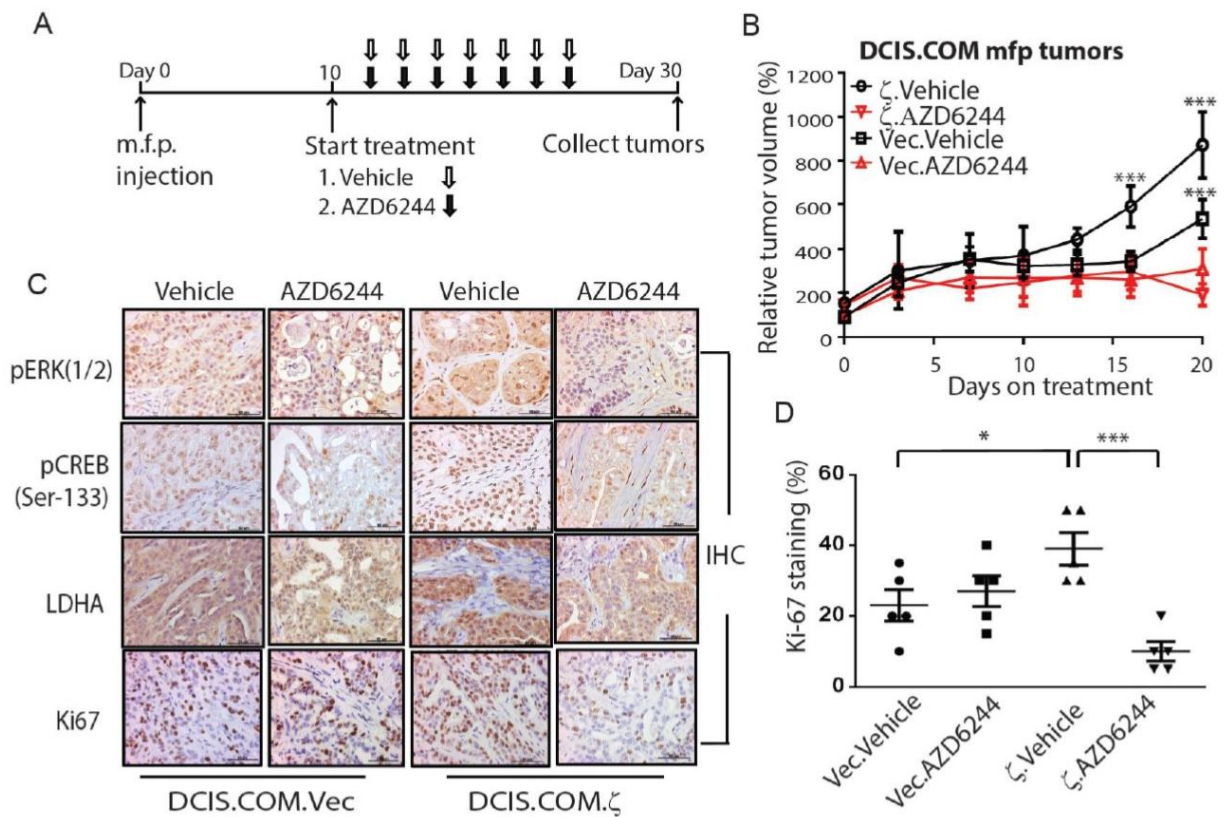
Figure 25. AZD6244 treatment inhibits DCIS.COM.ζ tumor growth. A. Experimental design of treating the DCIS.COM.Vec and DCIS.COM.ζ m.f.p. tumors in nude mice. After DCIS.COM.Vec and DCIS.COM.ζ xenograft tumors were established by day 10, mice were treated with vehicle or AZD6244 daily. B, The relative tumor volume of DCIS.COM.Vec.Vehicle and DCIS.COM.ζ.Vehicle were compared with their AZD6244

treatment groups, respectively. Bars indicate standard deviations. C, Representative images of IHC staining of phospho-ERK, phospho-CREB (Ser-133), LDHA and Ki-67 in DCIS.COM.Vec and DCIS.COM.ζ xenograft tumors from mice treated with vehicle and AZD6244. Scale bars, 50 μm. D, Quantitative analysis of Ki-67-positive cells in DCIS.COM.Vec and DCIS.COM.ζ xenograft tumors. *, $P<0.05$; ***, $P<0.001$ by the Student t-test. The data are in collaboration with Dr. Qingling Zhang.

Xenografts / Marker	DCIS.COM.Vec	DCIS.COM.ζ		
	Vehicle	Vehicle	AZD6244	P Value
14-3-3ζ	1.6±0.245	2.6±0.245	2.2±0.200	P=0.2415
pERK	1.6±0.400	2.8±0.200	1.6±0.245	P=0.0053**
pCREB	2.4±0.245	3.0±0.000	2.2±0.200	P=0.0039**
LDHA	1.6±0.245	2.6±0.245	1.6±0.245	P=0.0203*
Ki-67	23%±4.359	37%±5.831	10%±2.739	P=0.0006***
TUNEL	4±1.673	3.2±0.583	4.4±1.631	P=0.508

Table 4. Quantitative analyses of IHC staining of the ERK/CREB signaling pathways.
The IHC staining scores for 14-3-3ζ, p-CREB, LDHA were defined as 0, 1+, 2+, 3+, which indicate different level of expression. The Ki-67 index was defined as the percentage of Ki-67 positive cells on slides and the TUNEL index was counted the TUNEL positive cells on slides. *P* value was calculated between vehicle and AZD6244 treated DCIS.COM.ζ tumors. * indicates *P*<0.05, ** indicates *P*<0.01 and *** indicates *P*<0.001 by the Student t-test.

2.3.6 14-3-3ζ-LDHA axis as potential biomarkers

Having established that the 14-3-3ζ-mediated MEK/ERK/LDHA axis is potently active in nontransformed hMECs and highly correlated in early neoplastic breast lesions (R^2>0.8) (Figure 13). Next, I extended our examination by bioinformatics analysis of datasets generated from breast cancers. I found that the correlative relationship between the expression levels of 14-3-3ζ (YWHAZ) and LDHA reached R^2 of 0.31 and 0.32 (Figure 14 and Figure 15) in microarray-derived dataset GSE2109, and RNAseq-derived TCGA dataset (193, 194), respectively. The strength of such positive correlation is much weaker than that in early-stage diseases (Figure 26A), suggesting that with cancer progression into advanced stages, neoplastic cells may have metabolitically adapted to a complex tumor environment. Furthermore, when I examined LDHA levels in 14-3-3ζ overexpressing established breast cancer cell lines such as, HCC1954 HER2+ and MDA-MB-231 TNBC, I did not detect a significant up-regulation of LDHA or increase of glycolysis. These data suggest that the 14-3-3ζ/CREB/LDHA pathway may be more critical in the early-stage breast cancer initiation.

As the above bioinformatics analyses were performed on RNA data, I further evaluated the clinical relevance of 14-3-3ζ/CREB/LDHA axis at protein level using tissue microarray (TMA) of mixed stages of breast cancers. Indeed, IHC staining revealed that the 14-3-3ζ protein levels were significantly correlated with the LDHA protein levels in these breast cancer specimens (Figure 26B and Table 5). Importantly, the 14-3-3ζ expression levels were also significantly correlated with CREB phosphorylation in the consecutive TMA slides from the same group of patients (Figure 26B and Table 5).

Next, to evaluate whether 14-3-3ζ and LDHA levels hold prognostic values for breast cancer. As there is no early-lesion dataset with follow-up on clinical outcome, I instead used a breast cancer gene expression dataset (GSE3494) with disease-specific overall survival data. I found that concomitant high expression of 14-3-3ζ and LDHA predicts worse survival of breast cancer patients compared to high expression of either gene alone (P=0.00257 vs. P=0.0127 and P=0.0322) (Figure 26C). Furthermore, the 5-year survival rate for patients with concurrent high expression of both 14-3-3ζ and LDHA genes dropped almost 10% compared to high expression of either gene alone (Figure 26C). Continued, these data suggest that the expression levels of 14-3-3ζ and LDHA have a more power in predicting the clinical outcome of breast cancer patients. It is possible that 14-3-3ζ and LDHA expression levels together may have an even stronger power in predicting the clinical outcome of early-stage disease progression in patients, which should be investigated in future studies.
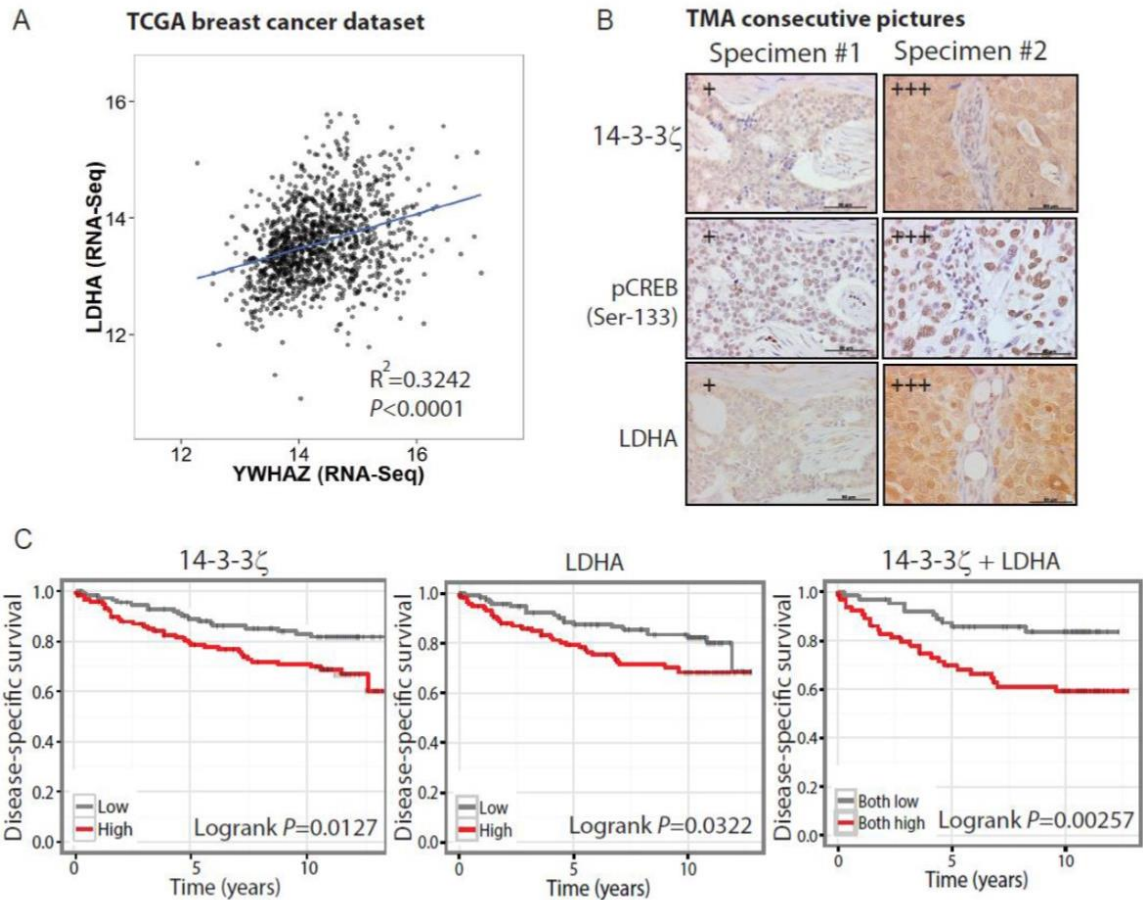
Figure 26. 14-3-3ζ-LDHA signaling axis holds prognostic value in predicting clinical outcome. A, Linear regression of the LDHA and 14-3-3ζ (YWHAZ) expression values in the TCGA breast cancer dataset. The square of Pearson coefficient R^2 is 0.324 and $P<0.0001$. B, Representative images of IHC staining of 14-3-3ζ, phospho-CREB (Ser-133) and LDHA, in a 208-core human breast cancer tissue microarray (TMA). A total of 187 (89%) cores were eligible for scoring and examined for the association of 14-3-3ζ and phosphor-CREB; a total of 183 (88%) cores were examined the association of 14-3-3ζ and LDHA. The IHC staining scores for 14-3-3ζ, p-CREB, LDHA were defined as 0, 1+, 2+, or 3+, where 3+ indicates higher positive expression; and 1+ indicates lower

positive expression. Scale bars, 50 µm. C, Kaplan-Meier survival curve of breast cancer

patients (GSE3494). Concomitant high expression of 14-3-3ζ and LDHA (logrank P<0.01)

predicts worse outcome than high 14-3-3ζ (YWHAZ) expression level (logrank P<0.05)

or high LDHA expression level (logrank P<0.05). The data are in collaboration with Dr.

Qingling Zhang and Dr. Hai Wang.

	14-3-3ζ expression						
Marker	0	1+	2+	3+	*P* value	R^2	N
LDHA expression							
0	4.2%	4.2%	5.3%	0.0%			
1+	5.3%	12.9%	10.6%	2.6%	0.047*	0.242	187
2+	6.4%	16.5%	9.6%	5.8%			
3+	1.6%	5.8%	3.7%	4.2%			
pCREB expression							
0	9.6%	5.5%	9.3%	0.5%			
1+	0.0%	9.8%	9.3%	4.4%	0.0006***	0.245	183
2+	0.0%	6.6%	9.8%	6.0%			
3+	3.8%	8.2%	12.0%	5.5%			

Table 5. Analyses of 14-3-3ζ association with LDHA and pCREB (Ser-133) in consecutive tissue microarray (TMA) slides. A total of 187 (89%) specimens were examined the association between 14-3-3ζ and LDHA; and a total of 183 (88%) specimens were examined the association between 14-3-3ζ and phospho-CREB (Ser-133). The square of Pearson coefficient R^2 is 0.242 between 14-3-3ζ and LDHA; and R^2 is 0.245 between 14-3-3ζ and phospho-CREB. The IHC staining scores for 14-3-3ζ, p-CREB, LDHA were defined as 0, 1+, 2+, 3+, which indicate different level of expression. The square of Pearson coefficient R^2 were calculated and indicated the correlation relationship. *P* value was calculated by Chi-square analysis. * indicates *P*<0.05 and *** indicates *P*<0.001 by Student t-test.

2.4 Conclusions

Mammary tumor progression manifests ten hallmarks of cancers, of which metabolic dysregulation is an important tumor-specific alteration (8, 212). Understanding the intrinsic link between cancer progression and metabolic alteration could be further developed into a promising "metabolic therapy" approach for cancer prevention or treatment (212, 213). The Warburg effect is a general phenomenon in cancer cells that fuels a high rate of glycolysis in order to produce biological intermediates for biosynthetic pathways, satisfying the cells' needs for active proliferation. Recent studies indicate that metabolic alteration may already occur at the early-stage of neoplasms and contribute to early transformation (103, 171). Understanding cancer cell metabolism may improve early identification and diagnosis for breast cancer treatment (214). Previously, Dr. Jing Lu's work (previous postdoc in my laboratory) have identified that 14-3-3ζ is a critical mediator to cooperate with receptor tyrosine-protein kinase 2 (ErbB2) to increase the transition of ductal carcinoma in situ (DCIS) to invasive breast cancer (162). The work in this chapter now demonstrates that overexpression of 14-3-3ζ in human breast epithelial cells upregulates LDHA, contributing to shift metabolic flux toward aerobic glycolysis, thereby facilitating cancer initiation and progression (Figure 27)

A bioinformatics analysis of datasets generated from premalignant breast lesions found that the expression level of 14-3-3ζ (YWHAZ) is highly correlated with LDHA ($R^2 > 0.8$) (Figure 13), however, when the disease progressed into late stages of breast cancer, the correlation between the 14-3-3ζ and LDHA become very weak. R^2 is 0.32 and 0.31 in TCGA invasive breast cancer dataset (193) and human breast cancer dataset (GSE2109), respectively (Figure 14 and Figure 15) (194). The data indicate that 14-3-3ζ-

mediated LDHA upregulation may be critical for early transformation features, but may be less desired for late stages of breast cancer for adaptation in a more complex tumor environment. Nonetheless, concurrent high expression of 14-3-3ζ and LDHA can still hold prognostic values for disease-specific overall survival for breast cancer (Figure 26C). A similar phenomenon was observed in the *in vitro* models. My works found that 14-3-3ζ overexpression clearly induced upregulation of LDHA and aerobic glycolysis in the hMEC and MCF10DCIS.COM cells that mimic the early-stage development of breast cancer. Intriguingly, further overexpression of 14-3-3ζ in aggressive human breast cancer cell lines HCC1954 (HER2 overexpressing breast cancer) and MB-MDA-231 (triple-negative breast cancer) did not lead to significantly higher LDHA levels or glycolytic activity. The findings suggest that 14-3-3ζ overexpression-induced metabolic dysregulation may be an early event during breast cancer initiation and progression, which may serve as a metabolic therapy target for early intervention.

A genome-wide promoter analysis has reported that *LDHA* is a CREB's target gene due to the conserved *c-AMP* response element (CRE), TGACGTCA on LDHA promoter, which is evolutionarily preserved either within 1000-bp upstream of the ATG start codon or within 250-bp of the 5'-UTR element in mouse and human genome (215). Transfecting the 65bp region with CRE binding site in 10A.ζ showed significantly higher luciferase activity than those with the 2000-bp promoter region (Figure. 21A), which suggests that CRE binding sequence is critical for LDHA transcription in 14-3-3ζ-overexpressing hMECs. Although CREB activation has been reported to be involved in multiple signaling transduction (216), my work is the first to demonstrate that 14-3-3ζ overexpression-mediated LDHA upregulation is through activation of MEK/ERK/CREB

signaling, which is important for early transformation and cancer initiation phenotype. Despite c-Myc has been reported as a master mediator for modulating LDHA expression in cancer (95, 217), my data suggest that CREB is a key transcription factor to induce expression of LDHA in 14-3-3ζ-overexpressing hMECs. Remarkably, the expression of 14-3-3ζ is strongly associated with the LDHA protein expression and CREB phosphorylation level in tissue microarray (TMA) with various stages of breast cancers, which validates and determines the importance of our findings.

Cancer cell metabolism is a cancer hallmark (218, 219), which provides different intermediates for cell survive and growth. Targeting aberrant metabolism becomes a potential therapeutic strategy (181, 220). However, unlike other targeted therapy which could easily distinguish between normal tissues and cancerous tissues in the body, a metabolic therapy may lead to high toxicity in tissues and adverse effects by patients. Therefore, the dose-limiting toxicity may be a challenge and need further investigation along metabolic drug development (114, 115, 221). After establishing the functional roles of the 14-3-3ζ/LDHA axis in 14-3-3ζ-mediated glycolysis, further inhibition of MEK/ERK pathway with AZD6244 leads to significantly reduced LDHA expression and tumor inhibition. The LDHA inhibitor Gossypol (AT-101) has already yielded encouraging results in multiple clinical trials (181-183), which may be worthy to further investigate in the future.

Many lines of study revealed that 14-3-3ζ is involved in numerous cellular pathways including therapy resistance, lipid metabolism, anti-apoptosis function, and metastasis (154, 222-224). This work suggest a novel link between 14-3-3ζ and cancer cell metabolism. In summary, my work demonstrate that 14-3-3ζ is a critical mediator of glycolysis, which may contribute to initiation, early transformation and progression of

breast cancer. The data in hMEC-derived DCIS preclinical model suggest that intervening 14-3-3ζ-mediated activation of MEK/ERK pathway can significantly reduce tumor growth. These findings have now provided new insights into the mechanistic understanding of 14-3-3ζ overexpression-mediated early transformation, which may serve as new biomarkers and therapeutic targets for early intervention in the clinic.

Since that chapter 2 has addressed the role of 14-3-3ζ in breast cancer initiation, the next chapter (chapter 3) will further focus on the investigation of the pathological role of 14-3-3ζ in breast tumor growth and progression.
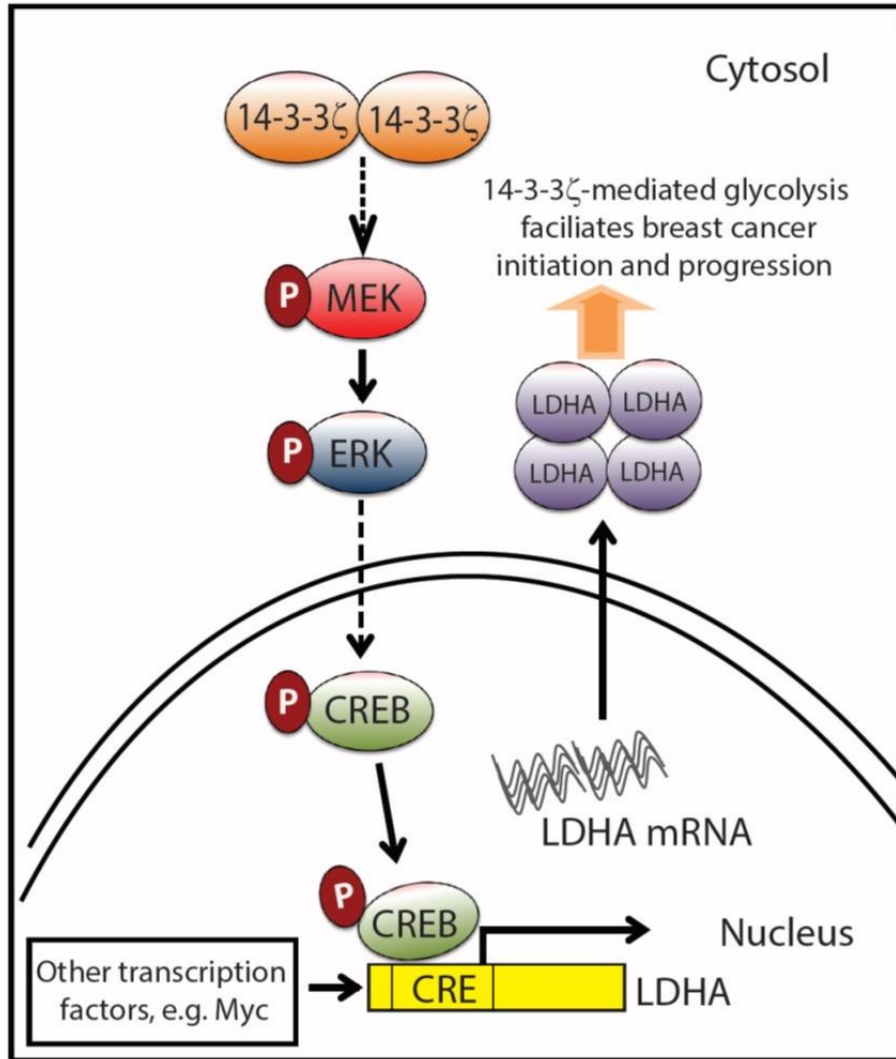
Figure 27. **Proposed model of 14-3-3ζ overexpression facilitates breast cancer tumorigenesis.** Schema showing that 14-3-3ζ overexpression activates the MEK/ERK/CREB pathway and transcriptionally upregulates LDHA which contributes to increasing glycolysis and promotes cancer initiation and growth. Dotted arrow points out that other transcription factors including Myc can regulate LDHA gene expression (95), reprogram cancer metabolism and contribute to cancer pathogenesis as well. 14-3-3ζ-

mediated LDHA upregulation shows the novel functional role of 14-3-3ζ in mediating metabolic dysregulation in cancer.

Chapter 3

**THE MIF-CXCR2-IL8 PATHWAY IS REQUIRED FOR 14-3-3ζ–
HIGH TUMOR CELLS TO INDUCE CELL COMPETITION**

3.1 Introduction

3.1.1 Clonal selection and tumor heterogeneity

Cancer is an evolutionary process of cell clone selection and expansion (116, 117); over time, a clone population arises with an increase in competitive abilities and fitness advantages and out-competes other tumor subclones for the limited space and resources within tumors (118). Somatic mutation, epigenetic dysregulation, cellular context and microenvironment stress contribute to different levels of positive selection of clones for fitness, which results in tumor heterogeneity (118, 119). Tumor heterogeneity explains the cellular complexity and dynamics that challenge current therapeutic strategies and alter treatment effectiveness (123). Understanding clonal evolution and dynamics of cell fitness may improve targeted therapy efficacy and enable efficient intervention in tumor progression.

3.1.2 Overview of cell competition

Cell competition is a type of cell-cell interaction that was originally described in Drosophila melanogaster development and is evolutionarily conserved in mammals (225, 226). The cell competition is initiated when cell populations ("loser" or "unfit" cells) are surrounded by better competing cell populations ("winner" or "fit" cells), thereby triggering winner-cell-induced apoptosis (227). Interestingly, loser cells can be viable in a homotypic environment, which means that the cell death is caused by the percentage of surrounding fit cells (225). The mechanism underlying winner-loser competition is that the winner cells contain better proliferative capacity and eliminate loser cell through inducing apoptosis, perhaps and most likely, through cell–cell contact-dependent signaling. Cell competition

is not limited to the defect in the *Minute* gene described in Drosophila; certain genes, such as dmyc, when their overexpression level is above that of the surrounding cells, can transform wild-type cells into super-competitors and eliminate neighboring cells (228-230). Cell competition has emerged in both tumor suppressor and oncogene function. Previous studies have shown that failure to substitute deficient T cell progenitors with healthy bone marrow progenitors results in T-lineage acute lymphoblastic leukemia (T-ALL) (231, 232). Those studies reveal that cell competition is a powerful tissue surveillance mechanism that prevents tumor formation from unfit cells. In addition to such protective efforts, cell competition could be exploited by oncogenes and critical for early-stage cancer initiation and development (233-236). Other signaling, such as Warts/Hippo pathway and Myc, have been shown to modulate tumor growth in Drosophila (237); Especially Myc, one of the well-characterized models in Drosophila, was further implied to drive cell competition in human cancers (238). It remains elusive how human cancer cells acquire the cell competition mechanism for tumor growth and survival during cancer development.

3.1.3 14-3-3ζ and cell competition mechanism

14-3-3ζ belongs to a highly conserved protein family and modulates numerous pathways in cancer (157). 14-3-3ζ may be relevant to cell competition because many of the 14-3-3ζ-mediated cellular networks have been shown to be involved in regulation of cell competition. In neoplasms, 14-3-3ζ overexpression induces aerobic glycolysis through upregulation of LDHA (159); leads to Akt phosphorylation by activation of the PI3K pathway (161); and destabilizes the p53/Smads complex by binding to YAP-1 (154). In cancers, 14-3-3ζ overexpression enhances MAPK/c-Jun signaling (163) and regulates tumor immune response by modulation of multiple cytokines' expression (164, 165).

Interestingly, quite a number of 14-3-3ζ-mediated cellular networks have been reported as involved in cell competition, such as the Hippo pathway, JNK pathway and PI3K-Akt pathway (166). These results suggest that cancer cells with high 14-3-3ζ expression may hijack cell competition machinery from the developmental stage to promote cancer initiation and progression.

3.1.4 Hypothesis

14-3-3ζ overexpression occurs at the early neoplastic stage of breast disease and persists throughout breast cancer progression (167). I therefore sought to examine the role of 14-3-3ζ in cell competition. I found that 14-3-3ζ expression was greatly heterogeneous at the neoplastic stage of breast cancer; as disease progressed, the expression expanded to 100% of tumor. 14-3-3ζ preferentially accumulated during breast cancer development. I therefore hypothesized that tumor cells selectively preserve high 14-3-3ζ expression and may take over the tumor population through regulating the cell fitness mechanism. I identified that cells expressing different levels of 14-3-3ζ responded inversely upon macrophage inhibitory factor (MIF) stimulation. 14-3-3ζ-high-expressing cells can efficiently sequester MIF in a ligand-limited tumor environment, and reduction of MIF stimulation in 14-3-3ζ-low cells led to cell death and gradual elimination of the cells from tumors. Taken together, my findings establish a novel role for how 14-3-3ζ exploits the inflammatory pathway to drive cell competition and eradicate loser cells. This proof-of-concept study shows that cancer is a disease caused by cell competition. Targeting mechanisms underlying cell competition may reduce oncogene-mediated cell fitness and be a potential therapeutic strategy to further inhibit tumor growth.

3.2 Materials and Methods

3.2.1 Cell lines and cell culture

HCC1954, HCC70, Hs 578t and BT549 cells were obtained from American Type Culture Collection (ATCC) and were cultured in DMEM/F-12 media (Caisson Laboratories, USA) supplemented with 10% fetal bovine serum. Cell lines were authenticated and characterized by the Characterized Cell Line Core Facility at MD Anderson Cancer Center.

3.2.2 Plasmids and shRNAs

Green and red fluorescent protein were constructed into pLOVE lentivirus-based vectors (Addgene). To produce lentiviral virus, all shRNA vectors and pLOVE vectors were transfected into 293FT cells together with second-generation lentiviral plasmids, pMD2.G and psPAX2 (Addgene), through a LipoD293 DNA in vitro transfection Ver. II kit (SignaGen Laboratories, USA) according to the manufacturer's protocol. Lentiviral supernatants were collected 48 hours after transfection. Lentiviral particles were precipitated and concentrated by PEG-it virus precipitation solution (SBI System Biosciences, USA) and freshly used to transduce cells in the presence of 8 µg/ml polybrene. For 14-3-3ζ-knockdown lines, cells were transfected with 14-3-3ζ shRNA (clone, NM_003406.2-418s1c1 or NM_003406.2-738s1c1, Sigma) or non-targeting scrambled shRNA (pLKO.1-puro #SHC002, Sigma) and selected with 2 µg/ml puromycin.

For IL-8-knockdown cell lines, HCC1954.Ctrl cells were transfected with IL-8 shRNA (NM_000584.2-727s1c1) or non-targeting shRNA (pLKO.1-puro) and selected with 3 µg/ml puromycin.

3.2.3 3D cell-culture system

Cells were cultured in DMEM/F-12 medium supplemented with 10% fetal bovine serum and 10% Matrigel (BD Biosciences, USA) and grown in Costar's clear flat-bottom ultra-low-attachment plates (Corning, USA) to mimic the natural tissue environment. Fresh media were added into each culture well every 3 days.

3.2.4 Reagents and chemicals

Recombinant human CXCL8 and MIF proteins were obtained from R&D Systems (Cat. 208-IL-010 and 289-MF-002). CXCR2 inhibitor SB225002 (Cat. sc-202803A) and MIF antagonist ISO 1 (ab142140) were purchased from Santa Cruz Biotechnology and Abcam, respectively. Both CXCR2 and MIF were freshly dissolved in 10% DMSO for animal treatment experiments. For cell death staining experiments, 4,6-diamidino-2-phenylindole (DAPI, D1306) and SYTOX Red dead-cell stain (Cat. S34859) were purchased from Thermo Fisher Scientific. 5-Bromo-2-deoxyuridine (BrdU), hyauronidase type IV-S (H3884-50 mg), hyauronidase I-S (H3506-500 mg), hyauronidase VIII (H3757-100 mg) and propidium iodide (PI) were obtained from Sigma. Collagenase A (Cat. 10103578001) was purchased from Roche.

3.2.5 BrdU incorporation and detection assay

In vitro: 5 mg/ml BrdU stock solution was prepared by dissolving 5 mg of BrdU in 1 ml sterilized phosphate-buffered saline (PBS, pH 7.4). 10 μl of BrdU stock solution was added into cell culture for 1 to 3 hours before cell fixation and permeabilization steps. In vivo: 10 mg/ml BrdU stock solution was prepared in sterilized PBS solution. Mice were given 1 mg BrdU through intraperitoneal (i.p.) injection for 3 times during 3 consecutive hours a day before tumor collection. Meanwhile, mice also fed with 1 mg/ml of BrdU water supplemented with 5% sucrose for 24 hours before tumor collection. Both in vitro and in vivo tumor cell BrdU staining and detection procedures were described previously.(239, 240)

3.2.6 Real-time PCR analyses

Total RNA from cells was isolated with Trizol reagent (Life Technologies). cDNA was generated by an iScript cDNA Synthesis Kit (Bio-Rad) following the manufacturer's protocol. mRNA expression levels of 14-3-3ζ, IL-8, CXCR2, MIF and IL-1β were determined by qRT-PCR using a KAPA PROBE Fast qPCR Kit (KAPA Biosystems) and TaqMan primers (Hs03044281_g1, Hs00174103_m1, Hs01891184_s1, Hs00236988_g1 and Hs00174097_m1) and normalized to 18S rRNA endogenous control (#4310893E).

3.2.7 Cell cycle analysis

Cells were harvested and fixed with ice-cold 70% ethanol at least 24 hours before cell cycle analysis. Every cell sample was washed twice with PBS to remove ethanol and incubated with 500 µl PI DNA staining solution (5 µl of a 100 µg/ml RNase stock, 50 µl of a 10 mg/ml bovine serum albumin stock, 25 µl of a 1 mg/ml propidium iodide (PI) stock and 420 µl ddH$_2$O) for 1 hour protected from light. The PI signal, which represents different stages of the cell cycle, was measured by the Canto II FACS system (BD) and analyzed by FlowJo software.

3.2.8 Annexin V staining and apoptosis assay

Cells were harvested and washed twice with Phosphate buffered saline (PBS) before suspending with 100 µl of 1X binding buffer (Cat. 556454, BD Biosciences) containing 5 µl of Pacific blue–labelled anti–Annexin V antibody and 1 µl of SYTOX Red dead-cell stain. Early and late apoptotic events were measured by flow cytometry system (BD) and analyzed by FlowJo software (http://www.flowjo.com/).

3.2.9 Cytometric Bead Array (CBA) analyses

The human inflammatory cytokine CBA kit (Cat. 551811, BD Biosciences) is a panel of six cytokines or chemokines for detection of protein expression levels in a sample. The required sample volume is about one-sixth of the volume used in conventional ELISA. Cell lysates or tumor fluids were first incubated with six-bead populations, which were coated with antibody specific for capture of IL-8, IL-1β, IL-6, IL-10, TNF and IL-12p70 proteins. Samples were then washed, measured and analyzed following the

manufacturer's instructions. The measurement and data analyses were done by a LSR II flow cytometry system and FCAP Array v3.0 Software (BD Biosciences).

3.2.10 Gene expression profiling

ζ-high, ζ-low and HET xenograft tumors were chopped into small pieces using blades and then transferred into a 15 ml tube to incubate with 3 ml digestion buffer at 37 °C for 15 minutes to generate a single-cell suspension. Digestion buffer was made by cell recovery solution (Cat. 354253, Corning), Trypsin-EDTA (25200-056, Thermo Fisher Scientific) and DMEM/F12 medium with a 2:1:1 ratio and supplemented with 1 mg/ml hyaluronidase and 1 mg/ml collagenase A. The dead cells in single-cell suspension were removed by the Dead Cell Removal Kit (Miltenyi Biotec) according to the manufacturer's instructions. FACS was then performed to sort out GFP+ (shCtrl) and TdR+ (shζ) cells from the live-cell fraction. Total RNA in GFP+ and TdR+ cells was extracted using a PureLink® RNA Mini Kit (Thermo Fisher Scientific). All RNA samples meet the quality criteria: OD260/280 ≥1.7, OD260/230 ≥1.5, RNA integrity number (RIN) ≥7 and concentration ≥33 ng/µL. Gene expression profiling of 12 samples was done on a HumanHT-12 v4 Expression BeadChip, which targets more than 47,000 probes (Illumina).

3.2.11 ELISA

Human IL-1β protein, human IL-8 protein and human active MIF protein were quantified by using ELISA kits (Cat. 447007, Cat. 431504, Cat. 438407; Biolegend) following the manufacturer's protocol.

3.2.12 Human cytokine array

35 µl of *in vivo* tumor fluids from HCC1954.shCtrl and HCC1954.shζ cells were assessed with human cytokine array panel A (Cat. ARY005, R&D Systems) following the manufacturer's procedure. Each dot represents a specific protein expression, which was quantified by ImageJ software (https://imagej.nih.gov/ij/).

3.2.13 Animal studies and drug treatment

All mouse experiments were performed following protocols approved by MD Anderson's institutional animal care and use committee. Tumor xenografts were established by injecting 1×10^6 HCC1954 subline cells in a 50 µl mixture of DMEM/F-12 and Matrigel (BD Biosciences) with a 1:1 ratio orthotopically into the m.f.p. in SWISS$^{nu/nu}$ mice, which were obtained from the Department of Experimental Radiation Oncology at MD Anderson. Tumor volume (V) was measured weekly after transplantation, and calculated using the formula: $V = \text{length} \times (\text{width})^2/2$ (200). To evaluate the potential therapeutic effect in mice, the dosage of ISO 1 (20 mg/kg) and SB225002 (2.5 mg/kg) were adjusted and followed studies described previously (241-243). To assess shCtrl-to-shζ cell ratio in tumors, we processed tumor using the methods described in the section "Gene expression profiling" and analyzed the GFP+ to TdR+ cell ratio, which indicated shCtrl and shζ, respectively, by flow cytometry.

3.2.14 Tissue specimens for 14-3-3ζ expression analysis

Tissue specimens including atypical ductal hyperplasia (ADH; 42 cases), DCIS (44 cases), and invasive ductal carcinoma (48 cases) were collected and processed in compliance with protocols (LAB10-0995) approved by the IRBs of MD Anderson Cancer Center and Southern Medical University (China), which was described previously (154). Consent forms were obtained from all patients. IHC staining of 14-3-3ζ expression was performed following procedures described in the section "IHC analyses". The percentage of 14-3-3ζ expression in every tissue slide was assessed and analyzed by a pathologist (Dr. Qingling Zhang MD).

3.2.15 Antibodies

We used the following antibodies for IHC staining and western blotting: anti–14-3-3ζ, anti-MIF, and anti-GAPDH (clone C-19, clone FL-115 and clone G-9 respectively, Santa Cruz Biotechnology); anti–β-actin (Sigma); anti-BrdU (Abcam); anti–red fluorescent protein (tdRed) (Rockland); anti-GFP, anti–phospho-Akt, anti-Akt, anti–phospho-c-Jun, anti–c-Jun, anti–cleaved caspase 3, anti–phospho-p38 MAPK (Thr180/Tyr182), anti–phospho-STAT1 (Tyr 701), anti-STAT1, and anti–c-IAP2 (catalog no. 2955, 4060, 2920, 3270, 9165, 9664, 4511, 9167, 14994 and 3130, respectively; Cell Signaling Technology); and anti–minichromosome maintenance 2 (MCM2) (clone EP40, Epitomics). For flow cytometry analyses, PE/Cy7- or APC-labelled anti–human CD182 (CXCR2) antibody, PE/Cy7-labelled anti–human CD184 (CXCR4) antibody and APC-labelled anti-BrdU antibody were purchased from BioLegend; Pacific blue–labelled anti–Annexin V was purchased from Thermo Fisher Scientific. The optimal antibody dilutions for IHC is 1:100; for western blotting is 1:1000.

3.2.16. Immunoblotting

Western blot samples including mouse xenograft tumors and cell lysates were prepared in RIPA buffer (10 mM Tris-Cl (pH 8.0), 1 mM EDTA, 0.5 mM EGTA, 1% Triton X-100, 0.1% SDS, 140 mM NaCl and 1x protease inhibitor). Immunoblotting was done as previously described (162) using antibodies listed in the "Antibodies" paragraph above.

3.2.17 IHC analyses and tissue microarray (TMA)

Mouse tumors were collected and embedded in paraffin following standard pathological procedures. Antigen retrieval and IHC analyses were performed as described previously (154). To achieve double IHC staining of proliferation marker BrdU or apoptotic marker cleaved caspase 3 together with staining for GFP and TdR expression, AEC substrate-chromogen (Dako) and DAB substrate-chromogen (Dako) were used following the manufacturer's procedures. AEC substrate-chromogen stained as pink to indicate GFP or TdR expression; DAB substrate-chromogen stained as brown to indicate the expression levels of BrdU or cleaved caspase 3. Antibodies for IHC double staining were listed in the "Antibodies" paragraph above. To assess the clinical relevance, we stained 14-3-3ζ and CXCR2 in a 70-case, 208-core breast cancer tissue microarray (catalog no. BR2085a trial, US Biomax Inc.), which contained normal breast tissue and different grades of breast cancer tissues. The scores for staining power were identified by pathologist Dr. Qingling Zhang as 0, 1+, 2+, or 3+, with 3+ indicating higher expression and 0 indicating no expression.

3.2.18 Statistical analyses

GraphPad Prism 6 and IBM SPSS Statistics 19 were used to analyze data. A Pearson's correction was used to investigate whether the expression levels of 14-3-3ζ and CXCR2 are positively correlated. Differences between groups were assessed using the Student's t test or ANOVA and were considered significant if P values were less than 0.05.

3.3 Results

3.3.1 Cells with higher 14-3-3ζ expression induce cell competition

14-3-3ζ expression is associated with disease progression, metastasis and poor survival (157, 158). In breast cancer, 14-3-3ζ was overexpressed in pre-cancerous breast lesions and was persistently overexpressed throughout disease progression (158). To gain insight into the 14-3-3ζ expression pattern during breast cancer progression, I detected 14-3-3ζ expression by IHC staining of specimens of different stages of breast cancer. Fascinatingly, 14-3-3ζ expression was highly heterogeneous at early neoplastic stages such as atypical ductal hyperplasia (ADH) and DCIS (Figure 28A); however, as disease progressed into invasive ductal carcinoma (IDC), the 14-3-3ζ expression expanded to up to 100% of tumor cells (Figure 28B). This result suggests that 14-3-3ζ expression is favorably enriched and may benefit cell survival during tumor progression.

To examine the oncogenic function of 14-3-3ζ in a relatively early stage of breast cancer, I knocked down 14-3-3ζ in HCC1954 cells (HCC1954.shζ), a cell line derived from stage IIA breast cancer (Figure 29A) (244, 245). HCC1954.shζ cells and vector control cells were labelled with red (TdR) and green fluorescence protein (GFP), respectively. To mimic the clinical scenario of heterogeneous cell types, I mixed 14-3-3ζ knockdown cells (shζ.TdR) and control cells (shCtrl.GFP) in a 1:1 ratio and orthotopically transplanted them into mouse mammary fat pads (m.f.p.) to form HET tumors (Figure 29B). Similar to what I observed in breast cancer patients, shCtrl.GFP cells always colonized the whole tumor population at the end stage of the tumorigenicity assay (Figure 29C). To avoid dye bias and to assess replicability of the study, a further dye-swap experiment was performed, and I observed an analogous phenomenon; again, 14-3-3ζ-high cells

(shCtrl.TdR) surpassed tumor populations at the late stage of the tumorigenicity assay (Figure 29C). In addition, there was no significant difference in terms of tumor growth between shCtrl (14-3-3ζ-high or "ζ-high") and shζ (14-3-3ζ-low or "ζ-low") tumors when they grew individually (Figure 29D). These data suggest that when shζ cells grew with shCtrl cells a distinct cell growth rate and cell death mechanism were induced in HET tumors.

To investigate when the cell-ratio change occurred in HET tumors, I analyzed the shCtrl-to-shζ ratio through GFP-to-TdR signal ratio by flow cytometry every consecutive week after xenograft implantation. At week 5, the shCtrl-to-shζ ratio amplified to 2.8, and it gradually increased to 8 at week 8 (Figure 30A). Yet individually grown ζ-high and ζ-low tumors maintained a similar growth rate, even when I directly dissect the tumor growth rate into cell number level (Figure 29D). Next, further examined the weekly shCtrl-to-shζ ratio of cells freshly extracted from individually grown ζ-high and ζ-low tumors, the shCtrl-to-shζ ratio maintained a ratio close to 1 throughout the assay (Figure 30A). These data suggest that when shCtrl and shζ cells grow together, the growth rate gradually changes in both cells. Intriguingly, I did not observe a significant difference in tumor size between HET tumors and individually grown ζ-high and ζ-low tumors (Figure 29D). The data indicate that shCtrl (14-3-3ζ-high) cells may induce cell death in shζ (14-3-3ζ-low) cells, thereby slowly changing the composition ratio of shCtrl and shζ cells in HET tumors. This cell competition mechanism seems to be preserved in the fly, in which integrity of tumor size was maintained under 14-3-3ζ variation (234).
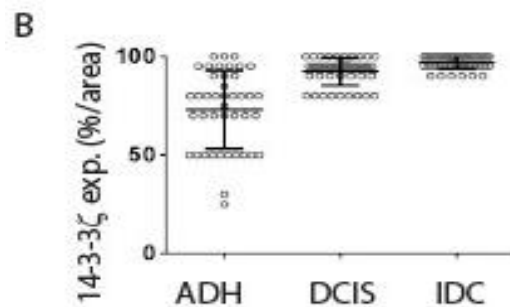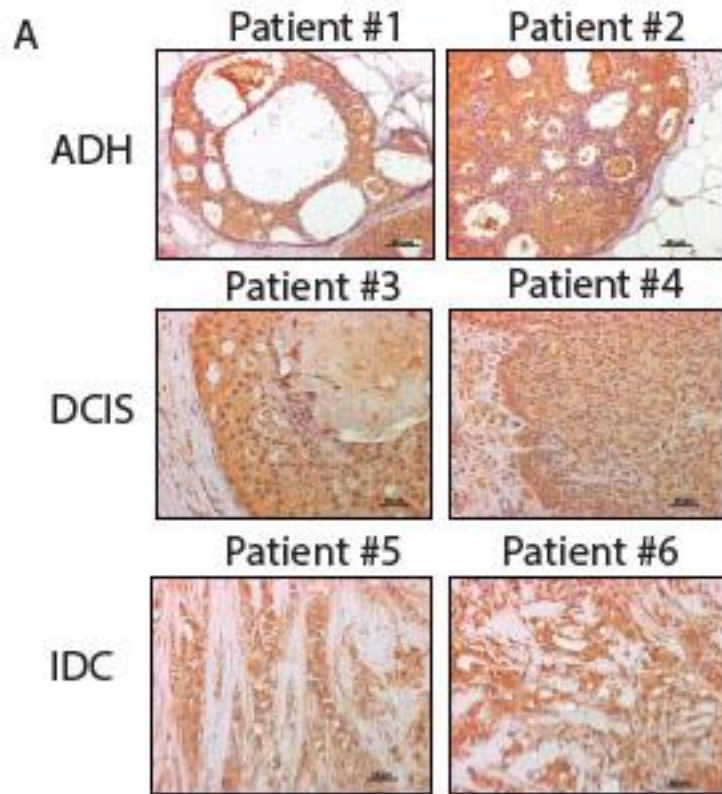
Figure 28. 14-3-3ζ overexpression is selectively elevated during breast cancer progression. A, Representative IHC staining for 14-3-3ζ in specimens from patients with different stages of breast cancer. ADH: atypical hyperplasia, DCIS: ductal carcinoma in situ, IDC: invasive ductal carcinoma. B, Percentage of tissue containing 14-3-3ζ expression in specimens from different stages of breast neoplasia. ADH, n=42; DCIS, n=44; IDC, n=48. The data are in collaboration with Dr. Qingling Zhang.
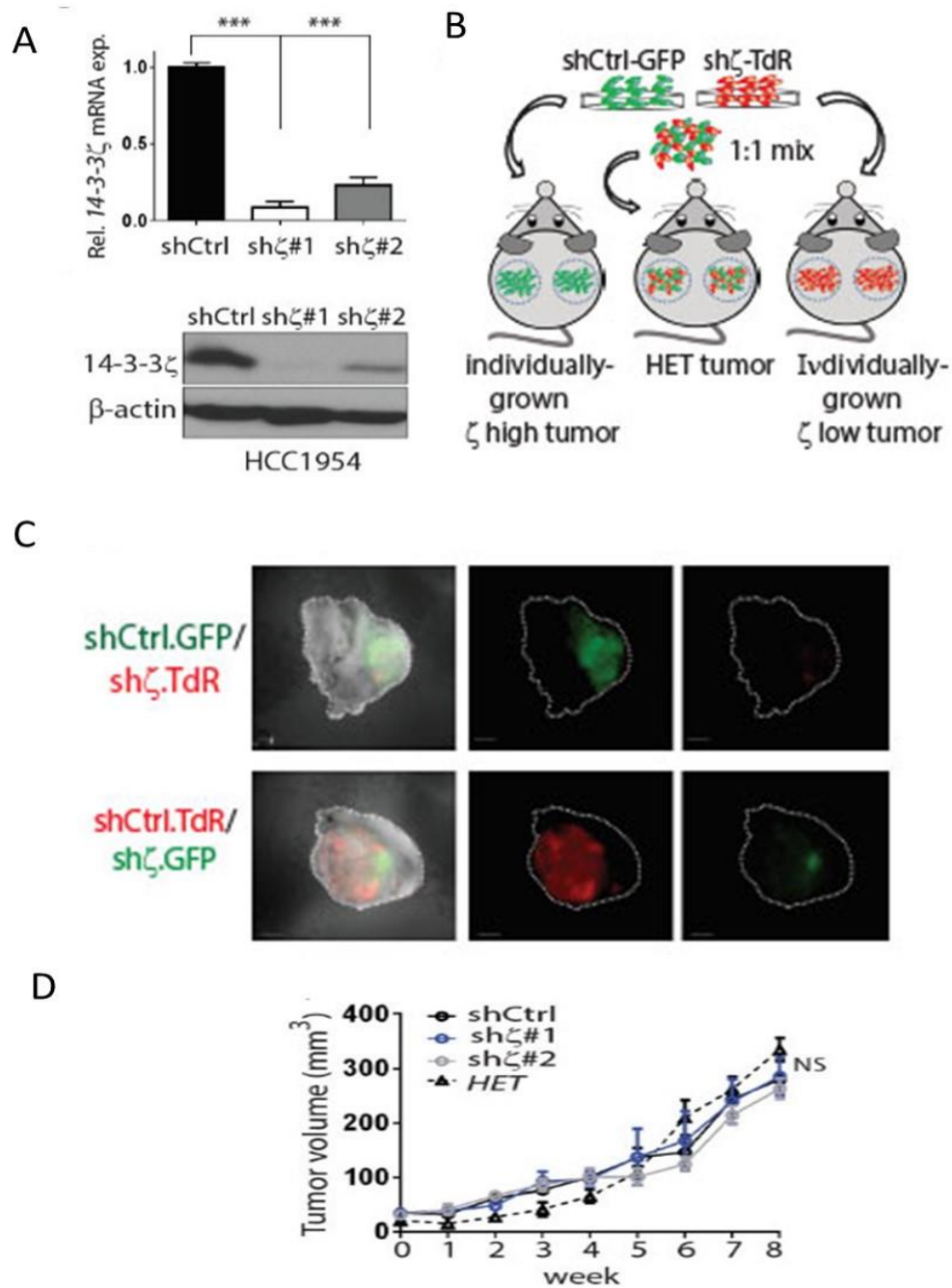
Figure 29. 14-3-3ζ high breast cancer cells have growth advantages in a HET tumors. A, Upper, qRT-PCR analysis of relative 14-3-3ζ mRNA expression in HCC1954 sublines was normalized by 18S rRNA expression. Bottom, western blotting of 14-3-3ζ

proteins in HCC1954 sublines. Schematic summary of individually grown ζ-high and ζ-low tumors, as well as HET tumor. B, HET tumor contains ζ-high and ζ-low cells implanted in a 1:1 ratio into m.f.p. to form tumor xenografts with heterogeneous 14-3-3ζ expression. C, Images of late-stage tumors at week 8. Top panel, shCtrl (GFP+) mixed with shζ (TdR+) cells to form HET tumor; bottom panel, dye-swap experiment with shCtrl (TdR+) mixed with shζ (GFP+) to form HET tumor. D, The tumor volumes of shCtrl, shζ#1, shζ#2 and HET tumors were measured every week after xenograft implantation.

To demonstrate cell proliferation and apoptosis in shCtrl and shζ cells from HET tumors, I performed IHC double staining for a proliferation marker (bromodeoxyuridine, BrdU) and an apoptosis marker (cleaved caspase 3) along with GFP or TdR staining. I analyzed the percentage of proliferative and apoptotic events in shCtrl (GFP positive staining) and shζ cells (TdR positive staining) at different time points of tumor progression. From week 4 to 8, shCtrl cells showed an increase in proliferation compared to shζ cells (Figure 30B), whereas from week 6 to 8, shζ cells showed an increase in apoptosis compared to shCtrl cells (Figure 30C). However, there was no significant difference in terms of proliferation and apoptosis between shCtrl and shζ cells in their individually grown ζ-high and ζ-low tumors (Figure 30D and 30E). To further detect which stages of apoptosis in shζ cells was altered by shCtrl cells, I stained cells extracted from HET tumors with apoptotic markers (Annexin V and Sytox Red DNA dye). Interestingly, shζ cells had increased late-stage apoptotic cells compared to shCtrl cells in HET tumors (Figure 30F). To confirm the results of cell proliferation between shCtrl and shζ cells in HET tumors, I stained shCtrl and shζ cells with BrdU along with GFP and TdR and then quantified the percentage of co-localization signal. Indeed, similar to the results of the IHC double staining data (Figure 30B), cell proliferation was increased in shCtrl cells compared to shζ cells (Figure 30G). Taken together, the data indicate that 14-3-3ζ mediates cell competition by increasing cell proliferation in 14-3-3ζ-high cells (winner cells) while increasing cell apoptosis in 14-3-3ζ-low cells (loser cells). 14-3-3ζ-low cells were gradually eradicated by 14-3-3ζ-high cells, which then proliferate to fill the space and gap left by the disappearing loser cells (Figure 31).
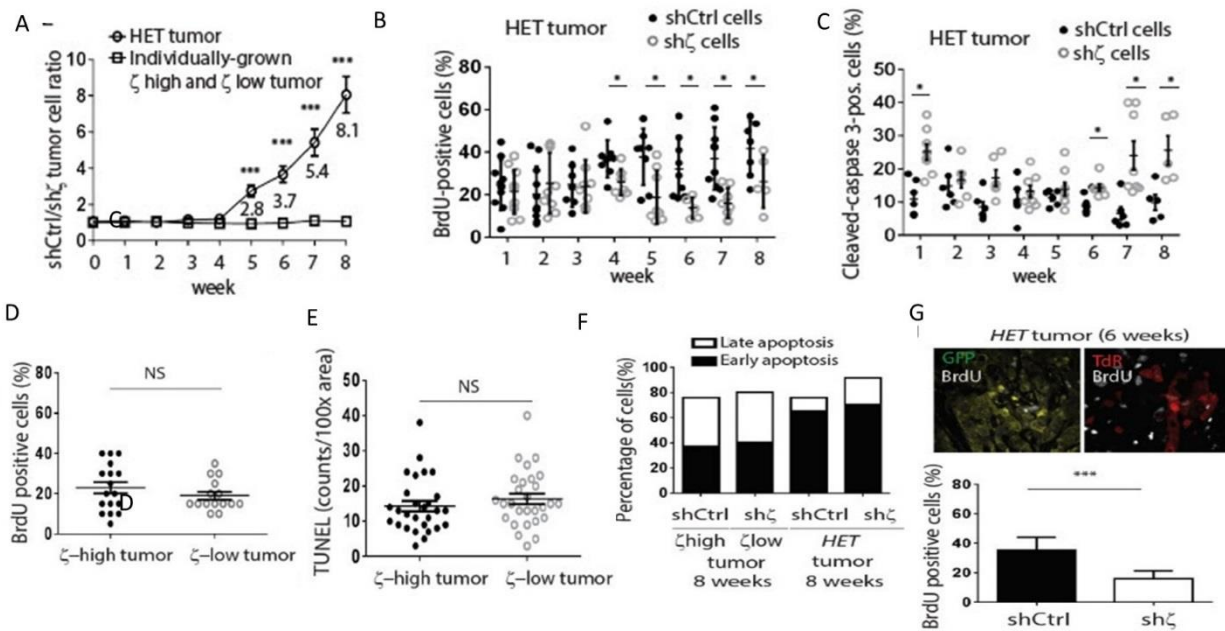
Figure 30. 14-3-3ζ-high cells induce growth rate changes in HET tumors. A, shCtrl-to-shζ ratio was analyzed through the GFP-to-TdR signal ratio by flow cytometry. The individually grown shCtrl-to-shζ ratio reflects the ratio for ζ-high tumors together with that for ζ-low tumors; the HET tumor ratio indicates the ratio from HET tumors in which the two types of cells were implanted together. B-C, Consecutive HET tumor slides stained with proliferation marker BrdU (B) or apoptosis marker cleaved caspase 3 (C) along with GFP staining (shCtrl) or TdR staining (shζ). Quantification of the percentage of BrdU-positive or apoptosis marker (B) or cleaved caspase 3 (C) IHC staining in shCtrl and shζ cells. D-E, IHC staining of proliferation marker BrdU-positive cells (D) and TUNEL-positive cells (E) in individually grown ζ-high (shCtrl) and ζ-low (shζ) tumors. F, Histograms show early and late apoptotic events in shCtrl and shζ cells extracted from ζ-high, ζ-low and HET tumors. G, Co-IF staining of BrdU marker and GFP or TdRed staining. Scale bar represents 50 μm. Error bars, S.D. *** indicates $P<0.001$ and * indicates $P<0.05$ by Student t-test. The data are in collaboration with Dr. Qingling Zhang
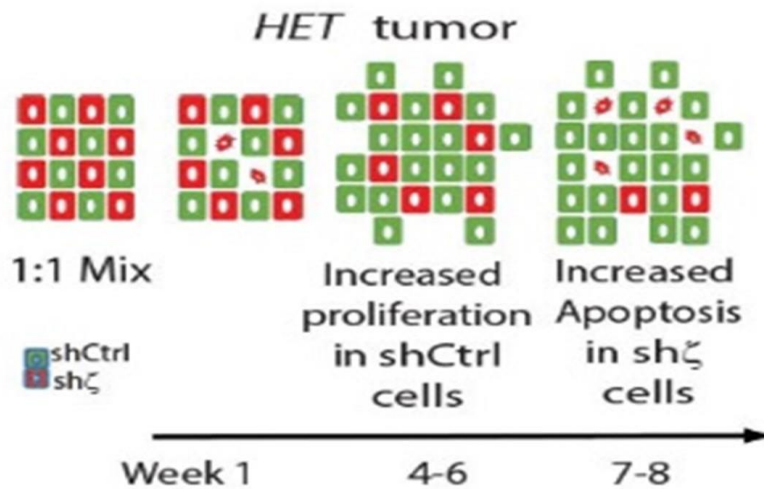
Figure 31. Schematic summary of how 14-3-3ζ mediates cell proliferation and apoptosis during cancer progression in HET tumors. When 14-3-3ζ-high cells grew with 14-3-3ζ-low cell in HET tumors, cell growth rate and cell death mechanism were changed in both cells. 14-3-3ζ-high cells (winner cells) increasing cell apoptosis in 14-3-3ζ-low cells (loser cells) at the early stage of tumorigenesis assay. During tumor progression, 14-3-3ζ-low cells were gradually eradicated by 14-3-3ζ-high cells, which then proliferated to fill the space and gap left by the disappearing loser cells. Green: shCtrl cells (14-3-3ζ-high cells or winner cells); red: shζ cells (14-3-3ζ-low cells or loser cells).

3.3.2 Upregulation of IL-8 in 14-3-3ζ-high cells is critical to drive cell competition

To dissect the molecular mechanism underlying the cell competition of the "winning" 14-3-3ζ-high over the "losing" 14-3-3ζ-low cells in HET tumors, I performed an unbiased-approach gene expression profiling analysis in shCtrl and shζ cells freshly extracted from HET tumors and individually grown ζ-high and ζ-low tumors. I noted the top hits that were upregulated in shCtrl cells versus shζ cells specifically in HET tumors. Remarkably, pro-inflammatory ligands, IL-1β and IL-8, were significantly upregulated in shCtrl cells compared to shζ cells (Figure 32A). Meanwhile, I analyzed the top 10% of genes that were altered between the shCtrl and shζ cells through Ingenuity pathway analysis (IPA). Interestingly, IL-1β and IL-8 signaling ranked among other top altered pathways (Figure 32B); the biological functions cell growth and cell survival were listed as the top two mechanisms (Figure 32C); revealed by IPA. These data suggest that 14-3-3ζ may modulate the pro-inflammatory pathway, thereby mediating cell competition.

To validate the array profiling data, I used qRT-PCR to examine mRNA expression of *IL-1β* and *IL-8* in shCtrl and shζ cells. shCtrl cells had an increase in mRNA expression of *IL-8* and *IL-1β* compared to shζ cells (Figure 33A and 33B). Importantly, IL-8 expression was upregulated only in shCtrl cells from HET tumors, but was only moderate effect in the shCtrl cells from individually grown ζ-high tumors (Figure 33B). To test protein expression of IL-8 and IL-1β in shCtrl and shζ cells, I performed cytometric bead array (CBA) analysis, which can measure multiple ligands, including IL-8 and IL-1β, with better sensitivity than traditional ELISA. In shCtrl cells, IL-8, IL-1β, IL-6 and IL-12p70 showed higher expression compared to shζ cells (Figure 33C). Among these inflammatory ligands,

IL-8 expression showed the highest increase in shCtrl cells compared to shζ cells (Figure 33C and 33D), whereas it did not show a consistent expression pattern in cells from individually grown tumors (Figure 33D). I also tested IL-8 in secretion form in tumor fluids; IL-8 was increased 2-fold in HET tumor compared to ζ-high and ζ-low tumors (Figure 33E). Because inter-mouse heterogeneity affects basal cytokine expression levels, the significant upregulation of secretory IL-8 in HET tumors versus ζ-high and ζ-low tumors was only observed when these tumors were implanted into the same mouse. These data suggest that increased IL-8 expression in shCtrl cells contributed to secretory IL-8 in HET tumors, which may be relevant to cell competition.

To investigate whether IL-8 is critical for 14-3-3ζ to mediate cell competition, I knocked down IL-8 in HCC1954.shCtrl (shCtrl.shIL-8) cells and implanted shCtrl.shIL-8 cells together with shζ cells in a 1-to-1 ratio to establish HET.shIL-8 m.f.p. tumors. I first verified secretory IL-8 in tumor fluids; indeed, secretory IL-8 was significantly reduced in both HET.shIL-8 tumors and shCtrl.shIL-8 tumors (Figure 34A). To investigate whether IL-8 is sufficient to induce cell competition, I analyzed the shCtrl.shIL-8–to-shζ ratio in HET.shIL-8 tumors. Excitingly, knockdown of IL-8 significantly reduced the competition ratio that was altered by 14-3-3ζ (Figure 34B). Additionally, knockdown of IL-8 significantly inhibited tumor growth in HET.shIL-8 tumors compared to vector control HET tumor (Figure 34C). These data indicate that upregulation of IL-8 is not only crucial for 14-3-3ζ-mediated cell fitness but also facilitates tumor growth.

Canonical Pathway	P value
Protein A signaling	2.38E-05
CDK5 signaling	3.62E-05
Stem cell into cardiac lineages	1.16E-04
IL-1 signaling	2.76E-04
Tight junction signaling	6.22E-04
IL-8 signaling	2.78E-03
PI3K/AKT signaling	2.96E-03
Toll-like Receptor signaling	4.48E-03
ERK/MAPK signaling	5.34E-03
BMP signaling	5.67E-03
NF-kB signaling	6.30E-03

Disease and Bio Functions	P value
Cancer	1.71E-15
Cellular Growth and Proliferation	4.73E-12
Cell Death and Survival	3.09E-09
Cellular Development	1.73E-06
Cellular Movement	9.58E-06
Cell Cycle	2.80E-05
Cellular Mophology	1.82E-04
Inflammatory Disease	3.58E-04
Cellular Function and Maintanance	6.69E-04
Tissue Development	1.05E-03
Embryonic Development	1.56E-03
Organ Morphology	5.42E-03
Molecular Transport	7.68E-03

Figure 32. Gene expression profiling analysis in shCtrl and shζ cells from HET tumors. A, Four HET tumors were collected at weeks 8, 10, and 12. IL-8, IL-1β and MIF showed significantly altered between shCtrl and shζ cells from HET tumors. B, IPA ranking of the most altered cancer pathways from the top 10% of genes in terms of differing expression between shCtrl and shζ cells. IL-1 and IL-8 were in higher positions. C, IPA ranking of the most altered disease and biological functions from the top 10% genes in terms of differing expression between shCtrl and shζ cells. Cell growth and cell death rank among the top dysregulated biological functions.
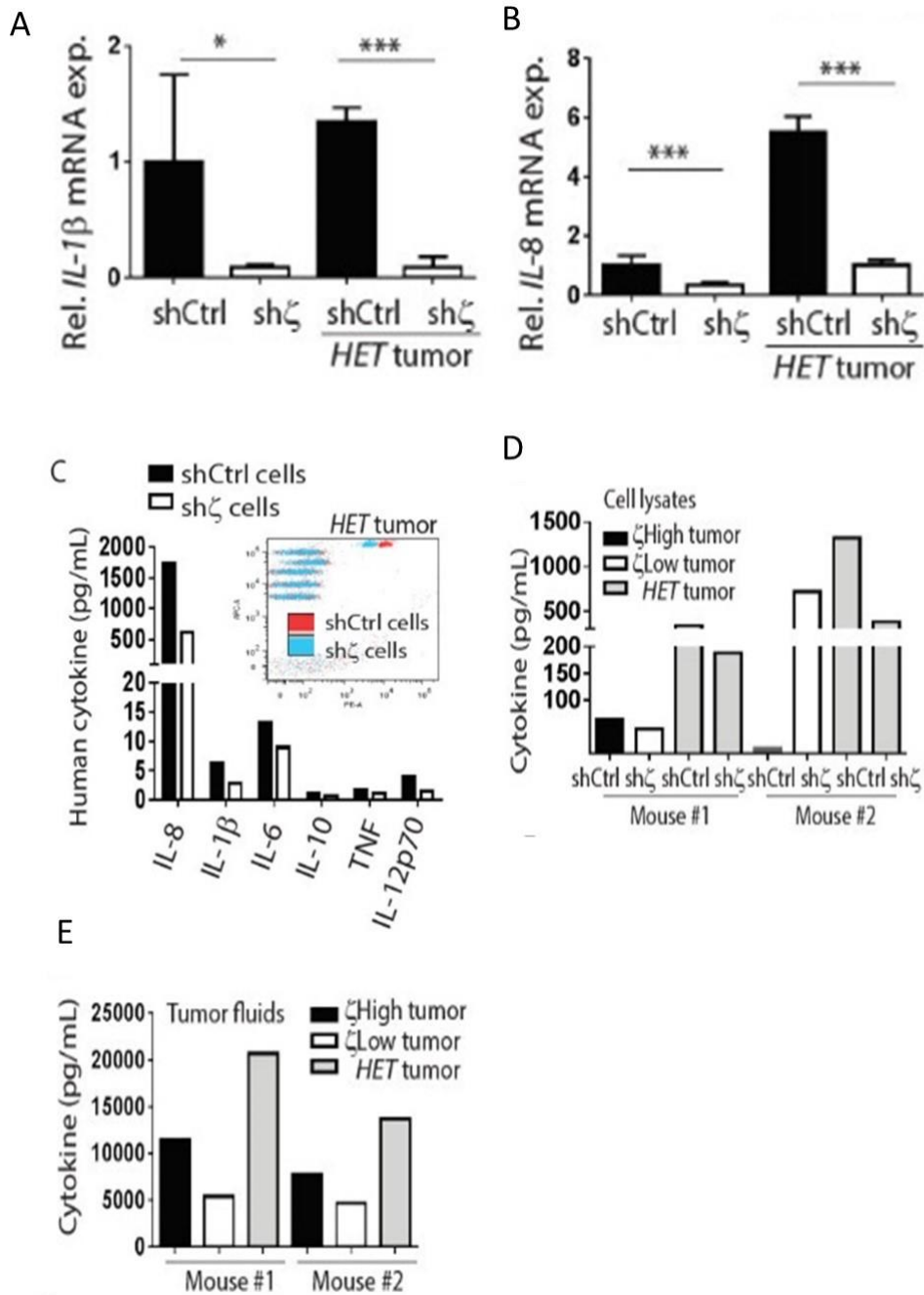
Figure 33. Upregulation of IL-8 in 14-3-3ζ-high cells contributes to tumor growth. A-B, qRT-PCR analysis of relative IL-1β (A) and IL-8 (B) mRNA expression in HCC1954 sublines, normalized by 18S rRNA expression. C, CBA analysis showed that shCtrl and shζ have different levels of cytokine expression. Histograms showed that four ligands (IL-

8, IL-1β, IL-6 and IL-10) were increased in shCtrl compared to shζ cells. Inset, among the four cytokines and chemokines, shCtrl cells (red) had a 3-fold increase in IL-8 expression compared to shζ cells (blue). D, CBA analyses revealed that ζ-high cells upregulated IL-8 expression compared to ζ-low cells in HET tumor. E, CBA analyses showed that HET tumor increased secretory IL-8 compared to individually grown ζ-high and ζ-low tumors. F All bars, S.D. *** indicates P<0.001 and * indicates P<0.05 by Student t-test.
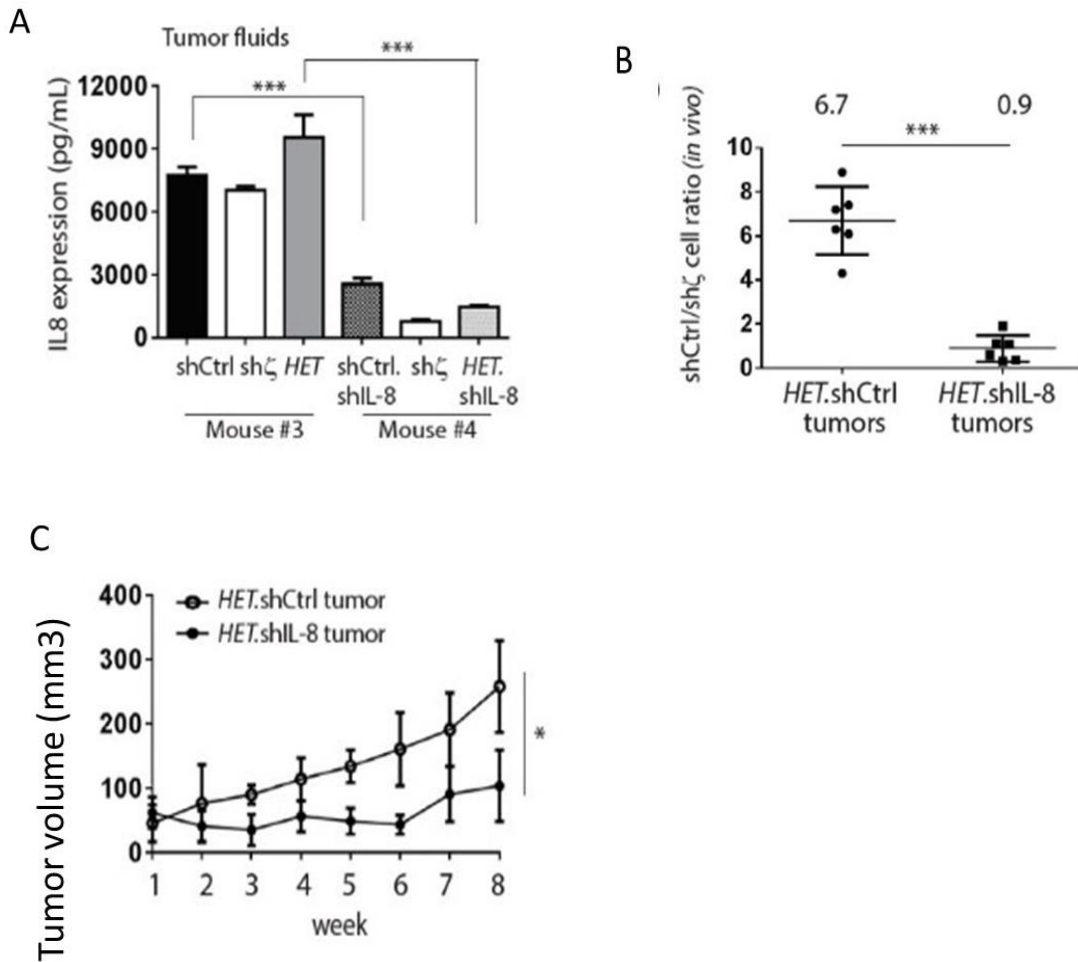
Figure 34. Upregulation of IL-8 in 14-3-3ζ high cell mediates cell competition. A, Knockdown of IL-8 significantly reduced secretory IL-8 in tumors, as shown by ELISA. B, Knockdown of IL-8 in shCtrl cells (shCtrl.shIL-8) significantly reduced cell competition, thereby decreasing the ζ-high to ζ-low ratio. HET.shIL-8 tumors indicate xenograft transplantation of shCtrl.shIL-8 cells together with shζ cells. C, Knockdown of IL-8 inhibited tumor growth. All error bars, S.D. *** indicates P<0.001 by Student t-test.

3.3.3 MIF-CXCR2-IL-8 axis is required for 14-3-3ζ to induce cell fitness

Several evidence showed that MIF induces IL-8 production through a heteromeric receptor complex (246, 247) and a functional MIF receptor complex includes CXCR2 and CXCR4, CD74 and/or other receptors (247, 248). I first analyzed CXCR2 expression in shCtrl and shζ cells and found CXCR2 expression was reduced in shζ cells compared to shCtrl cells (Figure 35A). Interestingly, certain evidence has showed that MIF is a pro-inflammatory cytokine originally discovered to be secreted in the immune response (249), which can stimulate IL-8 production by competing with other canonical ligands for binding to the CXCR2 receptor (248). To examine the upstream signaling that mediates IL-8 production in shCtrl cells in HET tumors, tumor fluids of ζ-high and ζ-low tumors were collected and analyzed with a human cytokine array. Among the cytokines, macrophage inhibitory factor (MIF) expression was higher in ζ-low tumors than in ζ-high tumors (Figure 35B), which was also observed in the microarray profiling (Figure 32A). To validate the results from the cytokine array, I examined intracellular MIF expression in shCtrl and shζ cells and found that MIF was upregulated in shζ cells compared to shCtrl cells (Figure 35C). In addition, MIF upregulation was observed in multiple 14-3-3ζ-knockdown cell lines, such as HCC70, Hs578T and BT-549 cells, compared to the corresponding control cells (Figure 35C). This finding suggests that MIF expression is modulated by 14-3-3ζ in breast cancer, where knockdown of 14-3-3ζ upregulates MIF expression. Interestingly, those data indicate that 14-3-3ζ modulates expression of cytokine MIF, and its own receptor CXCR2, which may affect survival-dependent pathway in cells.

CXCR2 forms complexes with CD74 and other receptors, which are essential for mediating MIF-induced inflammation function (248). To test whether IL-8 expression was

induced by MIF through CXCR2 (Figure 35D), I stimulated shCtrl cells with human recombinant protein MIF and blocked it with CXCR2 antagonist SB225002. Upon MIF induction, both IL-8 mRNA expression and secretory IL-8 were upregulated in shCtrl cells, and this changed expression was further disrupted by SB225002 (Figure 35E). The data indicate that IL-8 production was directly modulated through the MIF-CXCR2 axis in shCtrl cells. This finding suggests that shCtrl upregulated IL-8 expression in HET tumors may be due to exposure to more MIF in the tumor environment. IL-8 expression primarily regulated by MIF-CXCR2 axis, blocking CXCR2 activation successfully inhibited IL-8 production (Figure 35E).

To determine whether targeting the MIF-CXCR2 axis inhibited cell fitness induced by 14-3-3ζ, I first established HET tumor xenografts in mouse m.f.p., and started to treat mice with MIF antagonist ISO 1 and CXCR2 antagonist SB225002 in the third week after implantation. I analyzed shCtrl-to-shζ cell ratio between the treatment and vehicle groups. Vehicle treatment moderately affected the shCtrl-to-shζ cell ratio (mean=3.64) compared to the non-treatment group (mean=8.1) (Figures 30A and 36A). Interestingly, the ISO 1- and SB225002-treated groups significantly reduced the shCtrl-to-shζ cell ratio (mean=1.9 and 1.8, respectively) compared to the vehicle control group (mean=4.5) (Figure 36A). These data indicate that the impeding MIF-CXCR2 axis interrupted cell fitness induced by 14-3-3ζ in HET tumors.

To determine whether disturbing MIF-CXCR2 affects cell proliferation and cell apoptosis in shCtrl and shζ cells, I analyzed apoptosis and proliferation in both types of cells extracted from HET tumors. Remarkably, blocking MIF in the HET tumor increased apoptosis in shCtrl cells but reduced apoptosis in shζ cells (Figure 36B). Moreover,

disrupting MIF binding reduced proliferation in shCtrl cells but increased proliferation in shζ cells (Figure 36C). However, inhibiting CXCR2 activation primarily had effects on apoptosis but not proliferation (Figure 36B and 36C). The data suggest that MIF-CXCR2 signaling has distinct function in ζ-high (shCtrl) vs. ζ-low (shζ) expressing cells, whereas shζ cells are more dependent on the MIF-induced survival pathway. When shζ cells grew with shCtrl cells, shCtrl cells may compete with MIF from shζ that induce cell death in shζ cells.

To examine whether 14-3-3ζ-high cells competed to sequester limited MIF ligands in HET tumors, thereby inducing cell competition, I analyzed the internalization rate between shCtrl and shζ cells. I found that 14-3-3ζ-high cells drive cell competition by successfully outcompeting 14-3-3ζ-low cells to internalize MIF in the tumor environment (Figure 36D), and removing MIF from 14-3-3ζ-low cells caused cell death. Our data indicate that 14-3-3ζ-high cells have extremely competitive capacity to eradicate subclones in genetically heterogeneous tumors through competing with survival signal. Hindering MIF-CXCR2 significantly reduced cell fitness and tumor growth caused by 14-3-3ζ (Figure 36E). Thus, MIF and IL-8 are potential biomarkers for 14-3-3ζ-induced cell fitness in breast cancer.
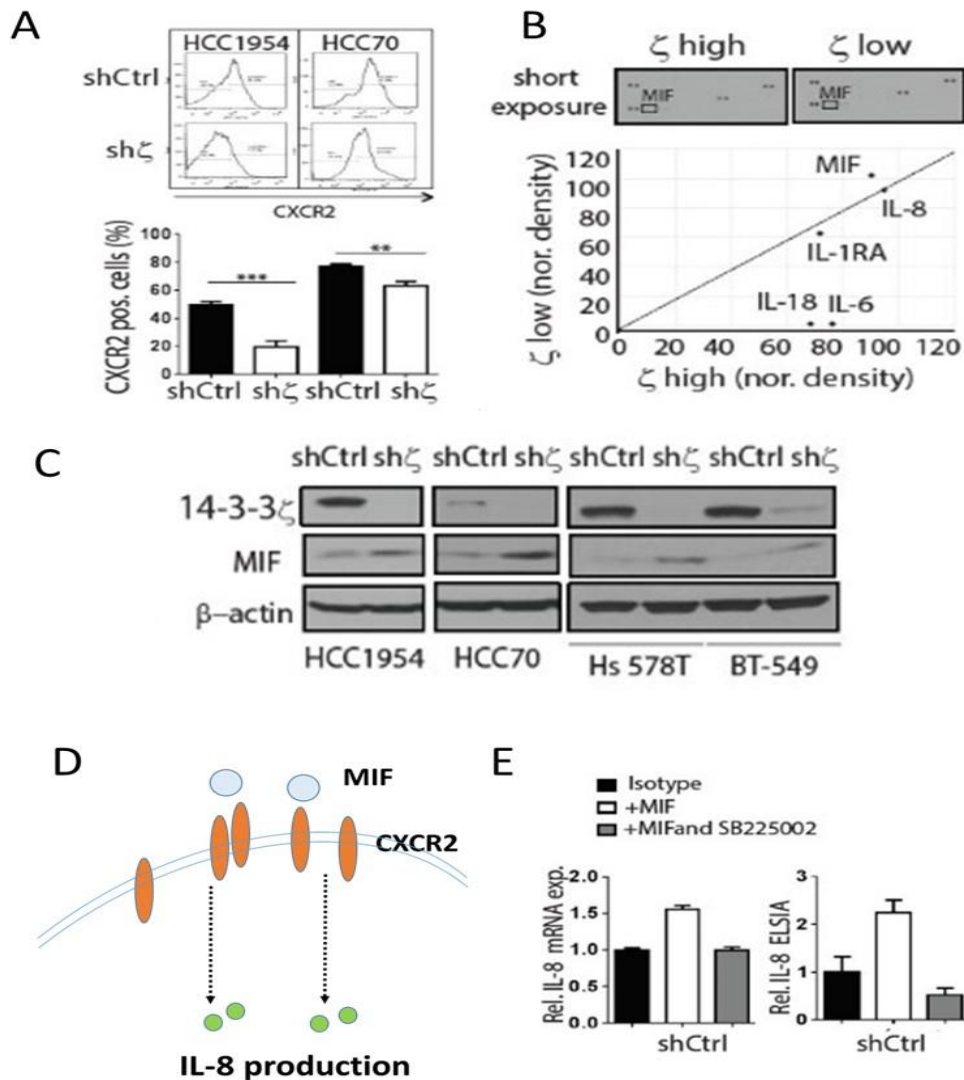
Figure 35. MIF-CXCR2 axis is regulated by 14-3-3ζ. A, Flow cytometry analyses revealed that ζ-high cells have higher expression of CXCR2 compared to ζ-low cells. B, Top, cytokine array of tumor fluids (35 μl) from ζ-high and ζ-low tumors (short exposure). C, Western blotting of MIF and β-actin in multiple breast cancer sublines. D. Proposed model reveals MIF may induce IL-8 production through CXCR2. E, mRNA levels and protein levels of IL-8 expression as detected by qRT-PCR and ELISA, respectively, in ζ-high cells (3D culture). All error bars, S.D. ** indicates P<0.01 by Student t-test.
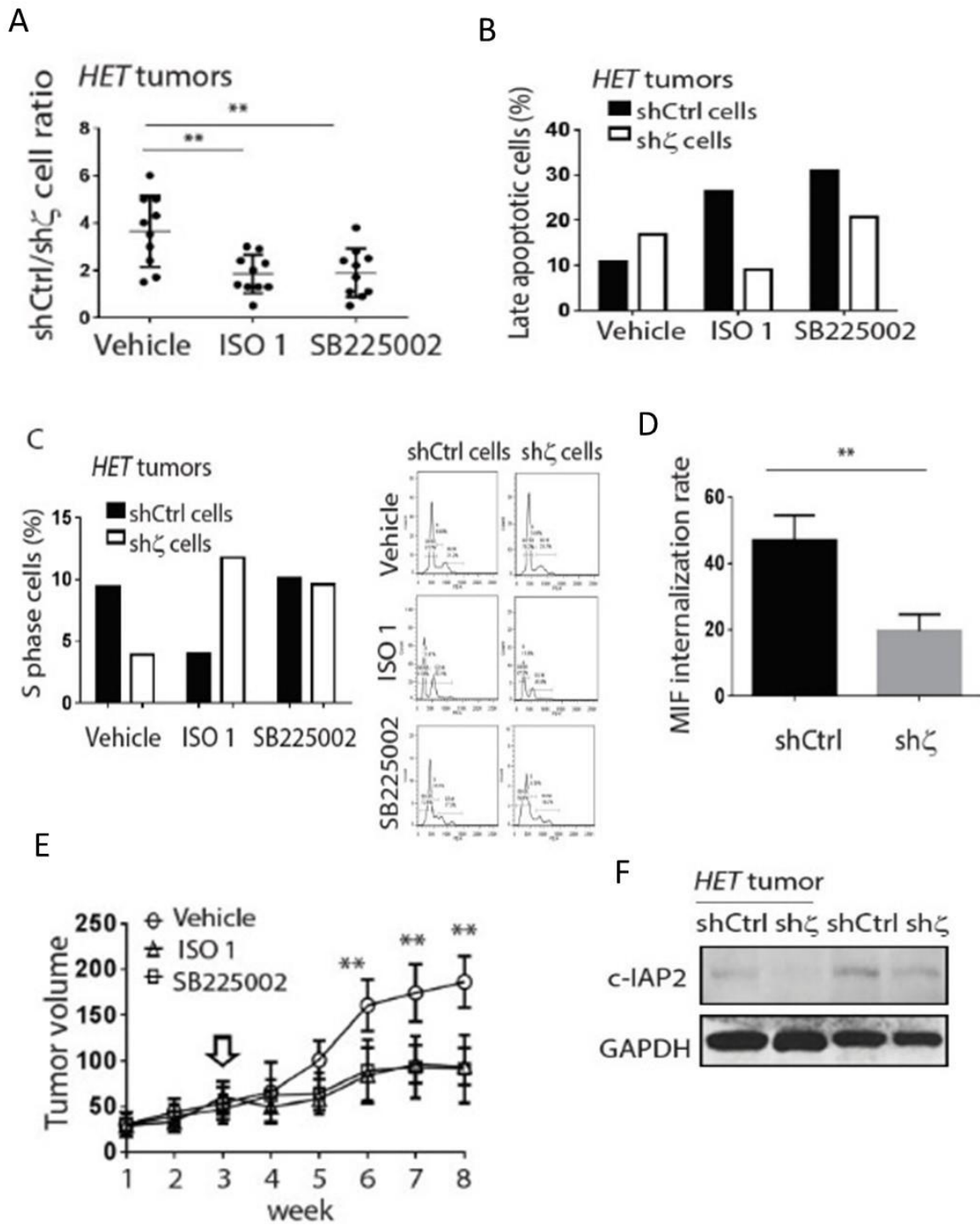
Figure 36. MIF-CXCR2 axis mediates cell competition. A, Targeting HET tumors with

MIF antagonist (ISO 1) or CXCR2 antagonist (SB225002) reduced the shCtrl-to-shζ ratio,

thereby inhibiting cell competition. B, Apoptosis was analyzed by Annexin V and SYTOX DNA dye, comparing MIF antagonist (ISO 1) and CXCR2 antagonist (SB225002) to vehicle control. C, Proliferation was affected by ISO 1 and CXCR2 inhibitor SB225002 which as seen through regular PI cell cycle staining. D, MIF internalization rate between shCtrl and shζ cells. E, Tumor volume in the ISO 1- and SB225002-treated groups, as well as a vehicle (DMSO) control group. All error bars, S.D. ** indicates P<0.01 by Student t-test

3.3.4 The MIF-CXCR2 axis predicts worse clinical outcome

Having established that the MIF-CXCR2 axis is potently regulated with regard to cell fitness and tumor growth by 14-3-3ζ breast cancer cells. Next, to assess whether each of MIF and IL-8 expression levels hold prognostic value for breast cancer, I then analyzed overall survival of the breast cancer dataset without subtype separation by an online Kaplan-Meier survival plotter (250). I found that high expression of MIF predicts poor survival of breast cancer patients (P=3.3e-08); high expression of IL-8 also predicts poor survival of breast cancer patients (P=0.00039) (Fig. 37A and 37B). These data suggest that inflammatory molecules MIF and IL-8 can predict worse clinical outcome in breast cancer. 14-3-3ζ mediated cell competition by regulating the inflammatory pathway, which increases the risk factors and is associated with shorter overall survival of breast cancer.
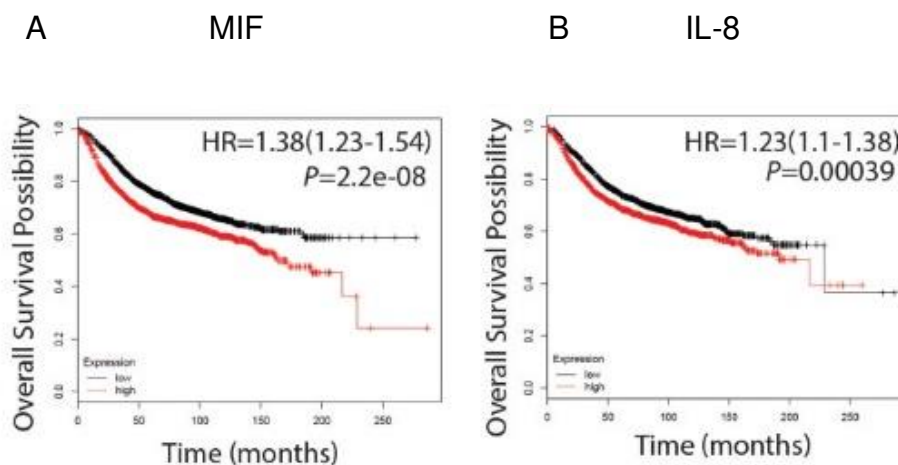
Figure 37. MIF-IL-8 axis proteins predict poor prognosis in breast cancer. A-B Kaplan-Meier overall survival curve of breast cancer patients. High expression of MIF (A) or IL-8 (B) was associated with poor overall survival (both log rank P<0.001).

3.4 Discussion

Cell competition, a unique mechanism that orchestrates cell fate during development (251), has emerged as having a role in tumor suppression and has been proposed to be required for the progression from a pre-cancerous lesion to a tumor (235). I found that, in contrast to the traditional mechanism of loser-cell elimination is recognized by cell-cell interactions, 14-3-3ζ mediates cell competition through coordination of part of the inflammatory system and gradually removes unfit cells in tumor populations. The level of 14-3-3ζ determined the outcome of competitive races for tumor populations; cells with relatively higher 14-3-3ζ expression increased proliferation, reduced apoptosis and eliminated the slow-proliferating surrounding cells (14-3-3ζ-low cells). Mechanistically, 14-3-3ζ-high cells outcompeted for survival ligand MIF via high expression of CXCR2 (Figure 36D), thereby driving cell death in 14-3-3ζ-low-expressing cells in tumors with mosaic expression of 14-3-3ζ (Figure 38). Interestingly, because MIF showed distinct functions in 14-3-3ζ-high versus 14-3-3ζ-low cells during the cell competition, the 14-3-3ζ-dependent MIF survival pathway becomes an Achilles heel and induce apoptosis in 14-3-3ζ-low cells when MIF was sequestered out by 14-3-3ζ-high cells. In HET tumor, 14-3-3ζ-high-expressing cells produce high levels of IL-8 through MIF-CXCR2 axis, which may further stimulate more IL-8 production as an autocrine signal, and contributes to cell fitness and tumor growth.

A type of cell competition occurs in the "race" for dominance between mutant cells and wild-type cells (233); however, only a small number of genes such as Myc, which has been identified to transform cells into super-competitor when they are overexpressed in cells. In cancer, whether tumor-promoting protein 14-3-3ζ can induce cell to become

super-competitor, which needs further investigation in normal breast tissue. In the meantime, I have established a mammary gland-specific inducible 14-3-3ζ mouse (Figure 39) that will allow further pursuit of these questions. Although it is unclear why the winner cells always require elimination of surrounding loser cells in order to proliferate, one explanation could be that loser cells may somehow restrain the growth capacity of winner cells through closely interacting with them (233).

The classical cell death mechanism in loser cells—involving JNK-dependent apoptosis, intercalation of cells through regulation of F-actin, cell engulfment, and binding to diffusible death signal secreted by winner cells (166, 234, 252)—has been observed from flies to mammalian cells. Previously, in chronic lymphocytic leukemia B lymphocytes, MIF activated the CD74-NFkB pathway and resulted in activation of the IL-8-Bcl2 survival pathway (246). However, in the model, reduction of c-IAP2 expression (Figure 36F) may be the primary mechanism to increase cell apoptosis in shζ cells and presents a novel means of cell competition regulation through the c-IAP pathway besides the Bcl2 pathway.

Meyer et al. reported that Myc induces cell competition by activating the innate immune system and triggering TRR-NF-κB-dependent apoptosis in the losing cells (253). In that model, winner and loser cells have distinct contexts, which are able to induce apoptosis in loser cells but not in winner cells. In the present study, 14-3-3ζ modulated expression levels of pro-inflammatory cytokines and their responding receptors. High endogenous 14-3-3ζ-expressing neoplastic clone upregulate CXCR2 expression on the cell surface, which efficiently creates more binding potential for ligands such as MIF in the tumor environment, which reduces the possibility of MIF-CXCR2 interaction in 14-3-3ζ-low-expressing cells at the same time. Remarkably, I also observed that CXCR2

expression levels gradually increased over time in a tumorigenesis assay (Figure S4A), where shCtrl cells always had higher expression of CXCR2 levels compared to shζ cells. Whether MIF-induced IL-8 production has impacts on induction of CXCR2 expression could be further investigated. 14-3-3ζ-high cells exploited and repurposed the function of the MIF-CXCR2-IL-8 axis to enhance cell fitness. Activation of MIF-CXCR2-IL-8 in nonimmune cells could be potential diagnostic markers for cell competition in breast cancer.

IL-8 signaling has been demonstrated to regulate invasion, migration and metastasis (254-256). During cell competition, endogenous higher-14-3-3ζ-expressing cells enhanced IL-8 signaling, which may be correlated to increased metastatic potential. In addition, upregulation of IL-8 was revealed to be an acquired therapeutic resistance mechanism in hepatocellular carcinoma (257). Chemotherapies, doxorubicin and paclitaxel, are commonly used for early-stage and advanced-stage breast cancer. Upregulation of IL-8 in 14-3-3ζ-high-expressing cells during breast cancer development may reduce drug sensitivity in patients who are receiving chemotherapy. The consequence of outcompeted cells in a heterogeneous tumor environment may enrich the potential to mediate therapy resistance and cancer metastasis.

Since the current field does not have an efficient way to target 14-3-3ζ, blocking 14-3-3ζ-high expressing cells with MIF or CXCR2 may be a potential therapeutic strategy to tackle tumor heterogeneity, cell fitness and potential metastasis or drug resistance. Altogether, my findings demonstrate that the MIF-CXCR2-IL-8 axis could be a critical cell competition feature in breast cancer and also show how cells gain advantages by efficiently acquiring extracellular ligands for cell proliferation and survival.
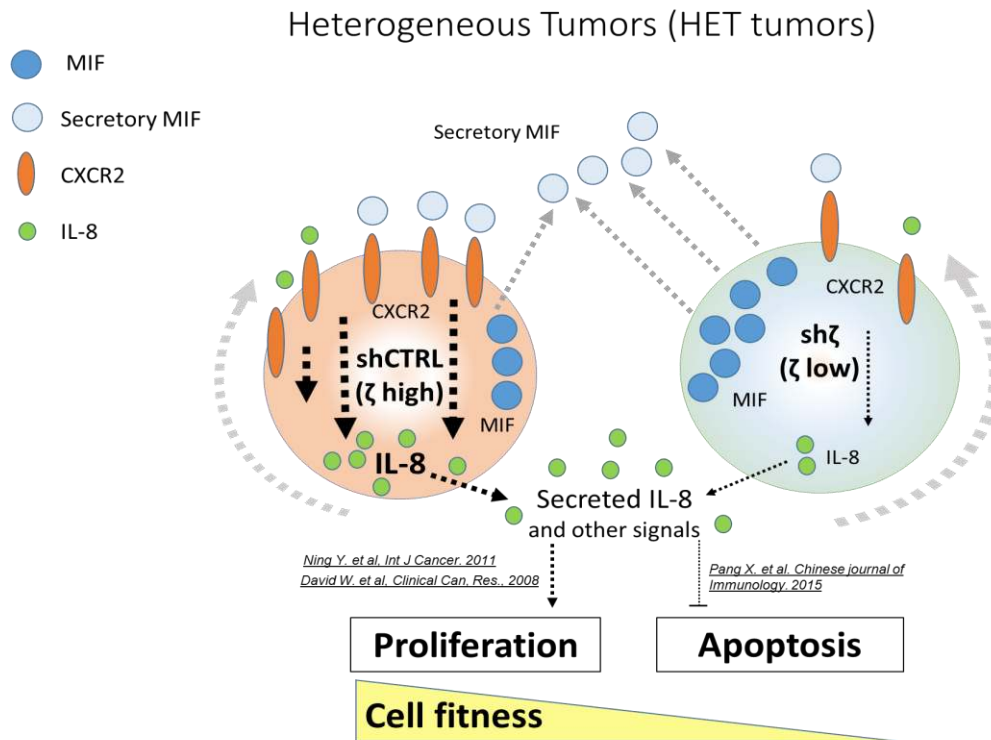
Figure 38. Proposed model of how 14-3-3ζ mediates cell competition and utilizes an inflammatory pathway. This schematic figure reveals how 14-3-3ζ modulates expression of cytokine and its own receptor, thereby changing cell context and survival-dependent pathway. Cancer cells expressing different levels of 14-3-3ζ responded inversely upon macrophage inhibitory factor (MIF) stimulation, with 14-3-3ζ-low cells critically dependent on the MIF survival pathway. 14-3-3ζ-high-expressing cells can efficiently sequester MIF in a ligand-limited tumor environment via high expression of CXCR2, and reduction of MIF stimulation in 14-3-3ζ-low cells led to cell death and gradual elimination of the cells from tumors. In HET tumor, 14-3-3ζ-high-expressing cells produce high levels of IL-8 through MIF-CXCR2 axis. IL-8 may further stimulate more IL-8 production by autocrine signal, which contributes to cell fitness and tumor growth. CXCR2 may or may not couple with other receptors to effectively produce IL-8.

Chapter 4
CONCLUDING REMARKS, FUTURE DIRECTIONS, AND PERSPECTIVES

4.1 Summary of findings

This work began with the clinical observations that early identification and intervention can greatly increase the 5-year overall survival rate in breast cancer patients. There is an urgent demand to identify the mechanism driving breast cancer initiation in order to rapidly develop targeted prevention strategies to interfere with breast cancer development. Additionally, 14-3-3ζ expression was found to be greatly heterogeneous at the early neoplastic stage of breast cancer; as the disease progressed, the expression expanded to 100% of the tumor cells. The data suggest that the preferential accumulation of 14-3-3ζ during breast cancer development is critical for tumor growth and cell survival. However, it remains unclear how cancer cells obtain growth and cell fitness advantages through increasing expression levels of 14-3-3ζ during cancer progression.

Metabolic alterations and cell competition during clonal selection are two important hallmarks of cancer. In this dissertation, I therefore pursued two major goals: first, to identify how 14-3-3ζ mediates metabolic alteration during early-stage breast cancer initiation **(Chapter 2)** and second, to examine how tumor cells selectively preserve high 14-3-3ζ expression and how this may allow them to take over the tumor population by regulating their cellular fitness and benefiting cell survival and proliferation during cancer progression **(Chapter 3)**.

The research presented herein led to the discovery that the 14-3-3ζ expression level is strongly associated with the expressions of glycolytic genes in the pre-neoplastic and early malignant breast lesions, which persistently exist in the advanced stages of

clinical breast cancer (Figure 14, 15 and 16). Importantly, I has demonstrated that 14-3-3ζ overexpression leads to increased glycolysis via upregulation of LDHA, facilitating breast cancer initiation and progression. Targeting 14-3-3ζ-overexpressing tumors with the MEK/ERK inhibitor AZD6244 can effectively inhibit mammary tumor growth **(discussed in Chapter 2)**. 14-3-3ζ has distinct functions at the early and late stages of breast cancer. In addition, previous studies reported that context-dependent signaling defines the roles of protein in different stages of disease (258-260). When considered in the context of cancer, spanning from early stage to advanced stages and containing various genetic and non-genetic regulations, proteins cooperate with 14-3-3ζ in widely differing ways. Another encouraging finding on 14-3-3ζ's role in cancer is that 14-3-3ζ exploits the inflammatory MIF-CXCR2-IL-8 axis, driving cell competition and eradicating the cells with lower 14-3-3ζ expression. This study led to the promising result that cancer is a disease caused by cell competition. Targeting mechanisms underlying cell competition may reduce 14-3-3ζ-mediated cell fitness and represent a potential therapeutic strategy to further inhibit tumor growth **(discussed in Chapter 3)**. Collectively, my work suggests that the Warburg effect and MIF-CXCR2-IL-8 axis are novel therapeutic targets for the treatment of 14-3-3ζ-overexpressing breast lesions.

A great deal of translational and clinical cancer research focuses on the development of biomarkers for earlier detection of cancer. Although modern technologies have allowed accurate diagnoses at relatively early stages of cancer, there remains a lack of promising biomarkers to result in a better prognostic assessment, especially without depending on a multi-marker testing strategy. Previous studies clearly showed

that the combination of multi-maker gene expression panels can lead to an accurate prognosis and better clinical decision making, but each gene expression panel may have limited specificity and sensitivity (261, 262). Indeed, the data in chapter 2 demonstrated that coexisting high expression of 14-3-3ζ and LDHA can be an efficacious prognostic biomarker in breast cancer, with more prediction power than either 14-3-3ζ or LDHA gene expression alone. My work has brought new insights into the molecular mechanism of early metabolic transformation, revealing that concurrent expression of 14-3-3ζ and LDHA could be applied into potential multi-marker panels for early intervention for breast cancer.

Cancer is a sequential process of cell clonal selection and competition. During tumor progression, the fittest clonal population (winner population) with better growth abilities outcompetes other subclonal populations for the limited resources within a tumor. The cell competition mechanism garnered attention because it not only orchestrates cell fate during development (251), but is probably also required for the progression from a pre-cancerous lesion to a tumor (235). Understanding clonal evolution and dynamics of cell fitness may improve targeted therapy efficacy and enable efficient intervention in tumor progression. My work specifically identified that the 14-3-3ζ protein preferentially accumulates during breast cancer development, utilizes the inflammatory pathway for cell survival, and induces winner-induced cell death in breast cancer patients and xenograft tumors. Although I have observed that 14-3-3ζ-low cells have relatively lower glycolytic activity compared to 14-3-3ζ-high cells, the difference of metabolic rate doesn't have significant impact on cell proliferation and cell competition. Interestingly, 14-3-3ζ can induce cell competition through 14-3-3ζ-mediated immune function. In cancers, 14-3-3ζ

overexpression enhances MAPK/c-Jun signaling (163), and regulates tumor immune response by modulation of multiple cytokines' expression (164, 165). Interestingly, 14-3-3ζ was found to directly interact with Stat3, which is essential for 14-3-3ζ-induced tumor inflammation. The evidence implicate that the role of 14-3-3ζ in tumor inflammation modulation and immune system.

I demonstrated that cells expressing different levels of 14-3-3ζ responded inversely upon macrophage inhibitory factor (MIF) stimulation, with 14-3-3ζ-low cells critically dependent on the MIF survival pathway. 14-3-3ζ-high-expressing cells can efficiently sequester MIF in a ligand-limited tumor environment, and reduction of MIF stimulation in 14-3-3ζ-low cells led to cell death and gradual elimination of the cells from tumors (Figure 38). At the end stage of a tumorigenicity assay, 14-3-3ζ-high-expressing cells were always observed to colonize the whole tumor population, which is similar to what I observed in clinical breast cancer cases (Figure 28 and 29C). The level of 14-3-3ζ determined the outcome of competitive races within tumor populations; cells with relatively higher 14-3-3ζ expression increased proliferation, reduced apoptosis, and eliminated the slower-proliferating, 14-3-3ζ-low surrounding cells. Interestingly, 14-3-3ζ-low cells can survive when they exist in a homotypic environment. But why should the winner clone (14-3-3ζ-high cells) always eliminate the loser clone (14-3-3ζ-low cells)? From a biological standpoint, it would make sense for the loser clone to be eliminated if it somehow restricted the growth of winner cells due to rivalry for limited resources in the tumor microenvironment. The exact feed-forward details were uncovered by utilizing inducible xenograft tumors to investigate the timing and biology of cell competition *in vivo*.

In present study, disturbing MIF-CXCR2 affects cell proliferation and cell apoptosis in shCtrl and shζ cells. Remarkably, blocking MIF in the HET tumor increased apoptosis in shCtrl cells but reduced apoptosis in shζ cells (Figure 36B). Moreover, disrupting MIF binding reduced proliferation in shCtrl cells but increased proliferation in shζ cells (Figure 36C). The data suggest that MIF-CXCR2 signaling has distinct function in ζ-high (shCtrl) vs. ζ-low (shζ) expressing cells, whereas shζ cells are more dependent on the MIF-induced survival pathway. When shζ cells grew with shCtrl cells, shCtrl cells may compete with limited MIF in the tumor environment from shζ cells, which induces cell death in shζ cells. Importantly, our data indicate that 14-3-3ζ-high cells have extremely competitive capacity to eradicate subclones in genetically heterogeneous tumors through competing with survival signal, MIF. 14-3-3ζ-high cells have higher CXCR2 expression compared to shζ cells. Hindering MIF-CXCR2 significantly reduced cell fitness and tumor growth caused by 14-3-3ζ (Figure 36E). Moreover, since IL-8 is increased in HET tumor compared to individually-grown tumors, I will further investigate whether IL-8 can serve as autocrine function to continuously maintain higher growth rate in shCtrl cells through binding to CXCR2. It is also important to further investigate whether IL-8 will compete wil MIF to bind to CXCR2.

In the present study, I demonstrated a novel role of 14-3-3ζ in cell competition both in *in vivo* and *ex vivo*. Similar to what was observed *in vivo*, when shCtrl cells were grown with shζ cells, the shCtrl-to-shζ ratio increased, whereas the shCtrl-to-shζ ratio remained constant when these cells were grown individually. However, the degree of cell competition was slightly different between *in vivo* and *in vitro* results. The shCtrl-to-shζ

ratio in the co-culture system (*in vitro*) can only reach a maximum of 3:1 after long-term culture, while the shCtrl-to-shζ ratio in HET tumors (*in vivo)* gradually increased up to 8:1 at late stage of tumorigenicity assay. These results suggest that the tumor microenvironment may further be involved in cell competition. One possible explanation is that increased IL-8 in the HET tumors may attract neutrophils to infiltrate into the tumor, and the neutrophils may accelerate the process of removing unfit cells within tumors, although this hypothesis merits further investigation. My work has added new weight to the generally accepted theory that cell competition may promote tumor progression.

4.2 14-3-3ζ as a therapeutic target for cancer metabolism and tumor heterogeneity

14-3-3ζ belongs to the highly conserved 14-3-3 scaffold protein family (157). 14-3-3ζ has been reported to modulate numerous pathways and cellular functions in cancer such as invasion, apoptosis resistance, metastasis, chemotherapy resistance, and disease recurrence. Additionally, a heritable increase in 14-3-3ζ expression in cancer is associated with poor prognosis (158). Recently, 14-3-3ζ has been shown to be involved in numerous metabolic alterations (186), such as modulating the function of hypoxia-inducible factor-1α (263), regulating adipogenesis (222), interacting with insulin signaling and facilitating glucose uptake (264), and binding to AMPK-target protein mTOR and coordinating cell growth (265). Furthermore, in cancer cells 14-3-3ζ physically interacts with phosphorylated LKB1 (192) and suppresses binding to and activation of its substrate, AMPK, a master sensor of cell metabolic flux, suggesting that 14-3-3ζ could be an important mediator of cellular metabolism. My work further demonstrated that 14-3-3ζ

overexpression is strongly correlated with the expression of glycolytic genes in breast cancer patients; and that 14-3-3ζ is a critical mediator of glycolysis, which may contribute to initiation, early transformation, and progression of breast cancer (Figure 27).

Immune cells have been found to play an important role against cancer (266, 267). Certain studies showed that immune cells have distinct metabolic changes undergo activation of their immune functions while encountering danger signals (268). While tumor cells opt for metabolic reprograming like glycolysis to support rapid proliferation, evidence suggests that infiltrating immune cells such as tumor associated macrophages, T cells, and tumor infiltrating lymphocyte, also undergo similar glucose alterations. For example, during tumor progression, increased glycolysis in tumor associated macrophages would induce inflammation and increase inflammatory cytokines release, supporting tumor-related inflammation. Activated effector T cell is marked by the by a switch from oxidative metabolism to glycolysis (71). Interestingly, cancer cells can compete for the limited glucose with tumor infiltrating lymphocyte in order to suppress the immune function in tumors (72, 73). Therefore, a better understanding of how metabolism fuels and modulates the maturation of immune responses may provide critical insights for cancer therapy (269, 270).

Much evidence indicates that 14-3-3ζ may be a potential therapeutic target in cancer. Existing protein targeting approaches include the peptide inhibitor R18 (271), and nonpeptide inhibitor BV02 (272, 273) for inhibiting 14-3-3; both have been tested *in vitro* and BV02, which targets the protein-binding groove of 14-3-3, exhibited high efficacy

killing cells. Many lines of research are underway to identify the effect of pan-14-3-3 inhibition in various diseases; yet, the development of a specific 14-3-3ζ inhibitor remains an urgent need in the field. Since there is currently no efficient way to target 14-3-3ζ, I may try to target 14-3-3ζ by interfering with its binding partners or downstream signaling pathways. In chapter 2, I have shown that inhibiting 14-3-3ζ-induced LDHA upregulation through targeting the 14-3-3ζ-downstream MEK/ERK pathway can effectively prevent the early-stage breast cancer progression *in vivo* by decreasing LDHA expression and reducing cell proliferation. In chapter 3, I have shown that inhibiting 14-3-3ζ-high-cell-induced cell competition, both by blocking 14-3-3ζ-high cells with MIF antagonist ISO 1 or CXCR2 antagonist SB225002, is explored as a potential therapeutic strategy to tackle tumor heterogeneity and cell fitness (Figure 34). Altogether, my findings help to provide novel therapeutic strategies to tackle 14-3-3ζ-overexpressing breast cancer, and are expected to provide new insights for translational research, perhaps even benefiting personalized medicine strategies to inhibit tumor growth.

4.3 Future directions

Cancer is recognized as a disease of altered metabolism for almost 100 years, and metabolic alterations are currently identified as one of the important cancer hallmarks. Many drugs that directly target metabolic enzymes have been investigated in clinical trials (115) and targeting cancer metabolism has become a promising anti-cancer approach. However, because of the intra-and inter-tumor metabolic heterogeneity within and between tumors (274, 275), drugs that are directly targeted against metabolic enzymes have encountered several hurdles which will need to be overcome in the future. According to the results from clinical studies, no single-agent metabolic inhibitor alone is likely to successfully control tumor growth due to the extensiveness of tumor heterogeneity. There is a growing recognition that developing combinatorial therapies is critical to increasing treatment efficacy. In this dissertation, 14-3-3ζ overexpression-mediated LDHA upregulation contributes to aerobic glycolysis and early transformation in early-stage breast cancer. Targeting 14-3-3ζ/ERK/CREB/LDHA axis by using the 14-3-3ζ-downstream pathway MEK/ERK inhibitor AZD6244 significantly inhibits tumor growth. The potent MEK/ERK inhibitor AZD6244 has also been used in combination with chemotherapies or other targeted therapies for treatment of advanced cancer (276), Consequently, AZD6244 may further combine with other agent such as an LDHA inhibitor in order to treat advanced breast cancer with overexpression of 14-3-3ζ. Several LDHA inhibitors have been developed and examined in preclinical and clinical studies such as FX-11 and AT-101 (181-183). I may further examine whether the combination of an LDHA inhibitor and MEK/ERK inhibitor AZD6244 has a synergistic effect for treating advanced

breast cancer. Another challenge in developing metabolism-targeted agents is that high dose-limiting toxicity frequently occurs in normal cells due to low specificity of metabolic enzyme activity for cancerous tissues. Although metabolic enzyme functions significantly impact tumorigenesis, on the other hand, they also conduct general physiological and signal transduction functions in normal cells throughout the body. The therapeutic window for cancer-targeted metabolic therapy may be too narrow for systemic administration, which can causes severe toxicity in patients. Synergistic combination strategies by using metabolic inhibitor(s) together with another first-line cancer drug may not only improve efficacy compared to single agent therapy, but also decrease drug toxicity by reducing the requisite drug dosage. Therefore, I will further investigate whether the combination of MEK/ERK inhibitor AZD6422 and an LDHA inhibitor can effectively inhibit the growth of 14-3-3ζ-overexpressing tumors.

Transgenic, gene knock-out, and gene knock-in mice are valuable models for studying human disease (277, 278). Inducible mouse models have been developed to overexpress and/or knock-out gene expression in order to investigate tumor biology at the desired time or stage of tumor development (279, 280). I have identified that increased expression of 14-3-3ζ in normal mammary epithelial cells leads to metabolic dysregulation, promotes mammary tumor initiation, triggers cell competition, and promotes breast cancer progression. To further investigate the role of 14-3-3ζ-mediated metabolic alteration in mammary gland development, mammary tumor initiation, and mammary tumor progression *in vivo*, use of transgenic mice with inducible mammary gland-specific 14-3-3ζ overexpression will be valuable for studying how 14-3-3ζ is involved in metabolic

dysregulation and tumorigenesis *in vivo*. Importantly, two previous lab members, Dr. Qingfei Wang and Dr. Jun Yang, have cloned a 14-3-3ζ PCR product with human influenza hemagglutinin (HA) tag into bidirectional inducible pBI-L vector for pronuclear injection and generation of transgenic mice. With the help of the genetically engineered mouse facility (GEM) at University of Texas MD Anderson Cancer Center, Tet-HA-14-3-3ζ mice have been successfully generated in a Friend virus b-type mice NIH Jackson (FVB/NJ) background. Tet-HA-14-3-3ζ mice were further crossed with a mouse strain whose mammary glands specifically and consistently express tetracycline-controlled transcriptional activation protein (rtTA) (mouse strain was given from Dr. Lewis Chodosh), to established mammary gland-specific, doxycycline-inducible 14-3-3ζ-expressing mice (MTB/T-HA-14-3-3ζ) (Figure 39A). The western blot (Figure 39B) and immunofluorescence (Figure 39C), results showed that upon doxycycline induction, inducible gene expression is tightly regulated and encodes HA-14-3-3ζ in mammary epithelial cells in the MTB/T-HA-14-3-3ζ mouse model, which can be used to examine the impact of 14-3-3ζ overexpression on cell metabolism and transformation (Figure 39).

My work has demonstrated that the 14-3-3ζ expression level is significantly correlated with the expression of glycolytic enzymes in pre-malignant and cancerous lesions. The MTB/T-HA-14-3-3ζ mouse model will serve as a valuable resource for investigating the significance of 14-3-3ζ and other glycolytic proteins, especially those that have been reported to be potential 14-3-3ζ partners including enzymes that are central to glycolysis such as pyruvate kinase (PK), glyceraldehyde-3-phosphate dehydrogenase (GADPH) and 6-phosphofructo-2-kinase (PFK-2) (191).

Lastly, in my present study, I found that the percentage of 14-3-3ζ expression was highly heterogeneous in early-stage breast cancer. However, when the breast cancer progressed into advanced stages, the percentage of 14-3-3ζ expression increased to almost 100% of breast lesions. Besides simply outcompeting the loser cells (14-3-3ζ-low cells) for limited resources in the tumor environment, it is important to understand whether there are other reasons why winner cells (14-3-3ζ-high cells) are positively selected during clonal evolution. During cell competition, endogenously high-14-3-3ζ-expressing cells enhanced IL-8 signaling, which was found to be able to drive cell competition. IL-8 signaling has been demonstrated to regulate invasion and metastasis (254-256). In addition, upregulation of IL-8 was revealed to be an acquired therapeutic resistance mechanism in cancer (257). Chemotherapies are commonly used to treat for early-stage and advanced-stage breast cancer patients. Elevated IL-8 expression in winner cells (14-3-3ζ-high cells) during the cell competition process may reduce drug sensitivity in patients who are receiving chemotherapy. Rather than simply select for cells with better proliferative capabilities, the consequence of cell competition in a heterogeneous tumor environment may be enriched potential to mediate therapy resistance and cancer metastasis. Therefore, an extended study to examine whether 14-3-3ζ-induced cell competition can further impact therapeutic resistance or metastasis is urgently needed. Altogether, my work demonstrates that the MIF-CXCR2-IL-8 axis may be a critical feature of cell competition. Ideally, in the future, I can further investigate whether MIF-CXCR2-IL-8 axis can be biomarkers for cell competition in cancer. Recently, a great deal of focus has shifted to the field of immuno-oncology because immunological checkpoint blockade and adoptive cell transfer have showed impressive response rates in cancer patients. My

work demonstrated that 14-3-3ζ utilizes an immune pathway to induce cell competition in solid cancer, a setting that has not thus far benefited from major gains in immmuno-oncology. Remarkably, blocking 14-3-3ζ-induced cell competition with MIF or CXCR2 antagonists can reduce tumor growth and cell fitness, which may be a potential therapeutic strategy to tackle tumor heterogeneity and cell fitness, potentially extending the survival benefits seen with immunotherapy for melanoma and cancers of the blood into solid cancers.

In summary, this work has discovered the two distinct roles of 14-3-3ζ in cancer metabolism and cell competition, and suggests two potential therapeutic strategies to tackle breast cancer initiation and progression.
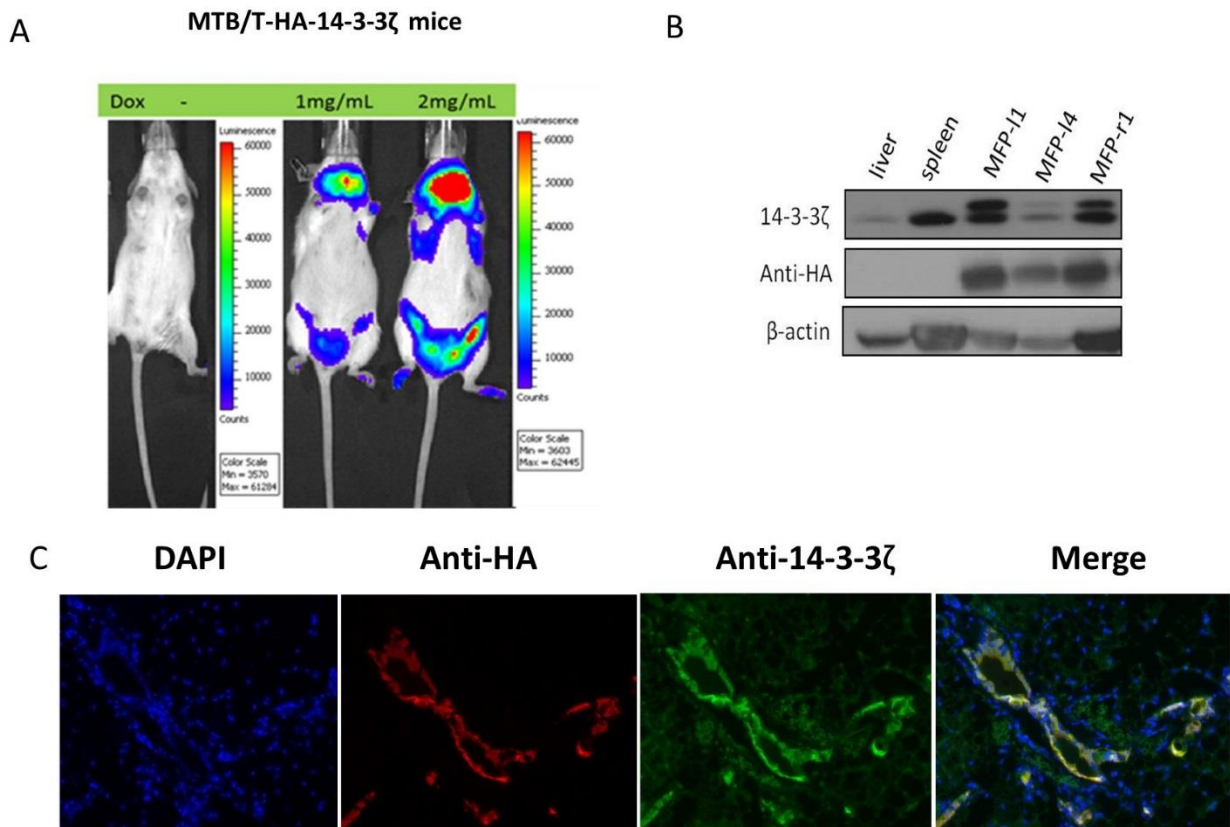
Figure 39. Tet-inducible MTB/T-HA14-3-3ζ bitransgenic mouse model. A, Mice were administrated doxycyclin (Dox) at 1 and 2mg/mL in drinking water for 3d and measured under IVIS bioluminescence imaging system. It shows gene expression in the MTB/T-HA14-3-3ζ is dox-dose-dependent indicating it can be induced at desired levels and desired time points. B, Western blot showed that inducible HA-14-3-3ζ only expressed in mammary glands (MFPl1, MFPl4 and MFPr1) whereas other organs such as liver and spleen have no inducible HA-14-3-3ζ signal. C, Immunofluorescence staining showed that the anti-HA specific signals co-localized with the anti-14-3-3ζ signals that further confirmed the histological staining results.

REFERENCES

1.   Siegel, R. L., K. D. Miller, and A. Jemal. 2016. Cancer statistics, 2016. *CA Cancer J Clin* 66: 7-30.

2.   Miller, K. D., R. L. Siegel, C. C. Lin, A. B. Mariotto, J. L. Kramer, J. H. Rowland, K. D. Stein, R. Alteri, and A. Jemal. 2016. Cancer treatment and survivorship statistics, 2016. *CA Cancer J Clin*.

3.   American Cancer Society, A. C. Key statistics for pancreatic cancer.

4.   American Cancer Society, A. C. Key statistics about liver cancer.

5.   American Cancer Society, A. C. Economic Impact of Cancer.

6.   (NCI), N. I. o. H. Cancer costs projected to reach at least $158 billion in 2020.

7.   Hanahan, D., and R. A. Weinberg. 2011. Hallmarks of cancer: the next generation. *Cell* 144: 646-674.

8.   Hanahan, D., and R. A. Weinberg. 2000. The hallmarks of cancer. *Cell* 100: 57-70.

9.   Witsch, E., M. Sela, and Y. Yarden. 2010. Roles for growth factors in cancer progression. *Physiology (Bethesda)* 25: 85-101.

10.   Lemmon, M. A., and J. Schlessinger. 2010. Cell signaling by receptor tyrosine kinases. *Cell* 141: 1117-1134.

11.   Fuchs, Y., and H. Steller. 2011. Programmed cell death in animal development and disease. *Cell* 147: 742-758.

12.   Everett, H., and G. McFadden. 1999. Apoptosis: an innate immune response to virus infection. *Trends Microbiol* 7: 160-165.

13.   Delbridge, A. R., and A. Strasser. 2015. The BCL-2 protein family, BH3-mimetics and cancer therapy. *Cell Death Differ* 22: 1071-1080.

14. Billard, C. 2013. BH3 mimetics: status of the field and new developments. *Mol Cancer Ther* 12: 1691-1700.

15. Ni Chonghaile, T., and A. Letai. 2008. Mimicking the BH3 domain to kill cancer cells. *Oncogene* 27 Suppl 1: S149-157.

16. Zhang, L., L. Ming, and J. Yu. 2007. BH3 mimetics to improve cancer therapy; mechanisms and examples. *Drug Resist Updat* 10: 207-217.

17. Butterworth, M., A. Pettitt, S. Varadarajan, and G. M. Cohen. 2016. BH3 profiling and a toolkit of BH3-mimetic drugs predict anti-apoptotic dependence of cancer cells. *Br J Cancer* 114: 638-641.

18. Harazono, Y., K. Nakajima, and A. Raz. 2014. Why anti-Bcl-2 clinical trials fail: a solution. *Cancer Metastasis Rev* 33: 285-294.

19. Folkman, J. 1971. Tumor angiogenesis: therapeutic implications. *N Engl J Med* 285: 1182-1186.

20. Cao, Y., and R. Langer. 2008. A review of Judah Folkman's remarkable achievements in biomedicine. *Proc Natl Acad Sci U S A* 105: 13203-13205.

21. Ribatti, D. 2008. Judah Folkman, a pioneer in the study of angiogenesis. *Angiogenesis* 11: 3-10.

22. Ribatti, D., A. Vacca, and M. Presta. 2001. An Italian pioneer in the study of tumor angiogenesis. *Haematologica* 86: 1234-1235.

23. Tischer, E., D. Gospodarowicz, R. Mitchell, M. Silva, J. Schilling, K. Lau, T. Crisp, J. C. Fiddes, and J. A. Abraham. 1989. Vascular endothelial growth factor: a new member of the platelet-derived growth factor gene family. *Biochem Biophys Res Commun* 165: 1198-1206.

24. Leung, D. W., G. Cachianes, W. J. Kuang, D. V. Goeddel, and N. Ferrara. 1989. Vascular endothelial growth factor is a secreted angiogenic mitogen. *Science* 246: 1306-1309.

25. Connolly, D. T., D. M. Heuvelman, R. Nelson, J. V. Olander, B. L. Eppley, J. J. Delfino, N. R. Siegel, R. M. Leimgruber, and J. Feder. 1989. Tumor vascular permeability factor stimulates endothelial cell growth and angiogenesis. *J Clin Invest* 84: 1470-1478.

26. Loupakis, F., A. Stein, M. Ychou, F. Hermann, A. Salud, and P. Osterlund. 2016. A Review of Clinical Studies and Practical Guide for the Administration of Triplet Chemotherapy Regimens with Bevacizumab in First-line Metastatic Colorectal Cancer. *Target Oncol* 11: 293-308.

27. Ozcelik, M., H. Odabas, O. Ercelep, S. Yuksel, A. G. Mert, D. Aydin, H. Surmeli, D. Isik, S. Isik, A. Oyman, B. B. Oven Ustaalioglu, M. Aliustaoglu, and M. Gumus. 2016. The efficacy and safety of capecitabine plus bevacizumab combination as first-line treatment in elderly metastatic colorectal cancer patients. *Clin Transl Oncol* 18: 617-624.

28. Rouyer, M., D. Smith, C. Laurent, Y. Becouarn, R. Guimbaud, P. Michel, N. Tubiana-Mathieu, A. Balestra, J. Jove, P. Robinson, P. Noize, N. Moore, A. Ravaud, A. Fourrier-Reglat, and E. s. group. 2016. Secondary Metastases Resection After Bevacizumab Plus Irinotecan-Based Chemotherapy in First-Line Therapy of Metastatic Colorectal Cancer in a Real-Life Setting: Results of the ETNA Cohort. *Target Oncol* 11: 83-92.

29. Rudolph, K. L. 2005. Telomeres and telomerase influence the course of human diseases, aging and carcinogenesis. *Curr Mol Med* 5: 133-134.

30. Chung, S. S., B. Oliva, S. Dwabe, and J. V. Vadgama. 2016. Combination treatment with flavonoid morin and telomerase inhibitor MST312 reduces cancer stem cell traits by targeting STAT3 and telomerase. *Int J Oncol* 49: 487-498.

31. Gavrilovic, I. T., and J. B. Posner. 2005. Brain metastases: epidemiology and pathophysiology. *J Neurooncol* 75: 5-14.

32. Patchell, R. A. 2003. The management of brain metastases. *Cancer Treat Rev* 29: 533-540.

33. Barnholtz-Sloan, J. S., A. E. Sloan, F. G. Davis, F. D. Vigneau, P. Lai, and R. E. Sawaya. 2004. Incidence proportions of brain metastases in patients diagnosed (1973 to 2001) in the Metropolitan Detroit Cancer Surveillance System. *J Clin Oncol* 22: 2865-2872.

34. Schouten, L. J., J. Rutten, H. A. Huveneers, and A. Twijnstra. 2002. Incidence of brain metastases in a cohort of patients with carcinoma of the breast, colon, kidney, and lung and melanoma. *Cancer* 94: 2698-2705.

35. Sawaya, R. 2001. Considerations in the diagnosis and management of brain metastases. *Oncology (Williston Park)* 15: 1144-1154, 1157-1148; discussion 1158, 1163-1145.

36. Talmadge, J. E., and I. J. Fidler. 2010. AACR centennial series: the biology of cancer metastasis: historical perspective. *Cancer Res* 70: 5649-5669.

37. Thompson, E. W., D. F. Newgreen, and D. Tarin. 2005. Carcinoma invasion and metastasis: a role for epithelial-mesenchymal transition? *Cancer Res* 65: 5991-5995; discussion 5995.

38. Tsai, J. H., and J. Yang. 2013. Epithelial-mesenchymal plasticity in carcinoma metastasis. *Genes Dev* 27: 2192-2206.

39. van Zijl, F., G. Krupitza, and W. Mikulits. 2011. Initial steps of metastasis: cell invasion and endothelial transmigration. *Mutat Res* 728: 23-34.

40. Cecchi, F., D. C. Rabe, and D. P. Bottaro. 2012. Targeting the HGF/Met signaling pathway in cancer therapy. *Expert Opin Ther Targets* 16: 553-572.

41. Birchmeier, C., W. Birchmeier, E. Gherardi, and G. F. Vande Woude. 2003. Met, metastasis, motility and more. *Nat Rev Mol Cell Biol* 4: 915-925.

42. Mazzone, M., and P. M. Comoglio. 2006. The Met pathway: master switch and drug target in cancer progression. *FASEB J* 20: 1611-1621.

43. Ho-Yen, C. M., J. L. Jones, and S. Kermorgant. 2015. The clinical and functional significance of c-Met in breast cancer: a review. *Breast Cancer Res* 17: 52.

44. Sierra, J. R., and M. S. Tsao. 2011. c-MET as a potential therapeutic target and biomarker in cancer. *Ther Adv Med Oncol* 3: S21-35.

45. Corso, S., C. Migliore, E. Ghiso, G. De Rosa, P. M. Comoglio, and S. Giordano. 2008. Silencing the MET oncogene leads to regression of experimental tumors and metastases. *Oncogene* 27: 684-693.

46. Surriga, O., V. K. Rajasekhar, G. Ambrosini, Y. Dogan, R. Huang, and G. K. Schwartz. 2013. Crizotinib, a c-Met inhibitor, prevents metastasis in a metastatic uveal melanoma model. *Mol Cancer Ther* 12: 2817-2826.

47. You, H., W. Ding, H. Dang, Y. Jiang, and C. B. Rountree. 2011. c-Met represents a potential therapeutic target for personalized treatment in hepatocellular carcinoma. *Hepatology* 54: 879-889.

48. Garajova, I., E. Giovannetti, G. Biasco, and G. J. Peters. 2015. c-Met as a Target for Personalized Therapy. *Transl Oncogenomics* 7: 13-31.

49. Pavlova, N. N., and C. B. Thompson. 2016. The Emerging Hallmarks of Cancer Metabolism. *Cell Metab* 23: 27-47.

50. Cairns, R. A., I. S. Harris, and T. W. Mak. 2011. Regulation of cancer cell metabolism. *Nat Rev Cancer* 11: 85-95.

51. Dang, C. V. 2012. Links between metabolism and cancer. *Genes Dev* 26: 877-890.

52. Wu, W., and S. Zhao. 2013. Metabolic changes in cancer: beyond the Warburg effect. *Acta Biochim Biophys Sin (Shanghai)* 45: 18-26.

53. Koppenol, W. H., P. L. Bounds, and C. V. Dang. 2011. Otto Warburg's contributions to current concepts of cancer metabolism. *Nat Rev Cancer* 11: 325-337.

54. Wong, J. L. 2011. From fertilization to cancer: a lifelong pursuit into how cells use oxygen. Otto Heinrich Warburg (October 8, 1883-August 1, 1970). *Mol Reprod Dev* 78: Fm i.

55. Warburg, O., F. Wind, and E. Negelein. 1927. The Metabolism of Tumors in the Body. *J Gen Physiol* 8: 519-530.

56. Warburg, O. 1956. On the origin of cancer cells. *Science* 123: 309-314.

57. Wallace, D. C. 2012. Mitochondria and cancer. *Nat Rev Cancer* 12: 685-698.

58. Weinhouse, S. 1956. On respiratory impairment in cancer cells. *Science* 124: 267-269.

59. Newsholme, E. A., B. Crabtree, and M. S. Ardawi. 1985. The role of high rates of glycolysis and glutamine utilization in rapidly dividing cells. *Biosci Rep* 5: 393-400.

60. Crabtree, H. G. 1929. Observations on the carbohydrate metabolism of tumours. *Biochem J* 23: 536-545.

61. Samudio, I., R. Harmancey, M. Fiegl, H. Kantarjian, M. Konopleva, B. Korchin, K. Kaluarachchi, W. Bornmann, S. Duvvuri, H. Taegtmeyer, and M. Andreeff. 2010. Pharmacologic inhibition of fatty acid oxidation sensitizes human leukemia cells to apoptosis induction. *J Clin Invest* 120: 142-156.

62. Vander Heiden, M. G., L. C. Cantley, and C. B. Thompson. 2009. Understanding the Warburg effect: the metabolic requirements of cell proliferation. *Science* 324: 1029-1033.

63. Locasale, J. W. 2012. The consequences of enhanced cell-autonomous glucose metabolism. *Trends Endocrinol Metab* 23: 545-551.

64. Liberti, M. V., and J. W. Locasale. 2016. The Warburg Effect: How Does it Benefit Cancer Cells? *Trends Biochem Sci* 41: 211-218.

65. Ward, P. S., and C. B. Thompson. 2012. Metabolic reprogramming: a cancer hallmark even warburg did not anticipate. *Cancer Cell* 21: 297-308.

66. Boroughs, L. K., and R. J. DeBerardinis. 2015. Metabolic pathways promoting cancer cell survival and growth. *Nat Cell Biol* 17: 351-359.

67. Pfeiffer, T., S. Schuster, and S. Bonhoeffer. 2001. Cooperation and competition in the evolution of ATP-producing pathways. *Science* 292: 504-507.

68.   Slavov, N., B. A. Budnik, D. Schwab, E. M. Airoldi, and A. van Oudenaarden. 2014. Constant growth rate can be supported by decreasing energy flux and increasing aerobic glycolysis. *Cell Rep* 7: 705-714.

69.   Labuschagne, C. F., N. J. van den Broek, G. M. Mackay, K. H. Vousden, and O. D. Maddocks. 2014. Serine, but not glycine, supports one-carbon metabolism and proliferation of cancer cells. *Cell Rep* 7: 1248-1258.

70.   Amelio, I., F. Cutruzzola, A. Antonov, M. Agostini, and G. Melino. 2014. Serine and glycine metabolism in cancer. *Trends Biochem Sci* 39: 191-198.

71.   Palmer, C. S., M. Ostrowski, B. Balderson, N. Christian, and S. M. Crowe. 2015. Glucose metabolism regulates T cell activation, differentiation, and functions. *Front Immunol* 6: 1.

72.   Chang, C. H., J. Qiu, D. O'Sullivan, M. D. Buck, T. Noguchi, J. D. Curtis, Q. Chen, M. Gindin, M. M. Gubin, G. J. van der Windt, E. Tonc, R. D. Schreiber, E. J. Pearce, and E. L. Pearce. 2015. Metabolic Competition in the Tumor Microenvironment Is a Driver of Cancer Progression. *Cell* 162: 1229-1241.

73.   Ho, P. C., J. D. Bihuniak, A. N. Macintyre, M. Staron, X. Liu, R. Amezquita, Y. C. Tsui, G. Cui, G. Micevic, J. C. Perales, S. H. Kleinstein, E. D. Abel, K. L. Insogna, S. Feske, J. W. Locasale, M. W. Bosenberg, J. C. Rathmell, and S. M. Kaech. 2015. Phosphoenolpyruvate Is a Metabolic Checkpoint of Anti-tumor T Cell Responses. *Cell* 162: 1217-1228.

74.   Estrella, V., T. Chen, M. Lloyd, J. Wojtkowiak, H. H. Cornnell, A. Ibrahim-Hashim, K. Bailey, Y. Balagurunathan, J. M. Rothberg, B. F. Sloane, J. Johnson, R. A.

Gatenby, and R. J. Gillies. 2013. Acidity generated by the tumor microenvironment drives local invasion. *Cancer Res* 73: 1524-1535.

75.   Colegio, O. R., N. Q. Chu, A. L. Szabo, T. Chu, A. M. Rhebergen, V. Jairam, N. Cyrus, C. E. Brokowski, S. C. Eisenbarth, G. M. Phillips, G. W. Cline, A. J. Phillips, and R. Medzhitov. 2014. Functional polarization of tumour-associated macrophages by tumour-derived lactic acid. *Nature* 513: 559-563.

76.   Locasale, J. W., and L. C. Cantley. 2011. Metabolic flux and the regulation of mammalian cell growth. *Cell Metab* 14: 443-451.

77.   Lu, W., Y. Hu, G. Chen, Z. Chen, H. Zhang, F. Wang, L. Feng, H. Pelicano, H. Wang, M. J. Keating, J. Liu, W. McKeehan, H. Wang, Y. Luo, and P. Huang. 2012. Novel role of NOX in supporting aerobic glycolysis in cancer cells with mitochondrial dysfunction and as a potential target for cancer therapy. *PLoS Biol* 10: e1001326.

78.   Sena, L. A., and N. S. Chandel. 2012. Physiological roles of mitochondrial reactive oxygen species. *Mol Cell* 48: 158-167.

79.   Shokolenko, I., N. Venediktova, A. Bochkareva, G. L. Wilson, and M. F. Alexeyev. 2009. Oxidative stress induces degradation of mitochondrial DNA. *Nucleic Acids Res* 37: 2539-2548.

80.   Cui, H., Y. Kong, and H. Zhang. 2012. Oxidative stress, mitochondrial dysfunction, and aging. *J Signal Transduct* 2012: 646354.

81.   Murphy, M. P. 2009. How mitochondria produce reactive oxygen species. *Biochem J* 417: 1-13.

82. Pelicano, H., W. Lu, Y. Zhou, W. Zhang, Z. Chen, Y. Hu, and P. Huang. 2009. Mitochondrial dysfunction and reactive oxygen species imbalance promote breast cancer cell motility through a CXCL14-mediated mechanism. *Cancer Res* 69: 2375-2383.

83. Yu, J., Y. Wu, and P. Yang. 2016. High glucose-induced oxidative stress represses sirtuin deacetylase expression and increases histone acetylation leading to neural tube defects. *J Neurochem* 137: 371-383.

84. Lu, C., and C. B. Thompson. 2012. Metabolic regulation of epigenetics. *Cell Metab* 16: 9-17.

85. Rodriguez, S., C. M. Denby, T. Van Vu, E. E. Baidoo, G. Wang, and J. D. Keasling. 2016. ATP citrate lyase mediated cytosolic acetyl-CoA biosynthesis increases mevalonate production in Saccharomyces cerevisiae. *Microb Cell Fact* 15: 48.

86. Griffiths, E. J., G. Hu, B. Fries, M. Caza, J. Wang, J. Gsponer, M. A. Gates-Hollingsworth, T. R. Kozel, L. De Repentigny, and J. W. Kronstad. 2012. A defect in ATP-citrate lyase links acetyl-CoA production, virulence factor elaboration and virulence in Cryptococcus neoformans. *Mol Microbiol* 86: 1404-1423.

87. Liu, X. S., J. B. Little, and Z. M. Yuan. 2015. Glycolytic metabolism influences global chromatin structure. *Oncotarget* 6: 4214-4225.

88. Zhao, S., W. Xu, W. Jiang, W. Yu, Y. Lin, T. Zhang, J. Yao, L. Zhou, Y. Zeng, H. Li, Y. Li, J. Shi, W. An, S. M. Hancock, F. He, L. Qin, J. Chin, P. Yang, X. Chen, Q. Lei, Y. Xiong, and K. L. Guan. 2010. Regulation of cellular metabolism by protein lysine acetylation. *Science* 327: 1000-1004.

89.   Stratton, S. A., and M. C. Barton. 2012. p53-Mediated regulation of hepatic lipid metabolism: forging links between metabolism, atherogenesis, and cancer. *J Hepatol* 56: 518-519.

90.   Won, K. Y., S. J. Lim, G. Y. Kim, Y. W. Kim, S. A. Han, J. Y. Song, and D. K. Lee. 2012. Regulatory role of p53 in cancer metabolism via SCO2 and TIGAR in human breast cancer. *Hum Pathol* 43: 221-228.

91.   Lago, C. U., H. J. Sung, W. Ma, P. Y. Wang, and P. M. Hwang. 2011. p53, aerobic metabolism, and cancer. *Antioxid Redox Signal* 15: 1739-1748.

92.   Courtnay, R., D. C. Ngo, N. Malik, K. Ververis, S. M. Tortorella, and T. C. Karagiannis. 2015. Cancer metabolism and the Warburg effect: the role of HIF-1 and PI3K. *Mol Biol Rep* 42: 841-851.

93.   Semenza, G. L. 2010. HIF-1: upstream and downstream of cancer metabolism. *Curr Opin Genet Dev* 20: 51-56.

94.   Miller, D. M., S. D. Thomas, A. Islam, D. Muench, and K. Sedoris. 2012. c-Myc and cancer metabolism. *Clin Cancer Res* 18: 5546-5553.

95.   Dang, C. V., A. Le, and P. Gao. 2009. MYC-induced cancer cell energy metabolism and therapeutic opportunities. *Clin Cancer Res* 15: 6479-6483.

96.   Luo, W., H. Hu, R. Chang, J. Zhong, M. Knabel, R. O'Meally, R. N. Cole, A. Pandey, and G. L. Semenza. 2011. Pyruvate kinase M2 is a PHD3-stimulated coactivator for hypoxia-inducible factor 1. *Cell* 145: 732-744.

97.   Christofk, H. R., M. G. Vander Heiden, M. H. Harris, A. Ramanathan, R. E. Gerszten, R. Wei, M. D. Fleming, S. L. Schreiber, and L. C. Cantley. 2008. The M2

splice isoform of pyruvate kinase is important for cancer metabolism and tumour growth. *Nature* 452: 230-233.

98.   Seton-Rogers, S. 2011. Cancer metabolism: feed it forward. *Nat Rev Cancer* 11: 461.

99.   Hosios, A. M., B. P. Fiske, D. Y. Gui, and M. G. Vander Heiden. 2015. Lack of Evidence for PKM2 Protein Kinase Activity. *Mol Cell* 59: 850-857.

100.   Hitosugi, T., S. Kang, M. G. Vander Heiden, T. W. Chung, S. Elf, K. Lythgoe, S. Dong, S. Lonial, X. Wang, G. Z. Chen, J. Xie, T. L. Gu, R. D. Polakiewicz, J. L. Roesel, T. J. Boggon, F. R. Khuri, D. G. Gilliland, L. C. Cantley, J. Kaufman, and J. Chen. 2009. Tyrosine phosphorylation inhibits PKM2 to promote the Warburg effect and tumor growth. *Sci Signal* 2: ra73.

101.   Lv, L., D. Li, D. Zhao, R. Lin, Y. Chu, H. Zhang, Z. Zha, Y. Liu, Z. Li, Y. Xu, G. Wang, Y. Huang, Y. Xiong, K. L. Guan, and Q. Y. Lei. 2011. Acetylation targets the M2 isoform of pyruvate kinase for degradation through chaperone-mediated autophagy and promotes tumor growth. *Mol Cell* 42: 719-730.

102.   Rees, M. L., J. Subramaniam, Y. Li, D. J. Hamilton, O. H. Frazier, and H. Taegtmeyer. 2015. A PKM2 signature in the failing heart. *Biochem Biophys Res Commun* 459: 430-436.

103.   Wikoff, W. R., D. Grapov, J. F. Fahrmann, B. DeFelice, W. N. Rom, H. I. Pass, K. Kim, U. Nguyen, S. L. Taylor, D. R. Gandara, K. Kelly, O. Fiehn, and S. Miyamoto. 2015. Metabolomic markers of altered nucleotide metabolism in early stage adenocarcinoma. *Cancer Prev Res (Phila)* 8: 410-418.

104. Cory, J. G., and A. H. Cory. 2006. Critical roles of glutamine as nitrogen donors in purine and pyrimidine nucleotide synthesis: asparaginase treatment in childhood acute lymphoblastic leukemia. *In Vivo* 20: 587-589.

105. Lowenstein, J. M. 1990. The purine nucleotide cycle revisited [corrected]. *Int J Sports Med* 11 Suppl 2: S37-46.

106. Bogusky, R. T., L. M. Lowenstein, and J. M. Lowenstein. 1976. The purine nucleotide cycle. A pathway for ammonia production in the rat kidney. *J Clin Invest* 58: 326-335.

107. Eagle, H. 1955. The specific amino acid requirements of a human carcinoma cell (Stain HeLa) in tissue culture. *J Exp Med* 102: 37-48.

108. Burgess, D. J. 2011. Metabolism: choose your carbon source. *Nat Rev Cancer* 11: 80.

109. Wellen, K. E., C. Lu, A. Mancuso, J. M. Lemons, M. Ryczko, J. W. Dennis, J. D. Rabinowitz, H. A. Coller, and C. B. Thompson. 2010. The hexosamine biosynthetic pathway couples growth factor-induced glutamine uptake to glucose metabolism. *Genes Dev* 24: 2784-2799.

110. Rathmell, J. C., C. J. Fox, D. R. Plas, P. S. Hammerman, R. M. Cinalli, and C. B. Thompson. 2003. Akt-directed glucose metabolism can prevent Bax conformation change and promote growth factor-independent survival. *Mol Cell Biol* 23: 7315-7328.

111. Medina, R. A., and G. I. Owen. 2002. Glucose transporters: expression, regulation and cancer. *Biol Res* 35: 9-26.

112. Tochio, T., H. Tanaka, and S. Nakata. 2013. Glucose transporter member 1 is involved in UVB-induced epidermal hyperplasia by enhancing proliferation in epidermal keratinocytes. *Int J Dermatol* 52: 300-308.

113. Denko, N. C. 2008. Hypoxia, HIF1 and glucose metabolism in the solid tumour. *Nat Rev Cancer* 8: 705-713.

114. Galluzzi, L., O. Kepp, M. G. Vander Heiden, and G. Kroemer. 2013. Metabolic targets for cancer therapy. *Nat Rev Drug Discov* 12: 829-846.

115. Martinez-Outschoorn, U. E., M. Peiris-Pages, R. G. Pestell, F. Sotgia, and M. P. Lisanti. 2016. Cancer metabolism: a therapeutic perspective. *Nat Rev Clin Oncol*.

116. Nowell, P. C. 1976. The clonal evolution of tumor cell populations. *Science* 194: 23-28.

117. Greaves, M., and C. C. Maley. 2012. Clonal evolution in cancer. *Nature* 481: 306-313.

118. Merlo, L. M., J. W. Pepper, B. J. Reid, and C. C. Maley. 2006. Cancer as an evolutionary and ecological process. *Nat Rev Cancer* 6: 924-935.

119. Nguyen, L. V., D. Pellacani, S. Lefort, N. Kannan, T. Osako, M. Makarem, C. L. Cox, W. Kennedy, P. Beer, A. Carles, M. Moksa, M. Bilenky, S. Balani, S. Babovic, I. Sun, M. Rosin, S. Aparicio, M. Hirst, and C. J. Eaves. 2015. Barcoding reveals complex clonal dynamics of de novo transformed human mammary cells. *Nature* 528: 267-271.

120. Oesper, L., G. Satas, and B. J. Raphael. 2014. Quantifying tumor heterogeneity in whole-genome and whole-exome sequencing data. *Bioinformatics* 30: 3532-3540.

121. Gerlinger, M., A. J. Rowan, S. Horswell, J. Larkin, D. Endesfelder, E. Gronroos, P. Martinez, N. Matthews, A. Stewart, P. Tarpey, I. Varela, B. Phillimore, S. Begum, N. Q. McDonald, A. Butler, D. Jones, K. Raine, C. Latimer, C. R. Santos, M. Nohadani, A. C. Eklund, B. Spencer-Dene, G. Clark, L. Pickering, G. Stamp, M. Gore, Z. Szallasi, J. Downward, P. A. Futreal, and C. Swanton. 2012. Intratumor heterogeneity and branched evolution revealed by multiregion sequencing. *N Engl J Med* 366: 883-892.

122. Bedard, P. L., A. R. Hansen, M. J. Ratain, and L. L. Siu. 2013. Tumour heterogeneity in the clinic. *Nature* 501: 355-364.

123. McGranahan, N., and C. Swanton. 2015. Biological and therapeutic impact of intratumor heterogeneity in cancer evolution. *Cancer Cell* 27: 15-26.

124. Marusyk, A., and K. Polyak. 2010. Tumor heterogeneity: causes and consequences. *Biochim Biophys Acta* 1805: 105-117.

125. Yothers, G., N. Song, and T. J. George, Jr. 2016. Cancer Hallmark-Based Gene Sets and Personalized Medicine for Patients With Stage II Colon Cancer. *JAMA Oncol* 2: 23-24.

126. Torre, L. A., A. M. Sauer, M. S. Chen, Jr., M. Kagawa-Singer, A. Jemal, and R. L. Siegel. 2016. Cancer statistics for Asian Americans, Native Hawaiians, and Pacific Islanders, 2016: Converging incidence in males and females. *CA Cancer J Clin* 66: 182-202.

127. DeSantis, C. E., R. L. Siegel, A. G. Sauer, K. D. Miller, S. A. Fedewa, K. I. Alcaraz, and A. Jemal. 2016. Cancer statistics for African Americans, 2016: Progress and opportunities in reducing racial disparities. *CA Cancer J Clin*.

128. Society, A. C. 2016. What are the key statistics about breast cancer?

129. Vargo-Gogola, T., and J. M. Rosen. 2007. Modelling breast cancer: one size does not fit all. *Nat Rev Cancer* 7: 659-672.

130. Polyak, K. 2007. Breast cancer: origins and evolution. *J Clin Invest* 117: 3155-3163.

131. Lakhani, S. R. 1999. The transition from hyperplasia to invasive carcinoma of the breast. *J Pathol* 187: 272-278.

132. Kroigard, A. B., M. J. Larsen, A. V. Laenkholm, A. S. Knoop, J. D. Jensen, M. Bak, J. Mollenhauer, T. A. Kruse, and M. Thomassen. 2015. Clonal expansion and linear genome evolution through breast cancer progression from pre-invasive stages to asynchronous metastasis. *Oncotarget* 6: 5634-5649.

133. Moulis, S., and D. C. Sgroi. 2008. Re-evaluating early breast neoplasia. *Breast Cancer Res* 10: 302.

134. Histology of DCIS. http://www.rnceus.com/dcis/sub.html

135. Cairns, J. 1975. Mutation selection and the natural history of cancer. *Nature* 255: 197-200.

136. Gray, J. W. 2003. Evidence emerges for early metastasis and parallel evolution of primary and metastatic tumors. *Cancer Cell* 4: 4-6.

137. Klein, C. A. 2009. Parallel progression of primary tumours and metastases. *Nat Rev Cancer* 9: 302-312.

138. Pinder, S. E. 2010. Ductal carcinoma in situ (DCIS): pathological features, differential diagnosis, prognostic factors and specimen evaluation. *Mod Pathol* 23 Suppl 2: S8-13.

139. Burstein, H. J., K. Polyak, J. S. Wong, S. C. Lester, and C. M. Kaelin. 2004. Ductal carcinoma in situ of the breast. *N Engl J Med* 350: 1430-1441.

140. Prat, A., J. S. Parker, O. Karginova, C. Fan, C. Livasy, J. I. Herschkowitz, X. He, and C. M. Perou. 2010. Phenotypic and molecular characterization of the claudin-low intrinsic subtype of breast cancer. *Breast Cancer Res* 12: R68.

141. Perou, C. M. 2011. Molecular stratification of triple-negative breast cancers. *Oncologist* 16 Suppl 1: 61-70.

142. Perou, C. M. 2010. Molecular stratification of triple-negative breast cancers. *Oncologist* 15 Suppl 5: 39-48.

143. Fumagalli, D., F. Andre, M. J. Piccart-Gebhart, C. Sotiriou, and C. Desmedt. 2012. Molecular biology in breast cancer: should molecular classifiers be assessed by conventional tools or by gene expression arrays? *Crit Rev Oncol Hematol* 84 Suppl 1: e58-69.

144. Jung, S. Y., H. Y. Kim, B. H. Nam, S. Y. Min, S. J. Lee, C. Park, Y. Kwon, E. A. Kim, K. L. Ko, K. H. Shin, K. S. Lee, I. H. Park, S. Lee, S. W. Kim, H. S. Kang, and J. Ro. 2010. Worse prognosis of metaplastic breast cancer patients than other patients with triple-negative breast cancer. *Breast Cancer Res Treat* 120: 627-637.

145. Niemantsverdriet, M., K. Wagner, M. Visser, and C. Backendorf. 2008. Cellular functions of 14-3-3 zeta in apoptosis and cell adhesion emphasize its oncogenic character. *Oncogene* 27: 1315-1319.

146. Fu, H., R. R. Subramanian, and S. C. Masters. 2000. 14-3-3 proteins: structure, function, and regulation. *Annu Rev Pharmacol Toxicol* 40: 617-647.

147. Yaffe, M. B. 2002. How do 14-3-3 proteins work?-- Gatekeeper phosphorylation and the molecular anvil hypothesis. *FEBS Lett* 513: 53-57.

148. Gohla, A., and G. M. Bokoch. 2002. 14-3-3 regulates actin dynamics by stabilizing phosphorylated cofilin. *Curr Biol* 12: 1704-1710.

149. Freeman, A. K., and D. K. Morrison. 2011. 14-3-3 Proteins: diverse functions in cell proliferation and cancer progression. *Semin Cell Dev Biol* 22: 681-687.

150. Yaffe, M. B., K. Rittinger, S. Volinia, P. R. Caron, A. Aitken, H. Leffers, S. J. Gamblin, S. J. Smerdon, and L. C. Cantley. 1997. The structural basis for 14-3-3:phosphopeptide binding specificity. *Cell* 91: 961-971.

151. van Heusden, G. P. 2005. 14-3-3 proteins: regulators of numerous eukaryotic proteins. *IUBMB Life* 57: 623-629.

152. Dougherty, M. K., and D. K. Morrison. 2004. Unlocking the code of 14-3-3. *J Cell Sci* 117: 1875-1884.

153. Muslin, A. J., and H. Xing. 2000. 14-3-3 proteins: regulation of subcellular localization by molecular interference. *Cell Signal* 12: 703-709.

154. Xu, J., S. Acharya, O. Sahin, Q. Zhang, Y. Saito, J. Yao, H. Wang, P. Li, L. Zhang, F. J. Lowery, W. L. Kuo, Y. Xiao, J. Ensor, A. A. Sahin, X. H. Zhang, M. C. Hung, J. D. Zhang, and D. Yu. 2015. 14-3-3zeta turns TGF-beta's function from tumor suppressor to metastasis promoter in breast cancer by contextual changes of Smad partners from p53 to Gli2. *Cancer Cell* 27: 177-192.

155. Ge, F., W. L. Li, L. J. Bi, S. C. Tao, Z. P. Zhang, and X. E. Zhang. 2010. Identification of novel 14-3-3zeta interacting proteins by quantitative

immunoprecipitation combined with knockdown (QUICK). *J Proteome Res* 9: 5848-5858.

156.   Jin, J., F. D. Smith, C. Stark, C. D. Wells, J. P. Fawcett, S. Kulkarni, P. Metalnikov, P. O'Donnell, P. Taylor, L. Taylor, A. Zougman, J. R. Woodgett, L. K. Langeberg, J. D. Scott, and T. Pawson. 2004. Proteomic, functional, and domain-based analysis of in vivo 14-3-3 binding proteins involved in cytoskeletal regulation and cellular organization. *Curr Biol* 14: 1436-1450.

157.   Neal, C. L., and D. Yu. 2010. 14-3-3zeta as a prognostic marker and therapeutic target for cancer. *Expert Opin Ther Targets* 14: 1343-1354.

158.   Neal, C. L., J. Yao, W. Yang, X. Zhou, N. T. Nguyen, J. Lu, C. G. Danes, H. Guo, K. H. Lan, J. Ensor, W. Hittelman, M. C. Hung, and D. Yu. 2009. 14-3-3zeta overexpression defines high risk for breast cancer recurrence and promotes cancer cell survival. *Cancer Res* 69: 3425-3432.

159.   Chang, C. C., C. Zhang, Q. Zhang, O. Sahin, H. Wang, J. Xu, Y. Xiao, J. Zhang, S. K. Rehman, P. Li, M. C. Hung, F. Behbod, and D. Yu. 2016. Upregulation of lactate dehydrogenase a by 14-3-3zeta leads to increased glycolysis critical for breast cancer initiation and progression. *Oncotarget*.

160.   Pozuelo Rubio, M., M. Peggie, B. H. Wong, N. Morrice, and C. MacKintosh. 2003. 14-3-3s regulate fructose-2,6-bisphosphate levels by binding to PKB-phosphorylated cardiac fructose-2,6-bisphosphate kinase/phosphatase. *EMBO J* 22: 3514-3523.

161. Neal, C. L., J. Xu, P. Li, S. Mori, J. Yang, N. N. Neal, X. Zhou, S. L. Wyszomierski, and D. Yu. 2012. Overexpression of 14-3-3zeta in cancer cells activates PI3K via binding the p85 regulatory subunit. *Oncogene* 31: 897-906.

162. Lu, J., H. Guo, W. Treekitkarnmongkol, P. Li, J. Zhang, B. Shi, C. Ling, X. Zhou, T. Chen, P. J. Chiao, X. Feng, V. L. Seewaldt, W. J. Muller, A. Sahin, M. C. Hung, and D. Yu. 2009. 14-3-3zeta Cooperates with ErbB2 to promote ductal carcinoma in situ progression to invasive breast cancer by inducing epithelial-mesenchymal transition. *Cancer Cell* 16: 195-207.

163. Rehman, S. K., S. H. Li, S. L. Wyszomierski, Q. Wang, P. Li, O. Sahin, Y. Xiao, S. Zhang, Y. Xiong, J. Yang, H. Wang, H. Guo, J. D. Zhang, D. Medina, W. J. Muller, and D. Yu. 2014. 14-3-3zeta orchestrates mammary tumor onset and progression via miR-221-mediated cell proliferation. *Cancer Res* 74: 363-373.

164. Matta, A., S. Bahadur, R. Duggal, S. D. Gupta, and R. Ralhan. 2007. Over-expression of 14-3-3zeta is an early event in oral cancer. *BMC Cancer* 7: 169.

165. Han, X., Y. Han, H. Jiao, and Y. Jie. 2015. 14-3-3zeta regulates immune response through Stat3 signaling in oral squamous cell carcinoma. *Mol Cells* 38: 112-121.

166. Levayer, R., B. Hauert, and E. Moreno. 2015. Cell mixing induced by myc is required for competitive tissue invasion and destruction. *Nature* 524: 476-480.

167. Danes, C. G., S. L. Wyszomierski, J. Lu, C. L. Neal, W. Yang, and D. Yu. 2008. 14-3-3 zeta down-regulates p53 in mammary epithelial cells and confers luminal filling. *Cancer Res* 68: 1760-1767.

168. Higgins, M. J., and J. Baselga. 2011. Targeted therapies for breast cancer. *J Clin Invest* 121: 3797-3803.

169. Carracedo, A., D. Weiss, A. K. Leliaert, M. Bhasin, V. C. de Boer, G. Laurent, A. C. Adams, M. Sundvall, S. J. Song, K. Ito, L. S. Finley, A. Egia, T. Libermann, Z. Gerhart-Hines, P. Puigserver, M. C. Haigis, E. Maratos-Flier, A. L. Richardson, Z. T. Schafer, and P. P. Pandolfi. 2012. A metabolic prosurvival role for PML in breast cancer. *J Clin Invest* 122: 3088-3100.

170. Di, L. J., A. G. Fernandez, A. De Siervi, D. L. Longo, and K. Gardner. 2010. Transcriptional regulation of BRCA1 expression by a metabolic switch. *Nat Struct Mol Biol* 17: 1406-1413.

171. Tiziani, S., V. Lopes, and U. L. Gunther. 2009. Early stage diagnosis of oral cancer using 1H NMR-based metabolomics. *Neoplasia* 11: 269-276.

172. Acharya, S., J. Xu, X. Wang, S. Jain, H. Wang, Q. Zhang, C. C. Chang, J. Bower, B. Arun, V. Seewaldt, and D. Yu. 2016. Downregulation of GLUT4 contributes to effective intervention of estrogen receptor-negative/HER2-overexpressing early stage breast disease progression by lapatinib. *Am J Cancer Res* 6: 981-995.

173. Dang, C. V. 2010. Rethinking the Warburg effect with Myc micromanaging glutamine metabolism. *Cancer Res* 70: 859-862.

174. Xie, H., J. Hanai, J. G. Ren, L. Kats, K. Burgess, P. Bhargava, S. Signoretti, J. Billiard, K. J. Duffy, A. Grant, X. Wang, P. K. Lorkiewicz, S. Schatzman, M. Bousamra, 2nd, A. N. Lane, R. M. Higashi, T. W. Fan, P. P. Pandolfi, V. P. Sukhatme, and P. Seth. 2014. Targeting lactate dehydrogenase--a inhibits tumorigenesis and tumor progression in mouse models of lung cancer and impacts tumor-initiating cells. *Cell Metab* 19: 795-809.

175. Le, A., C. R. Cooper, A. M. Gouw, R. Dinavahi, A. Maitra, L. M. Deck, R. E. Royer, D. L. Vander Jagt, G. L. Semenza, and C. V. Dang. 2010. Inhibition of lactate dehydrogenase A induces oxidative stress and inhibits tumor progression. *Proc Natl Acad Sci U S A* 107: 2037-2042.

176. Martinez-Outschoorn, U. E., F. Sotgia, and M. P. Lisanti. 2012. Power surge: supporting cells "fuel" cancer cell mitochondria. *Cell Metab* 15: 4-5.

177. Xiao, X., X. Huang, F. Ye, B. Chen, C. Song, J. Wen, Z. Zhang, G. Zheng, H. Tang, and X. Xie. 2016. The miR-34a-LDHA axis regulates glucose metabolism and tumor growth in breast cancer. *Sci Rep* 6: 21735.

178. Jiang, W., F. Zhou, N. Li, Q. Li, and L. Wang. 2015. FOXM1-LDHA signaling promoted gastric cancer glycolytic phenotype and progression. *Int J Clin Exp Pathol* 8: 6756-6763.

179. He, T. L., Y. J. Zhang, H. Jiang, X. H. Li, H. Zhu, and K. L. Zheng. 2015. The c-Myc-LDHA axis positively regulates aerobic glycolysis and promotes tumor progression in pancreatic cancer. *Med Oncol* 32: 187.

180. Yao, F., T. Zhao, C. Zhong, J. Zhu, and H. Zhao. 2013. LDHA is necessary for the tumorigenicity of esophageal squamous cell carcinoma. *Tumour Biol* 34: 25-31.

181. Doherty, J. R., and J. L. Cleveland. 2013. Targeting lactate metabolism for cancer therapeutics. *J Clin Invest* 123: 3685-3692.

182. Heist, R. S., J. Fain, B. Chinnasami, W. Khan, J. R. Molina, L. V. Sequist, J. S. Temel, P. Fidias, V. Brainerd, L. Leopold, and T. J. Lynch. 2010. Phase I/II study of AT-101 with topotecan in relapsed and refractory small cell lung cancer. *J Thorac Oncol* 5: 1637-1643.

183. Yu, Y., J. A. Deck, L. A. Hunsaker, L. M. Deck, R. E. Royer, E. Goldberg, and D. L. Vander Jagt. 2001. Selective active site inhibitors of human lactate dehydrogenases A4, B4, and C4. *Biochem Pharmacol* 62: 81-89.

184. Dutta, P., A. Le, D. L. Vander Jagt, T. Tsukamoto, G. V. Martinez, C. V. Dang, and R. J. Gillies. 2013. Evaluation of LDH-A and glutaminase inhibition in vivo by hyperpolarized 13C-pyruvate magnetic resonance spectroscopy of tumors. *Cancer Res* 73: 4190-4195.

185. Zhang, J., F. Chen, W. Li, Q. Xiong, M. Yang, P. Zheng, C. Li, J. Pei, and F. Ge. 2012. 14-3-3zeta interacts with stat3 and regulates its constitutive activation in multiple myeloma cells. *PLoS One* 7: e29554.

186. Kleppe, R., A. Martinez, S. O. Doskeland, and J. Haavik. 2011. The 14-3-3 proteins in regulation of cellular metabolism. *Semin Cell Dev Biol* 22: 713-719.

187. Gao, Y., K. Colletti, and G. S. Pari. 2008. Identification of human cytomegalovirus UL84 virus- and cell-encoded binding partners by using proteomics analysis. *J Virol* 82: 96-104.

188. Brajenovic, M., G. Joberty, B. Kuster, T. Bouwmeester, and G. Drewes. 2004. Comprehensive proteomic analysis of human Par protein complexes reveals an interconnected protein network. *J Biol Chem* 279: 12804-12811.

189. Pozuelo Rubio, M., K. M. Geraghty, B. H. Wong, N. T. Wood, D. G. Campbell, N. Morrice, and C. Mackintosh. 2004. 14-3-3-affinity purification of over 200 human phosphoproteins reveals new links to regulation of cellular metabolism, proliferation and trafficking. *Biochem J* 379: 395-408.

190. Benzinger, A., N. Muster, H. B. Koch, J. R. Yates, 3rd, and H. Hermeking. 2005. Targeted proteomic analysis of 14-3-3 sigma, a p53 effector commonly silenced in cancer. *Mol Cell Proteomics* 4: 785-795.

191. Meek, S. E., W. S. Lane, and H. Piwnica-Worms. 2004. Comprehensive proteomic analysis of interphase and mitotic 14-3-3-binding proteins. *J Biol Chem* 279: 32046-32054.

192. Bai, Y., T. Zhou, H. Fu, H. Sun, and B. Huang. 2012. 14-3-3 interacts with LKB1 via recognizing phosphorylated threonine 336 residue and suppresses LKB1 kinase function. *FEBS Lett* 586: 1111-1119.

193. Cancer Genome Atlas, N. 2012. Comprehensive molecular portraits of human breast tumours. *Nature* 490: 61-70.

194. Consortium, T. I. G. The Expression Project for Oncology.

195. Behbod, F., F. S. Kittrell, H. LaMarca, D. Edwards, S. Kerbawy, J. C. Heestand, E. Young, P. Mukhopadhyay, H. W. Yeh, D. C. Allred, M. Hu, K. Polyak, J. M. Rosen, and D. Medina. 2009. An intraductal human-in-mouse transplantation model mimics the subtypes of ductal carcinoma in situ. *Breast Cancer Res* 11: R66, 61-11.

196. Wang, W., L. Upshaw, D. M. Strong, R. P. Robertson, and J. Reems. 2005. Increased oxygen consumption rates in response to high glucose detected by a novel oxygen biosensor system in non-human primate and human islets. *J Endocrinol* 185: 445-455.

197. Xu, R. H., H. Pelicano, Y. Zhou, J. S. Carew, L. Feng, K. N. Bhalla, M. J. Keating, and P. Huang. 2005. Inhibition of glycolysis in cancer cells: a novel strategy to

overcome drug resistance associated with mitochondrial respiratory defect and hypoxia. *Cancer Res* 65: 613-621.

198. Impey, S., S. R. McCorkle, H. Cha-Molstad, J. M. Dwyer, G. S. Yochum, J. M. Boss, S. McWeeney, J. J. Dunn, G. Mandel, and R. H. Goodman. 2004. Defining the CREB regulon: a genome-wide analysis of transcription factor regulatory regions. *Cell* 119: 1041-1054.

199. Debnath, J., S. K. Muthuswamy, and J. S. Brugge. 2003. Morphogenesis and oncogenesis of MCF-10A mammary epithelial acini grown in three-dimensional basement membrane cultures. *Methods* 30: 256-268.

200. Tomayko, M. M., and C. P. Reynolds. 1989. Determination of subcutaneous tumor size in athymic (nude) mice. *Cancer Chemother Pharmacol* 24: 148-154.

201. Emery, L. A., A. Tripathi, C. King, M. Kavanah, J. Mendez, M. D. Stone, A. de las Morenas, P. Sebastiani, and C. L. Rosenberg. 2009. Early dysregulation of cell adhesion and extracellular matrix pathways in breast cancer progression. *Am J Pathol* 175: 1292-1302.

202. Guzinska-Ustymowicz, K., A. Pryczynicz, A. Kemona, and J. Czyzewska. 2009. Correlation between proliferation markers: PCNA, Ki-67, MCM-2 and antiapoptotic protein Bcl-2 in colorectal cancer. *Anticancer Res* 29: 3049-3052.

203. He, Y., J. R. Han, O. Chang, M. Oh, S. E. James, Q. Lu, Y. W. Seo, H. Kim, and K. Kim. 2013. 14-3-3varepsilon/zeta Affects the stability of delta-catenin and regulates delta-catenin-induced dendrogenesis. *FEBS Open Bio* 3: 16-21.

204. Schug, J. 2008. Using TESS to predict transcription factor binding sites in DNA sequence. *Curr Protoc Bioinformatics* Chapter 2: Unit 2 6.

205. Acevedo, S. F., K. K. Tsigkari, S. Grammenoudi, and E. M. Skoulakis. 2007. In vivo functional specificity and homeostasis of Drosophila 14-3-3 proteins. *Genetics* 177: 239-253.

206. Kolch, W. 2000. Meaningful relationships: the regulation of the Ras/Raf/MEK/ERK pathway by protein interactions. *Biochem J* 351 Pt 2: 289-305.

207. Pozuelo-Rubio, M. 2011. Regulation of autophagic activity by 14-3-3zeta proteins associated with class III phosphatidylinositol-3-kinase. *Cell death and differentiation* 18: 479-492.

208. Freed, E., M. Symons, S. G. Macdonald, F. McCormick, and R. Ruggieri. 1994. Binding of 14-3-3 proteins to the protein kinase Raf and effects on its activation. *Science* 265: 1713-1716.

209. Phuong, N. T., S. C. Lim, Y. M. Kim, and K. W. Kang. 2014. Aromatase induction in tamoxifen-resistant breast cancer: Role of phosphoinositide 3-kinase-dependent CREB activation. *Cancer Lett* 351: 91-99.

210. Chang, F., L. S. Steelman, J. T. Lee, J. G. Shelton, P. M. Navolanic, W. L. Blalock, R. A. Franklin, and J. A. McCubrey. 2003. Signal transduction mediated by the Ras/Raf/MEK/ERK pathway from cytokine receptors to transcription factors: potential targeting for therapeutic intervention. *Leukemia* 17: 1263-1293.

211. Klijn, C., S. Durinck, E. W. Stawiski, P. M. Haverty, Z. Jiang, H. Liu, J. Degenhardt, O. Mayba, F. Gnad, J. Liu, G. Pau, J. Reeder, Y. Cao, K. Mukhyala, S. K. Selvaraj, M. Yu, G. J. Zynda, M. J. Brauer, T. D. Wu, R. C. Gentleman, G. Manning, R. L. Yauch, R. Bourgon, D. Stokoe, Z. Modrusan, R. M. Neve, F. J. de Sauvage, J.

Settleman, S. Seshagiri, and Z. Zhang. 2015. A comprehensive transcriptional portrait of human cancer cell lines. *Nat Biotechnol* 33: 306-312.

212. Kroemer, G., and J. Pouyssegur. 2008. Tumor cell metabolism: cancer's Achilles' heel. *Cancer Cell* 13: 472-482.

213. Hirsch, H. A., D. Iliopoulos, P. N. Tsichlis, and K. Struhl. 2009. Metformin selectively targets cancer stem cells, and acts together with chemotherapy to block tumor growth and prolong remission. *Cancer Res* 69: 7507-7511.

214. Slupsky, C. M., H. Steed, T. H. Wells, K. Dabbs, A. Schepansky, V. Capstick, W. Faught, and M. B. Sawyer. 2010. Urine metabolite analysis offers potential early diagnosis of ovarian and breast cancers. *Clin Cancer Res* 16: 5835-5841.

215. Conkright, M. D., E. Guzman, L. Flechner, A. I. Su, J. B. Hogenesch, and M. Montminy. 2003. Genome-wide analysis of CREB target genes reveals a core promoter requirement for cAMP responsiveness. *Mol Cell* 11: 1101-1108.

216. Lonze, B. E., and D. D. Ginty. 2002. Function and regulation of CREB family transcription factors in the nervous system. *Neuron* 35: 605-623.

217. Shim, H., C. Dolde, B. C. Lewis, C. S. Wu, G. Dang, R. A. Jungmann, R. Dalla-Favera, and C. V. Dang. 1997. c-Myc transactivation of LDH-A: implications for tumor metabolism and growth. *Proc Natl Acad Sci U S A* 94: 6658-6663.

218. Johmura, Y., K. Watanabe, K. Kishimoto, T. Ueda, S. Shimada, S. Osada, M. Nishizuka, and M. Imagawa. 2009. Fad24 causes hyperplasia in adipose tissue and improves glucose metabolism. *Biol Pharm Bull* 32: 1656-1664.

219. Zamboni, P. F., M. Simone, A. Passaro, E. Doh Dalla Nora, R. Fellin, and A. Solini. 2003. Metabolic profile in patients with benign prostate hyperplasia or prostate cancer and normal glucose tolerance. *Horm Metab Res* 35: 296-300.

220. Raez, L. E., K. Papadopoulos, A. D. Ricart, E. G. Chiorean, R. S. Dipaola, M. N. Stein, C. M. Rocha Lima, J. J. Schlesselman, K. Tolba, V. K. Langmuir, S. Kroll, D. T. Jung, M. Kurtoglu, J. Rosenblatt, and T. J. Lampidis. 2013. A phase I dose-escalation trial of 2-deoxy-D-glucose alone or combined with docetaxel in patients with advanced solid tumors. *Cancer Chemother Pharmacol* 71: 523-530.

221. Tennant, D. A., R. V. Duran, and E. Gottlieb. 2010. Targeting metabolic transformation for cancer therapy. *Nat Rev Cancer* 10: 267-277.

222. Lim, G. E., T. Albrecht, M. Piske, K. Sarai, J. T. Lee, H. S. Ramshaw, S. Sinha, M. A. Guthridge, A. Acker-Palmer, A. F. Lopez, S. M. Clee, C. Nislow, and J. D. Johnson. 2015. 14-3-3zeta coordinates adipogenesis of visceral fat. *Nat Commun* 6: 7671.

223. Li, Y., L. Sun, Y. Zhang, D. Wang, F. Wang, J. Liang, B. Gui, and Y. Shang. 2011. The histone modifications governing TFF1 transcription mediated by estrogen receptor. *J Biol Chem* 286: 13925-13936.

224. Maxwell, S. A., Z. Li, D. Jaye, S. Ballard, J. Ferrell, and H. Fu. 2009. 14-3-3zeta mediates resistance of diffuse large B cell lymphoma to an anthracycline-based chemotherapeutic regimen. *J Biol Chem* 284: 22379-22389.

225. Morata, G., and P. Ripoll. 1975. Minutes: mutants of drosophila autonomously affecting cell division rate. *Dev Biol* 42: 211-221.

226. Oliver, E. R., T. L. Saunders, S. A. Tarle, and T. Glaser. 2004. Ribosomal protein L24 defect in belly spot and tail (Bst), a mouse Minute. *Development* 131: 3907-3920.

227. Amoyel, M., and E. A. Bach. 2014. Cell competition: how to eliminate your neighbours. *Development* 141: 988-1000.

228. de la Cova, C., M. Abril, P. Bellosta, P. Gallant, and L. A. Johnston. 2004. Drosophila myc regulates organ size by inducing cell competition. *Cell* 117: 107-116.

229. Moreno, E., and K. Basler. 2004. dMyc transforms cells into super-competitors. *Cell* 117: 117-129.

230. Claveria, C., G. Giovinazzo, R. Sierra, and M. Torres. 2013. Myc-driven endogenous cell competition in the early mammalian embryo. *Nature* 500: 39-44.

231. Martins, V. C., K. Busch, D. Juraeva, C. Blum, C. Ludwig, V. Rasche, F. Lasitschka, S. E. Mastitsky, B. Brors, T. Hielscher, H. J. Fehling, and H. R. Rodewald. 2014. Cell competition is a tumour suppressor mechanism in the thymus. *Nature* 509: 465-470.

232. Moreno, E. 2014. Cancer: Darwinian tumour suppression. *Nature* 509: 435-436.

233. Moreno, E. 2008. Is cell competition relevant to cancer? *Nat Rev Cancer* 8: 141-147.

234. Tamori, Y., and W. M. Deng. 2011. Cell competition and its implications for development and cancer. *J Genet Genomics* 38: 483-495.

235. Gil, J., and T. Rodriguez. 2016. Cancer: The Transforming Power of Cell Competition. *Curr Biol* 26: R164-166.

236. Wagstaff, L., G. Kolahgar, and E. Piddini. 2013. Competitive cell interactions in cancer: a cellular tug of war. *Trends Cell Biol* 23: 160-167.

237. Suijkerbuijk, S. J., G. Kolahgar, I. Kucinski, and E. Piddini. 2016. Cell Competition Drives the Growth of Intestinal Adenomas in Drosophila. *Curr Biol* 26: 428-438.

238. Johnston, L. A. 2014. Socializing with MYC: cell competition in development and as a model for premalignant cancer. *Cold Spring Harb Perspect Med* 4: a014274.

239. Darzynkiewicz, Z., and G. Juan. 2001. Analysis of DNA content and BrdU incorporation. *Curr Protoc Cytom* Chapter 7: Unit 7 7.

240. Cappella, P., F. Gasparri, M. Pulici, and J. Moll. 2015. Cell Proliferation Method: Click Chemistry Based on BrdU Coupling for Multiplex Antibody Staining. *Curr Protoc Cytom* 72: 7 34 31-17.

241. Al-Abed, Y., D. Dabideen, B. Aljabari, A. Valster, D. Messmer, M. Ochani, M. Tanovic, K. Ochani, M. Bacher, F. Nicoletti, C. Metz, V. A. Pavlov, E. J. Miller, and K. J. Tracey. 2005. ISO-1 binding to the tautomerase active site of MIF inhibits its pro-inflammatory activity and increases survival in severe sepsis. *J Biol Chem* 280: 36541-36544.

242. Jang, J. E., E. A. Hod, S. L. Spitalnik, and P. S. Frenette. 2011. CXCL1 and its receptor, CXCR2, mediate murine sickle cell vaso-occlusion during hemolytic transfusion reactions. *J Clin Invest* 121: 1397-1401.

243. Bento, A. F., D. F. Leite, R. F. Claudino, D. B. Hara, P. C. Leal, and J. B. Calixto. 2008. The selective nonpeptide CXCR2 antagonist SB225002 ameliorates acute experimental colitis in mice. *J Leukoc Biol* 84: 1213-1221.

244. Malladi, S., D. G. Macalinao, X. Jin, L. He, H. Basnet, Y. Zou, E. de Stanchina, and J. Massague. 2016. Metastatic Latency and Immune Evasion through Autocrine Inhibition of WNT. *Cell* 165: 45-60.

245. Gazdar, A. F., V. Kurvari, A. Virmani, L. Gollahon, M. Sakaguchi, M. Westerfield, D. Kodagoda, V. Stasny, H. T. Cunningham, Wistuba, II, G. Tomlinson, V. Tonk, R. Ashfaq, A. M. Leitch, J. D. Minna, and J. W. Shay. 1998. Characterization of paired tumor and non-tumor cell lines established from patients with breast cancer. *Int J Cancer* 78: 766-774.

246. Binsky, I., M. Haran, D. Starlets, Y. Gore, F. Lantner, N. Harpaz, L. Leng, D. M. Goldenberg, L. Shvidel, A. Berrebi, R. Bucala, and I. Shachar. 2007. IL-8 secreted in a macrophage migration-inhibitory factor- and CD74-dependent manner regulates B cell chronic lymphocytic leukemia survival. *Proc Natl Acad Sci U S A* 104: 13408-13413.

247. Tillmann, S., J. Bernhagen, and H. Noels. 2013. Arrest Functions of the MIF Ligand/Receptor Axes in Atherogenesis. *Front Immunol* 4: 115.

248. Bernhagen, J., R. Krohn, H. Lue, J. L. Gregory, A. Zernecke, R. R. Koenen, M. Dewor, I. Georgiev, A. Schober, L. Leng, T. Kooistra, G. Fingerle-Rowson, P. Ghezzi, R. Kleemann, S. R. McColl, R. Bucala, M. J. Hickey, and C. Weber. 2007. MIF is a noncognate ligand of CXC chemokine receptors in inflammatory and atherogenic cell recruitment. *Nat Med* 13: 587-596.

249. Baugh, J. A., and R. Bucala. 2002. Macrophage migration inhibitory factor. *Crit Care Med* 30: S27-S35.

250. Gyorffy, B., P. Surowiak, J. Budczies, and A. Lanczky. 2013. Online survival analysis software to assess the prognostic value of biomarkers using transcriptomic data in non-small-cell lung cancer. *PLoS One* 8: e82241.

251. Walck-Shannon, E., and J. Hardin. 2014. Cell intercalation from top to bottom. *Nat Rev Mol Cell Biol* 15: 34-48.

252. Levayer, R., and E. Moreno. 2013. Mechanisms of cell competition: themes and variations. *J Cell Biol* 200: 689-698.

253. Meyer, S. N., M. Amoyel, C. Bergantinos, C. de la Cova, C. Schertel, K. Basler, and L. A. Johnston. 2014. An ancient defense system eliminates unfit cells from developing tissues during cell competition. *Science* 346: 1258236.

254. Ning, Y., P. C. Manegold, Y. K. Hong, W. Zhang, A. Pohl, G. Lurje, T. Winder, D. Yang, M. J. LaBonte, P. M. Wilson, R. D. Ladner, and H. J. Lenz. 2011. Interleukin-8 is associated with proliferation, migration, angiogenesis and chemosensitivity in vitro and in vivo in colon cancer cell line models. *Int J Cancer* 128: 2038-2049.

255. Inoue, K., J. W. Slaton, B. Y. Eve, S. J. Kim, P. Perrotte, M. D. Balbay, S. Yano, M. Bar-Eli, R. Radinsky, C. A. Pettaway, and C. P. Dinney. 2000. Interleukin 8 expression regulates tumorigenicity and metastases in androgen-independent prostate cancer. *Clin Cancer Res* 6: 2104-2119.

256. De Larco, J. E., B. R. Wuertz, K. A. Rosner, S. A. Erickson, D. E. Gamache, J. C. Manivel, and L. T. Furcht. 2001. A potential role for interleukin-8 in the metastatic phenotype of breast carcinoma cells. *Am J Pathol* 158: 639-646.

257. Park, S. Y., J. Han, J. B. Kim, M. G. Yang, Y. J. Kim, H. J. Lim, S. Y. An, and J. H. Kim. 2014. Interleukin-8 is related to poor chemotherapeutic response and tumourigenicity in hepatocellular carcinoma. *Eur J Cancer* 50: 341-350.

258. Chen, H., J. Brady Ridgway, T. Sai, J. Lai, S. Warming, H. Chen, M. Roose-Girma, G. Zhang, W. Shou, and M. Yan. 2013. Context-dependent signaling defines roles of BMP9 and BMP10 in embryonic and postnatal development. *Proc Natl Acad Sci U S A* 110: 11887-11892.

259. Ju, X., T. O. Ishikawa, K. Naka, K. Ito, Y. Ito, and M. Oshima. 2014. Context-dependent activation of Wnt signaling by tumor suppressor RUNX3 in gastric cancer cells. *Cancer Sci* 105: 418-424.

260. Fernandes, M. T., E. Dejardin, and N. R. dos Santos. 2016. Context-dependent roles for lymphotoxin-beta receptor signaling in cancer development. *Biochim Biophys Acta* 1865: 204-219.

261. Marrone, M., K. K. Filipski, E. M. Gillanders, S. D. Schully, and A. N. Freedman. 2014. Multi-marker Solid Tumor Panels Using Next-generation Sequencing to Direct Molecularly Targeted Therapies. *PLoS Curr* 6.

262. Schneider, E., and G. Mizejewski. 2006. Multi-marker testing for cancer: what can we learn from modern prenatal testing for Trisomy-21. *Cancer Inform* 2: 44-47.

263. Tang, Y., S. Liu, N. Li, W. Guo, J. Shi, H. Yu, L. Zhang, K. Wang, S. Liu, and S. Cheng. 2016. 14-3-3zeta promotes hepatocellular carcinoma venous metastasis by modulating hypoxia-inducible factor-1alpha. *Oncotarget* 7: 15854-15867.

264. Ogihara, T., T. Isobe, T. Ichimura, M. Taoka, M. Funaki, H. Sakoda, Y. Onishi, K. Inukai, M. Anai, Y. Fukushima, M. Kikuchi, Y. Yazaki, Y. Oka, and T. Asano. 1997.

14-3-3 protein binds to insulin receptor substrate-1, one of the binding sites of which is in the phosphotyrosine binding domain. *J Biol Chem* 272: 25267-25274.

265. Gwinn, D. M., D. B. Shackelford, D. F. Egan, M. M. Mihaylova, A. Mery, D. S. Vasquez, B. E. Turk, and R. J. Shaw. 2008. AMPK phosphorylation of raptor mediates a metabolic checkpoint. *Mol Cell* 30: 214-226.

266. Chawla, A., A. V. Philips, G. Alatrash, and E. Mittendorf. 2014. Immune checkpoints: A therapeutic target in triple negative breast cancer. *Oncoimmunology* 3: e28325.

267. Olweus, J., and A. Kolstad. 2012. [Can the immune system target cancer?]. *Tidsskr Nor Laegeforen* 132: 784-785.

268. Biswas, S. K. 2015. Metabolic Reprogramming of Immune Cells in Cancer Progression. *Immunity* 43: 435-449.

269. Assmann, N., and D. K. Finlay. 2016. Metabolic regulation of immune responses: therapeutic opportunities. *J Clin Invest* 126: 2031-2039.

270. Ganeshan, K., and A. Chawla. 2014. Metabolic regulation of immune responses. *Annu Rev Immunol* 32: 609-634.

271. Yam, P. T., C. B. Kent, S. Morin, W. T. Farmer, R. Alchini, L. Lepelletier, D. R. Colman, M. Tessier-Lavigne, A. E. Fournier, and F. Charron. 2012. 14-3-3 proteins regulate a cell-intrinsic switch from sonic hedgehog-mediated commissural axon attraction to repulsion after midline crossing. *Neuron* 76: 735-749.

272. Mancini, M., V. Corradi, S. Petta, E. Barbieri, F. Manetti, M. Botta, and M. A. Santucci. 2011. A new nonpeptidic inhibitor of 14-3-3 induces apoptotic cell death

in chronic myeloid leukemia sensitive or resistant to imatinib. *J Pharmacol Exp Ther* 336: 596-604.

273. Mohammad, D. K., B. F. Nore, A. Hussain, M. O. Gustafsson, A. J. Mohamed, and C. I. Smith. 2013. Dual phosphorylation of Btk by Akt/protein kinase b provides docking for 14-3-3zeta, regulates shuttling, and attenuates both tonic and induced signaling in B cells. *Mol Cell Biol* 33: 3214-3226.

274. Sengupta, D., and G. Pratx. 2016. Imaging metabolic heterogeneity in cancer. *Mol Cancer* 15: 4.

275. Xu, H. N., G. Zheng, J. Tchou, S. Nioka, and L. Z. Li. 2013. Characterizing the metabolic heterogeneity in human breast cancer xenografts by 3D high resolution fluorescence imaging. *Springerplus* 2: 73.

276. Carvajal, R. D., J. A. Sosman, J. F. Quevedo, M. M. Milhem, A. M. Joshua, R. R. Kudchadkar, G. P. Linette, T. F. Gajewski, J. Lutzky, D. H. Lawson, C. D. Lao, P. J. Flynn, M. R. Albertini, T. Sato, K. Lewis, A. Doyle, K. Ancell, K. S. Panageas, M. Bluth, C. Hedvat, J. Erinjeri, G. Ambrosini, B. Marr, D. H. Abramson, M. A. Dickson, J. D. Wolchok, P. B. Chapman, and G. K. Schwartz. 2014. Effect of selumetinib vs chemotherapy on progression-free survival in uveal melanoma: a randomized clinical trial. *JAMA* 311: 2397-2405.

277. Doyle, A., M. P. McGarry, N. A. Lee, and J. J. Lee. 2012. The construction of transgenic and gene knockout/knockin mouse models of human disease. *Transgenic Res* 21: 327-349.

278. Hanahan, D., E. F. Wagner, and R. D. Palmiter. 2007. The origins of oncomice: a history of the first transgenic mice genetically engineered to develop cancer. *Genes Dev* 21: 2258-2270.

279. Roh, M., J. Kim, C. Song, M. Wills, and S. A. Abdulkadir. 2006. Transgenic mice for Cre-inducible overexpression of the oncogenes c-MYC and Pim-1 in multiple tissues. *Genesis* 44: 447-453.

280. Gunther, E. J., G. K. Belka, G. B. Wertheim, J. Wang, J. L. Hartman, R. B. Boxer, and L. A. Chodosh. 2002. A novel doxycycline-inducible system for the transgenic analysis of mammary gland biology. *FASEB J* 16: 283-292.

VITA

Chia-Chi Chang was born in Taipei, Taiwan, on August 16th, 1983, the daughter of Ray Chang, M.D., M.S. and Ruling Chen, M.S. After graduating from Tunghai University in Taichung, Taiwan in 2005, she immediately enrolled at National Taiwan University in Taipei, Taiwan. She graduated from National Taiwan University with a Master's degree in Science in 2007, with a basic science training in both Biochemistry and Biophysics. She worked as a research assistant in the Department of Chemistry at Academia Sinica, the highest academic institution in Taiwan, for two years before she entered The University of Texas Graduate School of Biomedical Sciences at Houston in pursuance of a Doctor of Philosophy degree in Cancer Biology in 2009.

Permanent address:

2180 Bancroft lane,

Houston, TX 77027